NUCLEOSOME REPOSITIONING UNDERLIES GENE EXPRESSION DYNAMICS

A Dissertation

Presented to the Faculty of the Weill Cornell Graduate School

of Medical Sciences

In Partial Fulfillment of the Requirements for the Degree of

Doctor of Philosophy

By

Nicolas Nocetti

May 2016

BIOGRAPHICAL SKETCH

Before beginning his graduate career at Weill Cornell, Nicolas attended Rutgers University as an undergraduate, majoring in molecular biology and biochemistry, with a minor in music. He performed his undergraduate research in the lab of Dr. Steven Brill, in search of a suppressor of *sgs1*Δ*slx4*Δ synthetic lethality, in *S. cerevisiae*. Nicolas was fortunate enough to take an epigenetics class in his senior year at Rutgers, stoking an interest in the control of gene expression that brought him to the lab of Iestyn Whitehouse at Sloan Kettering Institute. His work from his time in Iestyn's lab, aimed at mechanistically describing transcriptional dynamics through yeast metabolic oscillations, has been published in *Genes & Development*.

NUCLEOSOME REPOSITIOING UNDERLIES GENE EXPRESSION DYNAMICS

Nicolas Nocetti, Ph.D.

Cornell University 2016

Nucleosome repositioning at gene promoters is a fundamental aspect of the regulation of gene expression. Yet the extent to which nucleosome repositioning is utilized within eukaryotic genomes is poorly understood. Here we report a comprehensive analysis of nucleosome positions as budding yeast transit through an ultradian cycle in which expression of >50% of all genes is highly synchronized. We present evidence of extensive nucleosome repositioning at thousands of gene promoters as genes are activated and repressed. During activation, nucleosomes are relocated to allow sites of general transcription factor binding and transcription initiation to become accessible. The extent of nucleosome shifting is closely related to the dynamic range of gene transcription and generally related to DNA sequence properties and use of the co-activators TFIID or SAGA. While nucleosome repositioning occurs pervasively, we find that a class of genes required for growth experience acute nucleosome shifting as cells enter the cell cycle. Significantly, our data identifies that the ATP-dependent chromatin-remodeling enzyme Snf2, plays a fundamental role in nucleosome repositioning and the expression of growth genes. Collectively our data and analysis provide a framework for understanding nucleosome dynamics in relation to fundamental DNA dependent transactions. Further, given the tight association between promoter nucleosomes and transcription initiation, we also investigated the relationship between transcription start site selection and nucleosome positioning. The

data clearly demonstrate that the transition from promoter scanning to productive initiation by RNA polymerase is made upon invasion of the +1 nucleosome, and that transcripts initiating upstream of nucleosomes are targeted for rapid degradation.

Dedicated to Mom, Dad, Nina, Iestyn, Duncan, Sean, Jenny, and Tejas.

Table of Contents

List of Figures

List of Tables

Preface

Though genomes are comprised of many thousands of genes, only a subset of those genes are expressed by a cell at any given moment. Control of gene expression is crucial in responding to both intrinsic and exogenous factors, as well as determining and maintaining cell identity in eukaryotic organisms. In their Nobel Prize winning work, Jacob and Monod described the e .coli lac operon, and in so doing established many of the paradigms that have been exploited in studying the control of gene expression in organisms ranging from simple bacteria to the budding yeast, Saccharomyces cerevisiae, to humans. In studying this locus, Jacob and Monod, established and developed the concepts of "inducible" and "constitutive" systems, competition between activators and repressors, and linked the structural components of the locus to their functions. While the work described in this text is aimed at understanding how transcription is regulated in a more complex organism (S. cerevisiae), on a much broader scale (genome-wide as opposed to a single locus), all of the results presented here can be understood in the context of the concepts first described in over fifty years ago.

Transcription in budding yeast is achieved by three RNA Polymerase enzymes: I, II, and III. The activity of RNA Polymerase II (RNAPII) will be the focus of this work as it is responsible for the production of coding mRNA transcripts, among other non-coding transcripts. In order to produce an mRNA molecule, the polymerase must overcome several rate-limiting steps. RNAPII must be recruited to a promoter region,

where the RNAPII holoenzyme is assembled prior to the initiation of transcription. However, as yeast is a eukaryotic organism, its genome is packaged in nucleosomes. In order for the polymerase to gain access to its DNA template at promoter regions the nucleosomes must be cleared by ATP-dependent chromatin remodeling factors at many promoters. This introduction examines the role of chromatin and ATP-dependent remodelers, SWI/SNF in particular, in positioning promoter nucleosomes, thereby controlling levels transcriptional output. Subsequently, I introduce the Yeast Metabolic Cycle (YMC) and highlight the strengths of the YMC as a model system for studying the relationship between transcription initiation and chromatin remodeling events.

Chapter 1 - Introduction: Promoter Chromatin in *S. cerevisiae*

1.1 Transcription Initiation in Nucleosome Depleted Regions

Olins and Olins were the first to describe the famous "particles on a string" structure of chromatin, in 1974 (Olins and Olins 1974). The authors referred to the "particles" as ν-bodies, however they would quickly come to be known as nucleosomes following the publication of several seminal publications authored by Roger Kornberg and others. These early papers demonstrated that the repeating unit of chromatin is composed of ~200bp of double stranded DNA and and octameric complex of histones (Kornberg 1974; Finch et al. 1975; Oudet et al. 1975).

From structural analysis of the nucleosome utilizing X-Ray crystallography, we now know more precisely that 146bp of DNA wraps 1.6 times around the histone octamer, and that the octamer is composed of a single H3(2)-H4(2) tetramer, and two H2A-H2B dimers. Histone fold domains in each of the four histones allow the formation of "cresent-shaped" heterodimeric pairs comprised of H3-H4 or H2A-H2B. Additionally, interactions between H2B and H4 allow for assembly of H2A-H2B dimers into nucleosomes. Each histone pair, H3-H4 or H2A-H2B, physically interacts with 26-27bp of DNA, or roughly 2.5 turns of the helix (Luger et al. 1997).

The high degree of compaction achieved by nucleosomes restricts access to the underlying DNA, such that fundamental genomic processes like transcription, replication, recombination and repair must actively overcome the nucleosome barrier

(Eaton et al. 2010; Pan et al. 2011; Chambers and Downs 2012; Voss and Hager 2014). Eukaryotic promoter regions are characterized by many factors, including DNA sequence elements, post-translational modifications of histones, and the presence of chromatin remodeling factors and histone variants (Raisner et al. 2005; Badis et al. 2008; Hartley and Madhani 2009; Zhang et al. 2009; Rhee and Pugh 2012; Yen et al. 2012), though the most common feature among nearly all eukaryotic promoters is the Nucleosome Depleted Region (NDR) (Mavrich et al. 2008; Jiang and Pugh 2009a) (Figure 1-1).

NDRs in budding yeast are long linker regions between nucleosomes ranging from approximately 80-200 base pairs. These linkers are flanked by two remarkably well positioned nucleosomes, -1 and +1, upstream and downstream, respectively (Jiang and Pugh 2009b) (Figure 1-1). +1 nucleosomes are enriched for various post-translational modifications such as H4K5Ac, H3K4Ac, H3K9Ac and H3K14Ac, and the histone variant Htz1, also known as H2A.Z (Jenuwein and Allis 2001; Liu et al. 2005; Raisner et al. 2005; Luk et al. 2010). The composition of DNA within the NDR is highly AT-rich, which disfavors nucleosome assembly. Further, NDRs are enriched for sequence motifs that are recognized by various transcription factors, the most notable of these motifs being the TATA-element (TATAWAWR) (Badis et al. 2008; Rhee and Pugh 2012).

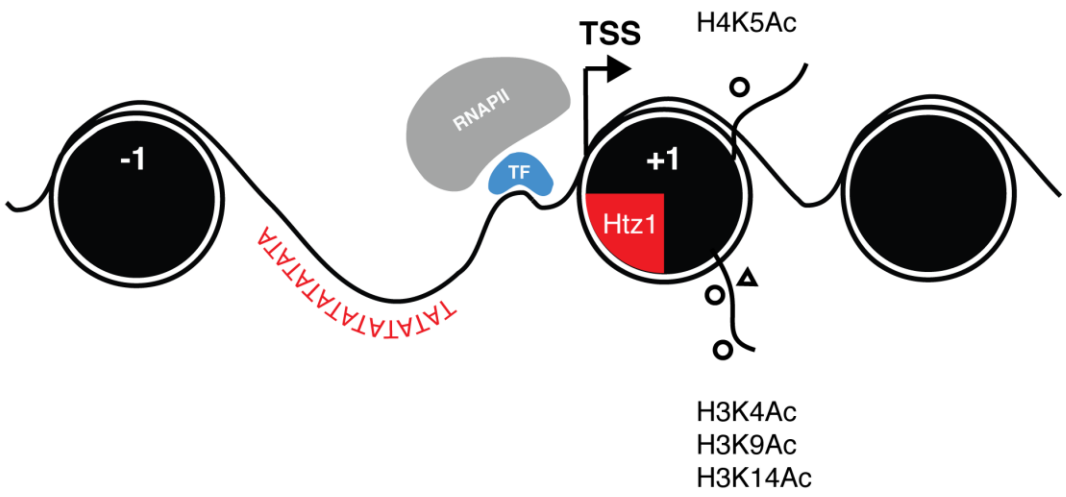

Figure 1-1 Illustration of Typical Promoter in *S. cerevisiae*

Common features of eukaryotic promoters are highlighted, specifically the AT-richness within the NFR, positions of -1 and +1 nucleosomes, binding of transcription factors (TF) and RNA Polymerase II (RNAPII), post-translational modification of histone tails, and incorporation of histone variant Htz1 in the +1 nucleosome. Also, illustrated is the positioning of transcription start site within the upstream edge of the +1 nucleosome.

The TATA Binding Protein (TBP), encoded by *SPT15* in *S. cerevisiae*, is tasked with simultaneously recognizing DNA the aforementioned TATA-element, and interacting with General Transcription Factors (GTFs) that physically interact with RNAPII. Binding of TBP to a promoter induces a large structural change in the topology of the DNA in the form of a roughly 90˚ bend (Horikoshi et al. 1992; Tan et al. 1996). Once TBP occupies a promoter, it recruits a second GTF, known as TFIIB, which stabilizes the TBP-DNA interaction, and functions to bridge TBP and RNAPII. The binding of TFIIA further stabilizes this complex of proteins at promoters via direct physical interactions with both TFIID and TBP (Tan et al. 1996). This collection of proteins, along with TFIIE, TFIIH, and TFIIF, bound to a promoter represents the

closed complex, also known as the pre-initiation complex (PIC) (Hampsey 1998; Chen and Hahn 2003; Rhee and Pugh 2012; Sainsbury et al. 2015) (Figure 1-2).

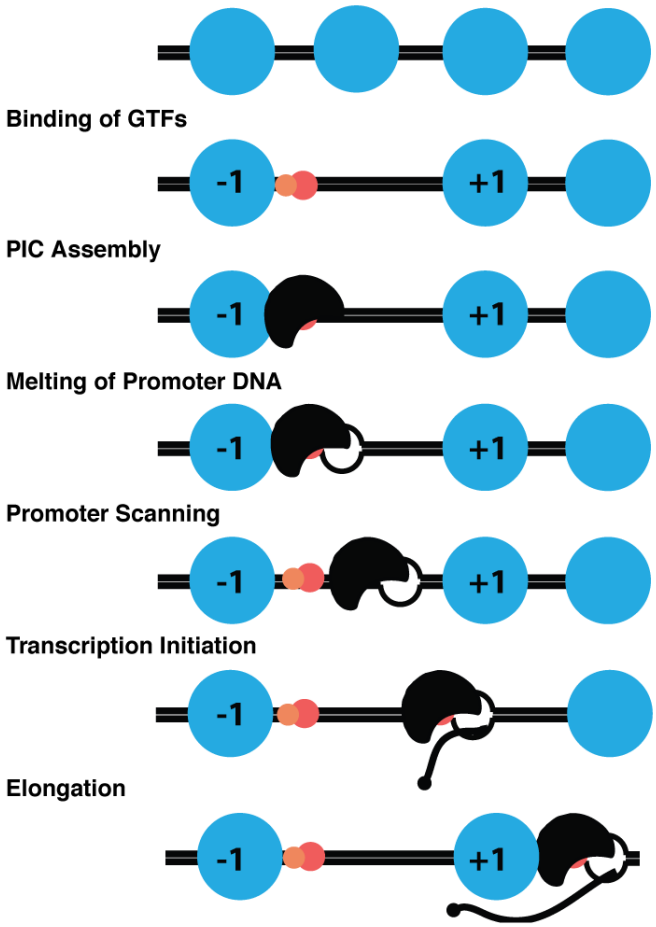

Figure 1-2 – Rate Limiting Steps of Transcription

Nucleosomes are represented in blue. Orange and red spheres denote transcription factors. RNAPII is illustrated as a black crescent.

In order to initiate transcription, the polymerase must next generate a single-stranded DNA template (Figure 1-2). The event of promoter melting marks the transition from the closed complex to the open complex, and is mediated by the helicase activity of the TFIIH. RNAPII is unique from the other RNA polymerases in

that it requires ATP to unwind promoter DNA (Grunberg et al. 2012). RNAPI and RNAPIII can initiate synthesis without the prerequisite of ATP hydrolysis. The dependence of transcription initiation on the ATPase activity of TFIIH can be overcome *in vitro* by introducing mismatch mutations in promoter DNA such that a single stranded bubble surrounding the TSS is created (Tantin and Carey 1994). Once the polymerase has initiated transcription it can proceed to the elongation phase of transcription.

1.2 Two Modes of Delivery of TBP to Promoters : TFIID and SAGA

Recognition of the TATA-element generally occurs with TBP as a member of either the TFIID or SAGA complex (Lee et al. 2000; Huisinga and Pugh 2004). Cumulatively, SAGA and TFIID are involved in the transcription of nearly all genes in *S. cerevisiae* (Huisinga and Pugh 2004). While there is redundancy between the two pathways, most promoters exhibit higher sensitivity to perturbation of either SAGA or TFIID. Between 10-20% of budding yeast promoters are dominated by the SAGA complex, while the others belong to the TFIID pathway (Basehoar et al. 2004; Huisinga and Pugh 2004).

The SAGA complex is a 1.8MDa complex containing 19-20 proteins (Han et al. 2014). Genes dominated by the SAGA (Spt-Ada-Gcn5-acetyltransferse) pathway tend to be inducible in response to various intrinsic and extrinsic factors, and exhibit broad ranges of expression (Basehoar et al. 2004; Huisinga and Pugh 2004). Further, these promoters are likely to exhibit perfect matches to the consensus TATA-element

sequence (Rhee and Pugh 2012). The acetyltransferase activity of the Gcn5 subunit has the ability to acetylate histone H3 at residues 9, 14, and 18 when functioning as a member of the SAGA complex (Zhang et al. 1998; Grant et al. 1999). Additionally, acetylation of SAGA components Sgf73, Spt7, and Ada3 is lost in a *gcn5*Δ genetic background, suggesting that Gcn5 is capable of acting upon non-histone substrates (Cai et al. 2011).

The TFIID complex is composed of TBP along with 14 TBP Associated Factors (TAFs) (Yatherajam et al. 2003). The majority of TAFs are associated exclusively with the TFIID complex, while others (Taf5, Taf6, Taf9, Taf10, and Taf12) can be found in both TFIID and SAGA (Grant et al. 1998). The presence of Taf1 has been used to specify a promoter as belonging to the TFIID class. Further, the requirement for consensus TATA-elements is much less stringent at TFIID promoters. These promoters are also more likely than their SAGA counterparts to maintain an Inr element (YYANWYY), a sequence motif recognized by TAF proteins, surrounding the TSS (Kaufmann and Smale 1994; Yang et al. 2007). In contrast to SAGA promoters which have been associated with stress response, and maintain the potential for broad ranges of dynamic expression, TFIID promoters tend to exhibit more static levels of expression and are often though of as so-called "housekeeping" genes (Basehoar et al. 2004; Huisinga and Pugh 2004).

Perhaps the most interesting distinction between SAGA and TFIID promoters is the unique relationship each class maintains with chromatin. TFIID promoters

maintain very well defined NDRs, and GTFs at these loci universally align to the upstream edge of the +1 nucleosome, as assayed by ChIP-exo. This is in stark contrast to GTFs at SAGA regulated promoters, which are bound throughout the body of the +1 nucleosome, suggesting that GTFs and nucleosomes are in competition for binding at these loci (Rhee and Pugh 2012).

1.3 Nucleosomal Affinity for DNA Is to Governed In Part by DNA Sequence

Though the vast majority of contacts between the histone octamer and DNA are made with the phosphate backbone, and the underlying sequence of the DNA can have profound effects on nucleosome stability (Luger et al. 1997). It has long been known that AT-rich sequences disfavor nucleosome assembly, and are rarely found near nucleosome dyads (Kunkel and Martinson 1981; Satchwell et al. 1986). Additionally, poly(dA-dT) tracts are important for constitutive expression of several genes in yeast, presumably due to their role in maintaining promoter accessibility for transcription factors (Struhl 1985). Experiments examining the effect of DNA sequence on nucleosome positioning *in vitro* demonstrate that yeast promoters inherently disfavor nucleosome assembly, and that flanking is much more amenable to nucleosomes (Segal et al. 2006; Zhang et al. 2011).

However, the *in vivo* nucleosomes surrounding NDRs exhibit markedly different rotational phasing than their *in vitro* assembled counterparts (Zhang et al.

2009). *In vitro* assembled nucleosomes adopt thermodynamically favorable positions with respect to the intrinsic 10bp AA/TT/AT dinucleotide periodicity found in the yeast genome, which allows for optimal DNA bending around nucleosomes (Segal et al. 2006). The effects of this dinucleotide periodicity are not as pronounced on promoter nucleosomes *in vivo*, as they are the subject of chromatin remodeling enzymes, such as SWI/SNF or ISWI, which utilize ATP to overcome DNA mediated positioning effects, allowing them to occupy thermodynamically unfavorable positions (Whitehouse and Tsukiyama 2006; Hartley and Madhani 2009; Gkikopoulos et al. 2011; Yen et al. 2012).

1.4 The SWI/SNF ATP-Dependant Chromatin Remodeler

The SWI/SNF complex is named after the two independent screens that discovered it. It was simultaneously described in screens searching for genes involved in the fermentation of sucrose and mating type switching in *S. cerevisiae* (Neigeborn and Carlson 1984; Stern et al. 1984). Null alleles of *SNF2*, encoding the catalytic subunit of the complex, are unable to complete either process. SWI/SNF has since been shown to alter chromatin structure by nucleosome sliding and nucleosome disassembly (Owen-Hughes et al. 1996; Whitehouse et al. 1999; Gkikopoulos et al. 2009).

Snf2 was identified in a screen for sucrose fermentation because it is absolutely required for the activation of *SUC2*, the protein product of which, invertase, converts sucrose into glucose and galactose (Neumann and Lampen 1967). *SUC2* is

transcriptionally silent in the presence of glucose, and repression of the locus is coincident with nucleosome positioning over the promoter such that there is no NDR and transcription factor binding sites are blocked (Wu and Winston 1997). Further, corepressors Ssn6-Tup1 and Mig1 occupy the promoter under glucose-repressed conditions (Treitel and Carlson 1995; Bu and Schmidt 1998). Derepression and activation of *SUC2* requires the chromatin remodeling activity of SWI/SNF to remodel promoter chromatin such that an NDR is formed and transcription factor binding sites such as the TATA-element and the Upstream Activating Sequence (UAS) become accessible (Wu and Winston 1997; Geng and Laurent 2004) (Figure 1-3). In the absence of Snf2 the promoter remains occluded by nucleosomes under derepressing conditions as assayed by sensitivity to MNase digestion (Wu and Winston 1997). This is consistent with *in vitro* studies demonstrating that SWI/SNF facilitates the binding of the Gal4 transcriptional activator to nucleosomal templates (Cote et al. 1994; Burns and Peterson 1997).

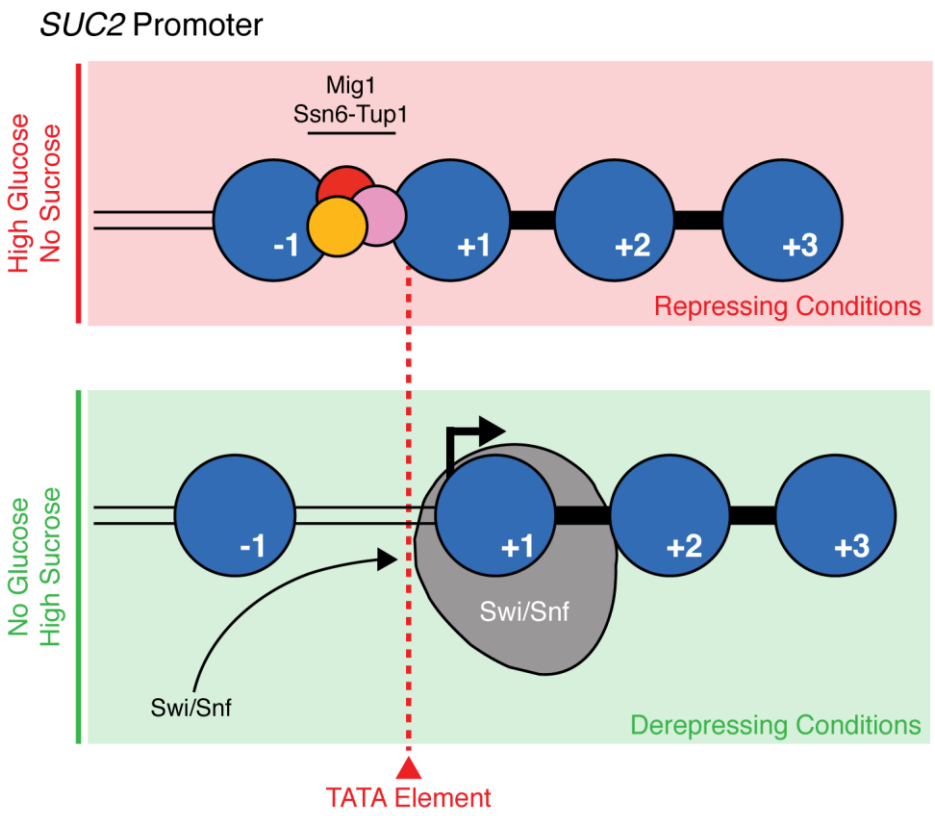

Figure 1-3 – Activation of *SUC2* transcription by SWI/SNF

The *SUC2* promoter under repressive (top) and activating (bottom) conditions is illustrated. The red dotted line highlights the position of the TATA Element.

SWI/SNF has since been shown to perform a similar role in the activation of myriad genes, many involved in the regulation of metabolism. For instance, the complex regulates the expression of *PHO5*, *PHO11*, *PHO12*, and *PHO84* in response to levels of P_i (Sudarsanam et al. 2000; Neef and Kladde 2003; Steger et al. 2003). Expression of *PHO5* is repressed by four promoter nucleosomes occluding the promoter region in phosphate-rich media (Adkins et al. 2007; Ertel et al. 2010; Korber and Barbaric 2014). Upon depletion of inorganic phosphate, promoter chromatin at *PHO5* is remodeled by SWI/SNF to allow for transcriptional activation. In a similar

fashion, activation of *PHO8* also exhibits a requirement for SWI/SNF (Gregory et al. 1999).

In an additional example of SWI/SNF regulating transcription in response to intracellular metabolite concentration, activation of transcription of Ty transposable elements in adenine starvation also requires the activity of SWI/SNF (Todeschini et al. 2005).

1.6.1 SWI/SNF in Mating Type Switiching

Haploid yeast adopt one of two mating types, a or alpha. The genes encoding the factors that determine the mating type are present at three loci present on chromosome III: HML(Hidden MAT Left)alpha, HMR(Hidden MAT right)a, and MAT (Haber 2012). While both HMLalpha and HMRa each encode the information capable of specifying mating type, both of these loci are transcriptionally silent. However, one of these two alleles can be found in a second copy at the MAT locus, and as the only transcriptionally active of the three loci the identity of the MAT locus determines whether a cell is a or alpha. Mating type switching in budding yeast occurs subsequent to cell division, and is initiated by the formation of a double strand break at the HO site located in the MAT locus leading to a gene conversion event (Jensen et al. 1983). *SNF2*, also known as *SWI2*, is essential for activating the expression of the HO endonuclease required for the initiation of the process (Krebs et al. 1999; Mitra et al. 2006). Thus, in addition to regulating the expression of relevant

genes in response metabolic cues, SWI/SNF is also responsible for regulating the only cell identity decision made in *S. cerevisiae*.

1.8 Domains of SWI/SNF

SWI/SNF is a large complex weighing >1.1MD comprised of 11 proteins: Snf2, Swi3, Swi1, Swp73, Snf5, Arp7, Arp9, Swp82, Snf6, Snf11, and Taf14 (Vignali et al. 2000; Dechassa et al. 2008). There exists a trough on the surface of SWI/SNF large enough to accommodate a nucleosome. When enveloped by the complex, the nucleosome makes many direct physical contacts with the catalytically active Snf2 subunit along the side-face of the nucleosome, interacting with all four histones. In addition, Snf2 makes contacts with nucleosomal DNA around the surface of the nucleosome (Dechassa et al. 2008). Snf2 contains a signature domain that is conserved in chromatin remodeling factors throughout eukaryotes (Smith and Peterson 2005; Durr et al. 2006). The Snf2-domain contains two RecA-like folds and bears significant homology to the helicase motifs, though Snf2 is incapable of unwinding DNA (Durr et al. 2006; Ryan and Owen-Hughes 2011). The Snf2-domain domain instead functions as a DNA translocase allowing it to use ATP-hydrolysis to slide double stranded DNA over the surface of the nucleosome or disrupt histone-DNA interactions (Dechassa et al. 2008).

Snf2 also contains a bromodomain, which mediates interactions with acetylated histone tails and is required for proper targeting and regulation of the complex (Hassan et al. 2001; Hassan et al. 2006). *In vitro* studies have shown that the

affinity of SWI/SNF nucleosomes is enhanced when nucleosomes are acetylated with either of the SAGA or NuA4 histone acetyltransferases (Hassan et al. 2002; Chandy et al. 2006). Further, activity is chromatin remodeling activity is preferentially directed towards acetylated histones over non-acetylated histones in an array of nucleosomes, and displacement of nucleosomes containing acetylated histones requires the bromodomain located on the C-terminal end of Snf2 (Hassan et al. 2002; Chandy et al. 2006).

1.9 Histone Acetyltransferase (HAT) Activity and SWI/SNF at Promoters

Acetylation of SUC2 promoter histones by the Gcn5 acetyltransferase is required for induction of expression, and in *gcn5*Δ strains acetylation of histone H3 at this locus is severely impaired (Figure 1-4). In the absence of SWI/SNF, acetylation of *SUC2* promoter histones proceeds normally, suggesting that Gcn5 activity precedes that of SWI/SNF in this instance, though the two factors appear to be recruited simultaneously (Geng and Laurent 2004). Additionally, SUC2 co-repressors , Ssn6-Tup1, have been shown to physically interact with the Rpd3 histone deacetylase (Watson et al. 2000). Thus, acetylation is associated with activation of the locus, while non-acetylated nucleosomes are indicative of a repressed transcriptional state.

The promoter of the HO endonuclease gene experiences periodic Gcn5-dependent histone acetylation with respect to the cell cycle. Specifically, nucleosomes positioned over the TATA-element and Swi4/Swi6 binding sites are targeted. Similar to the activation of the *SUC2* promoter, deletion of *GCN5* impairs the binding of

SWI/SNF to the HO promoter, demonstrating that the ability of SWI/SNF to activate transcription is augmented by acetylation of promoter nucleosomes (Mitra et al. 2006). In the absence of GCN5 the HO locus remains transcriptionally silent (Mitra et al. 2006).

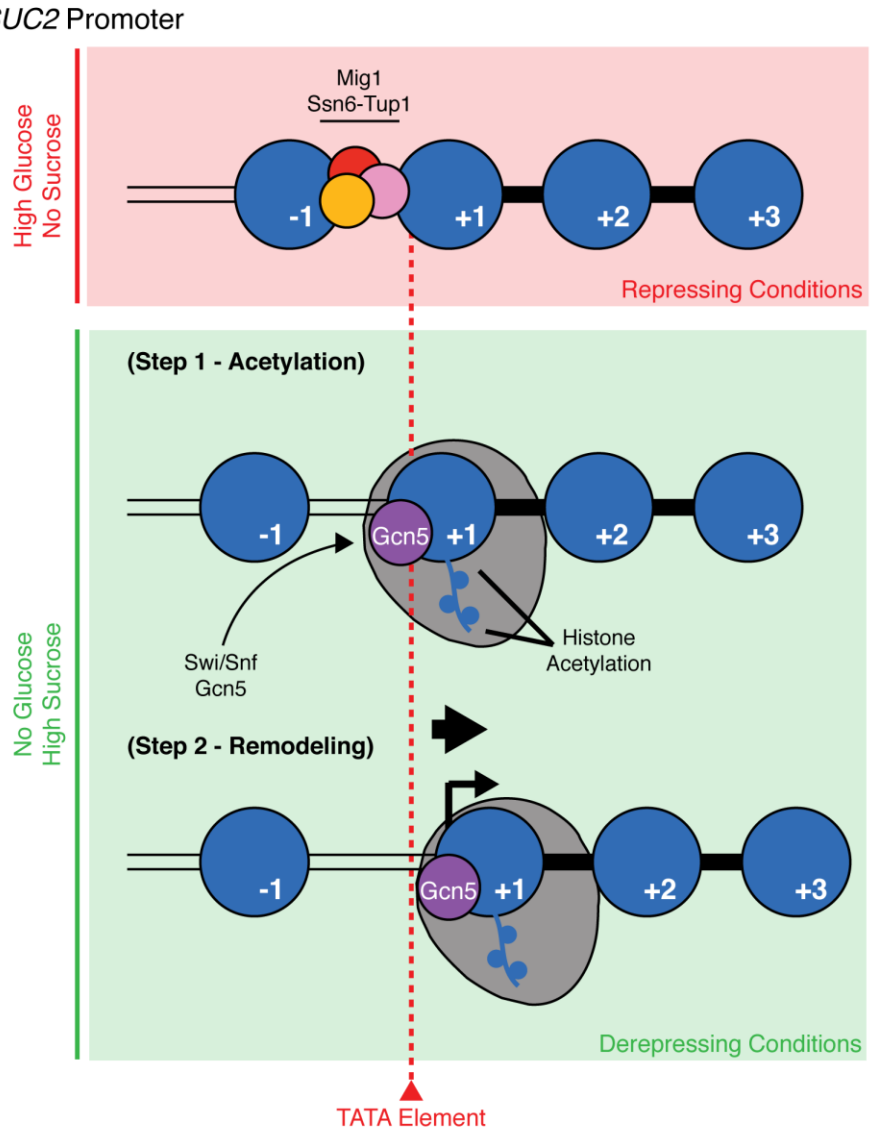

Figure 1-4 Acetylation Precedes Chromatin Remodeling at the *SUC2* Locus

The *SUC2* promoter under repressive (top) and activating (middle and bottom) conditions is illustrated. The red dotted line highlights the position of the TATA Element. Acetylation of the +1 nucleosome by Gcn5 precedes the activity of SWI/SNF.

SAGA and SWI/SNF also display a cooperative relationship in the activation of *PHO8*: in activating conditions (P_i poor), the *PHO8* promoter undegoes a limited degree of remodeling in the absence of GCN5, indicating that SWI/SNF is still recruited to some extent (Gregory et al. 1999). However, this remodeling is not sufficient to induce transcriptional activation, and full derepression of *PHO8* involves both SWI/SNF and SAGA (Gregory et al. 1999). Thus, SWI/SNF can recognize the *PHO8* promoter without acetylation, though acetylation of the locus triggers the full activation of the complex.

1.9.1 SWI/SNF inactivation by Gcn5

Acetylation of histones by Gcn5 has been implicated in mediating the recruitment of SWI/SNF and augmenting its activity towards promoter nucleosomes. However, Gcn5 has many substrates other than histones, including other members of the SAGA complex, and Snf2 itself (Kim et al. 2010b; Cai et al. 2011; Dutta et al. 2014). In contrast to its role in promoting SWI/SNF activity when acetylating histones, Gcn5 mediates the suppression of SWI/SNF activity upon acetylation of Snf2. The sites of this modification on Snf2 lie between two AT-hook domains found towards the N-terminal end of the protein. These AT-hook domains mediate interactions between SWI/SNF and DNA, thus it was proposed that acetylation by Gcn5 could mediate the release of SWI/SNF from chromatin. Indeed, by mutating the two acetylated lysine residues to arginine, thereby neutralizing their charge, an

increased occupancy of SWI/SNF is observed, both *in vivo* and *in vitro* (Kim et al. 2010b; Dutta et al. 2014).

1.10 Transcriptional Activators and SWI/SNF

While the acetylation of promoter nucleosomes facilitates recognition by SWI/SNF, recruitment of SWI/SNF *in vivo* often requires interactions with transcriptional activators (Neely et al. 1999; Yudkovsky et al. 1999; Neely et al. 2002). The Gal4-VP16 fusion protein is an excellent example of an activator, as it functions as a potent recruiter of SWI/SNF on the basis of a strong interaction between the acidic portion of VP16 and SWI/SNF (Yudkovsky et al. 1999). The DNA-binding portion of the protein recognizes the Gal4 motif (CGG-N_{11}-CCG,) allowing for the recruitment of the remodeler to specific sites (Giniger et al. 1985). Many activator proteins, such as Gcn4 and Hap4, exhibit a similar domain architecture in that they contain a DNA-binding domain and an acidic activation domain capable of physically interacting with SWI/SNF, through subunits Snf5 and Swi1 (Arndt and Fink 1986; Forsburg and Guarente 1989; Neely et al. 2002).

1.7 Context Dependence of SWI/SNF Activity and the Role of SWI/SNF in Mediating a Response to Stress

Genes involved in the response to heat shock are activated extremely rapidly in response to elevated temperatures. Expression of *HSP12*, *SSA4*, *HSP82* are all induced upon acute heat-shock conditions, and studies examining the activation of these three

genes found that their activation requires the displacement of promoter histones (Erkina et al. 2008; Erkina et al. 2010). In a subsequent genome-wide study examining the role of chromatin remodeling in response to heat-shock stress, repression of ribosomal protein (RP) genes in response to heat-shock was delayed in the *snf2*Δ genetic background (Shivaswamy and Iyer 2008). However, the same class of genes, RP, exhibited a decrease in transcriptional activity at standard temperature of 30˚C in the absence of *SNF2* relative to wildtype (Shivaswamy and Iyer 2008). Thus, SWI/SNF is involved in maintaining RP activation under normal conditions, but subsequently plays a role in repressing the same class of genes during stress response. The role of SWI/SNF is therefore highly context dependent.

Though SWI/SNF plays the role of activator in the majority of the cases described above, the complex has also been shown to function as the repressor in studies examining activation the *SER3* locus, and transcriptional repression at the rDNA loci and telomeres (Dror and Winston 2004; Martens et al. 2004; Martens et al. 2005). In addition, a genome-wide microarray based study examining the effects of *snf2*Δ and *swi1*Δ on gene expression found that many genes are activated in both mutant backgrounds, indicating that SWI/SNF was mediating their repression (Sudarsanam et al. 2000)(Figure 1-5 A).

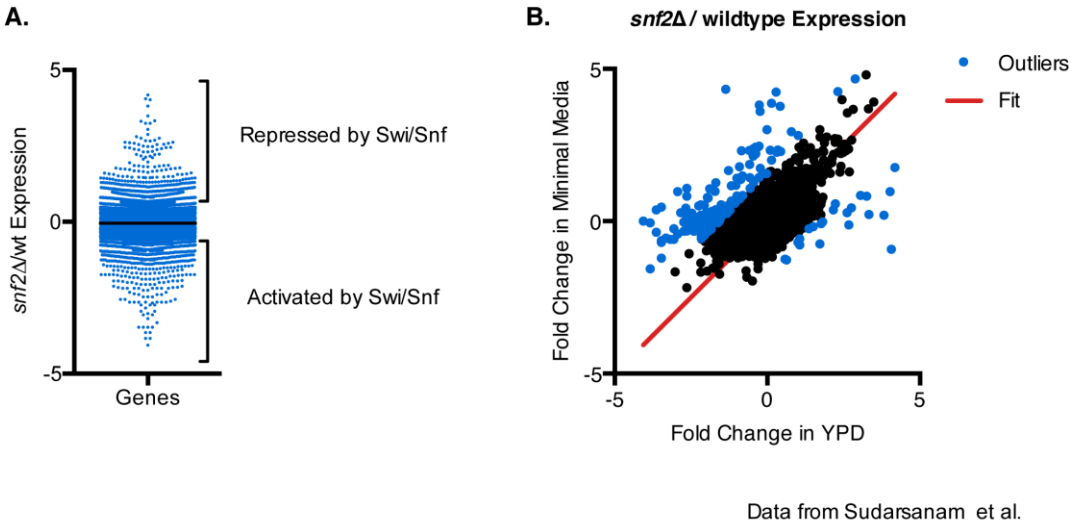

Figure 1-5 – The Complex and Context Dependent Role of SWI/SNF in Regulating Transcription

A. Fold change in expression in *snf2*Δ mutant versus wildtype. Loss of SWI/SNF activity leads to both transcriptional activation and repression. B. Comparison of the role SWI/SNF in regulating transcription in rich and minimal media. Linear fit (y=x) in red. Outliers represented in blue.

In analyzing the genome-wide effects of *snf2*Δ in transcription, the authors compared global transcription output of the mutant to that of the wildtype when grown in both rich (YPD), and minimal media (Sudarsanam et al. 2000). While the fold-change difference between mutant and wildtype for many genes is similar regardless of the growth conditions, other genes exhibit a drastic increase in sensitivity to *snf2*Δ depending on the growth condition. To illustrate this I have plotted the fold-change in expression for both growth conditions against one another, and fit the data to a linear regression (Figure 1-4 B). Data-points that do not conform to the linear fit are highlighted in blue. Many genes exhibit a significant fold-change in the absence of SWI/SNF when grown in YPD that is not observed when grown in minimal media, and visa versa.

The broad and pleiotropic effects resulting from of inactivation of SWI/SNF demonstrate how central a role the complex plays in regulating transcription genome-wide and highlight the difficulties and complexities of studying chromatin remodeling complexes.

1.11 The Yeast Metabolic Cycle

With the exception of studies examining the cell cycle, the vast majority of experiments utilizing yeast as a model organism sample asynchronous populations of cells. This asynchronisity can result in either the calling of false negatives when biologically significant events occur at a small frequency in the population, or introduce ambiguity due to an inability to segregate the behavior of distinct populations. These issues are particularly relevant to genome-wide datasets attempting to map and assess nucleosome positions and occupancy. For instance, as mentioned earlier in the introduction, the relationship between +1 nucleosomes and general transcription factors at SAGA-regulated promoters is unclear. The positions of nucleosome dyads, or midpoints of regions of nucleosomal protection, at SAGA-regulated promoters appear to occlude access of transcription factors to their binding sites. This observation could be due to competition between +1 nucleosomes and PICs, however, due to the asynchronous conditions under which the experiment was performed the authors are unable to temporally segregate the occupancy of these two factors, and both nucleosomes and transcription factors are observed ‘co-occupying’ the same locations.

Further, there are many genome-wide datasets mapping nucleosome positions in *S. cerevisiae*. From each of these datasets it is abundantly clear that nucleosomes are most precisely positioned closer to gene 5' ends and that rigid phasing of nucleosomes diminishes within gene bodies. Nucleosomes lacking precise positioning are referred to as 'fuzzy'. Are 'fuzzy' nucleosomes truly stochastically positioned, or is the diffuse occupancy observed at these sites the result of averaging multiple distinct populations? To further investigate the genome-wide relationship between nucleosomes and transcription we sought a system that would allow for the isolation of distinct populations.

The Yeast Metabolic Cycle (YMC) offers a highly robust and synchronized system in which over half of coding transcripts exhibit periodic expression (Klevecz et al. 2004; Tu et al. 2005). This system affords the temporal segregation of events that cannot be achieved in an asynchronous culture of logarithmically growing yeast. Oscillation is achieved in a chemostat by first growing a culture to saturation in nutrient limited conditions (Novick and Szilard 1950). Starved of a carbon source, the cells are maintained at saturation for several hours, allowing the culture to synchronize in a non-respiratory metabolic state. Upon the re-addition of glucose to the culture, the cells begin to respire synchronously, and this is monitored by the concentration of dissolved oxygen available to the culture (Figure 1-6).

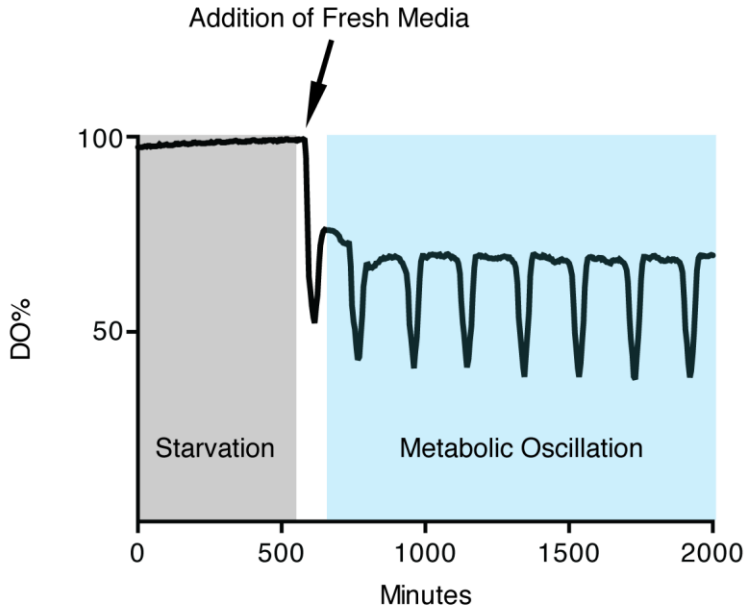

Figure 1-6 – Dissolved Oxygen Trace Through the Yeast Metabolic Cycle

A trace of dissolved oxygen (y-axis) over time (x-axis) through metabolic oscillations. During starvation conditions (grey) dissolved oxygen levels plateau at 100%. Upon the addition of fresh media containing 1% glucose, the culture begins to synchronously undergo respiratory/metabolic oscillations (blue).

Initial studies of transcription in the YMC described three temporally segregated clusters of metabolic activity: Oxidative (Ox), Reductive Building (RB), and Reductive Charging (RC) (Figure 1-7). Ox associated genes are maximally expressed as the culture consumes O_2, while R/B and R/C genes are transcribed as O_2 reenters the culture and subsequently plateaus, respectively (Tu et al. 2005; Tu et al. 2007). Within each category, the genes transcribed reflect the demands facing the culture (Cai and Tu 2012). For instance, the Ox phase is characterized by a burst of ribosome biogenesis, and the genes expressed during Ox are largely involved in this process and amino acid synthesis. Subsequently, in the R/B phase, within which S phase takes place, genes involved in DNA synthesis, DNA repair, and chromatin

assembly exhibit peak expression. Levels of the storage carbohydrate, trehalose, trigger the expression of factors involved in autophagy during the R/C phase (Tu et al. 2005; Tu et al. 2007; Cai et al. 2011; Cai and Tu 2012).

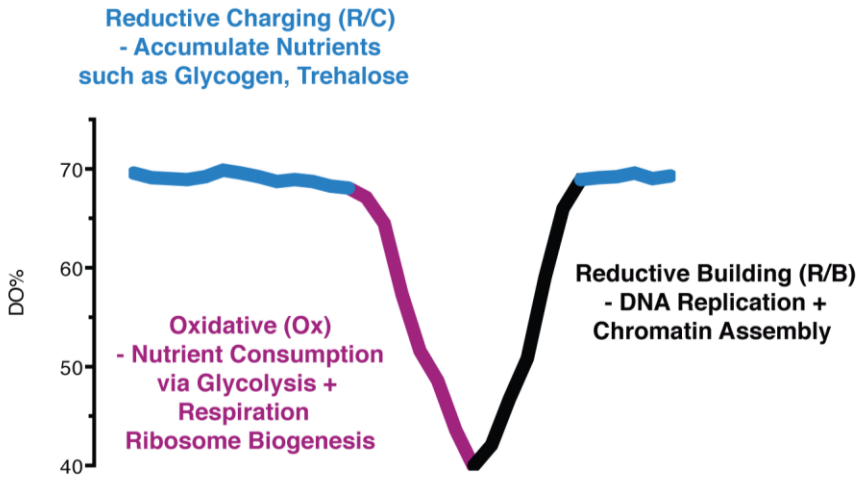

Figure 1-7 – Phases of the Yeast Metabolic Cycle

A trace of dissolved oxygen (DO%) content during a single metabolic oscillation. R/C (blue) occurs when the DO% plateaus, followed by the Ox phase which is coincident with the consumption of oxygen and an observed drop in DO%. The Ox phase is followed by the R/B during which respiration ceases and the culture is no longer actively consuming O_2. The biological processes associated with each phase are described.

The intersection between chromatin and metabolism in the YMC is perhaps best highlighted in the Ox phase, when a spike of acetyl-CoA stimulates the acetyltransferase activity of the SAGA complex (Cai et al. 2011). Acetylation of promoter histones subsequently drives expression of ribosomal and other growth genes. Eventually, acetyl-CoA levels recede as the metabolite is consumed by the citric acid cycle, SAGA driven gene expression drops accordingly, and the Ox phase gives way to R/B. A recent study examining the dynamics of histone post-translational modifications through the YMC found that the appearance of many histone post-

translational modifications at promoters is dynamic, and often highly predictive of transcriptional behavior (Kuang et al. 2014). Further, the histone acetyltransferases and methyltransferases responsible for these modifications are transiently associated with the loci they modify (Kuang et al. 2014).

To examine the dynamics of nucleosome positioning in the YMC we generated 12-paired end MNase-seq libraries of time points taken through a metabolic oscillation. In addition, we generated RNA-seq libraries from the same samples to determine how changes in nucleosome positioning come to bear on transcriptional output.

Chapter 2 - Materials and Methods : Analysis of Chromatin in the YMC

2.1 Introduction

With the goal of determining whether or not changes in transcriptional output throughout metabolic cycles could be correlated to changes in nucleosome positioning we set out to generate nucleosome maps from time-points throughout the cycle.

Once we were able to achieve the metabolic oscillations, twelve time points were taken sampling all three phases of the YMC. Chromatin from each sample was crosslinked with formaldehyde and subsequently digested with Micrococcal nuclease (MNase), an endo/exo-nuclease that preferentially digests naked DNA. Nucleosomal DNA fragments were then prepared for sequencing on the Illumina HiSeq platform (Figure 2-1). Additionally, RNA samples were taken from each sample to generate corresponding RNA-seq data.

2.2 Establishing the Yeast Metabolic Cycle

The strain used achieve metabolic cycling was a prototrophic version of CEN.PK (*MAT*a; *URA3*; *TRP1*; *LEU2*; *HIS3*; *MAL2-8C*; *SUC2;* Strain yIW385). YMC Media was prepared in batches of 10 liters according to the recipe published by Tu et al (Tu et al. 2005). First, 9L of media containing all components except the glucose was sterilized by autoclaving for 1 hour. Subsequently, 1L of 10% glucose

(filter sterilized) was added to bring the volume to 10L. Additionally, 5ml of Antifoam 204 (Sigma) was then added to a final concentration of 0.5ml/L. 1.5L of YMC media was added to the sterile fermenter and the pH of the media was brought to pH 3.4 with 500mM sodium hydroxide. Media inside the fermenter was brought to 30˚C, and a saturated starter culture of 15ml of prototrophic CEN.PK yeast grown in YPD (Yeast extract 10g/L, Bacto peptone 20g/L, 2% Dextrose) was spun down, washed with sterile ddH_20, and added to the media in the fermenter. 1.5L of air/minute was pumped into the culture, and the stirrer was set to 600 RPM and the culture was grown to saturation (OD_{600} =~11) overnight. Under saturation conditions the dissolved oxygen content of the media reaches the upper limit (DO% = 100), as all available carbon has been consumed and respiration is no longer possible. Saturation/starvation conditions were allowed to persist for a minimum of 6 hours before the addition of fresh YMC media containing glucose. To initiate the oscillations, fresh YMC media was added to the culture at a rate of 150ml of per hour. Simultaneously, media was pumped out of the culture to maintain a constant volume of 1.5L. Metabolic oscillations were observed by measuring the dissolved oxygen (DO%) content of the culture. A constant pH of 3.4 was maintained by the automated the addition of 500mM stock Sodium hydroxide.

Table 2-1 – Recipe for 10L of YMC Media

Chemical	**Amount**
$(NH_4)_2SO_4$	50 g
KH_2PO_4	20 g
$MgSO_4 \cdot 7H_20$	5 g
$CaCl_2 \cdot 2H20$	1 g
$FeSO_4 \cdot 7H_20$	0.2 g
$ZnSO_4 \cdot 7H_20$	0.1 g
$CuSO_4 \cdot 5H_20$	0.05 g
$MnCl_2 \cdot 4H_20$	0.01 g
Yeast Extract	10 g
H_2SO_4	5 ml

2.3 Digestion of Chromatin with Micrococcal Nuclease (MNase)

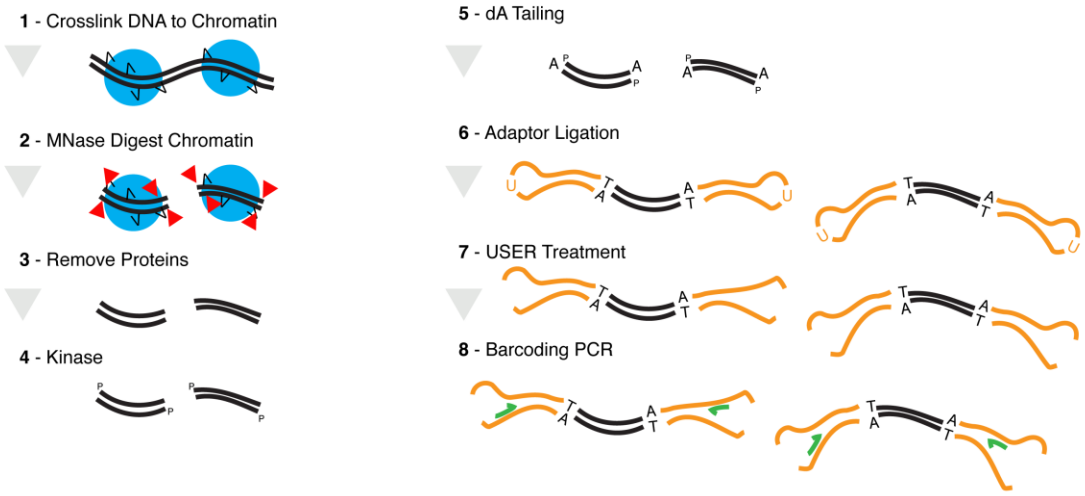

Figure 2-1 – Outline of the MNase-Seq Method

Genomic DNA – black, Nucleosomes – Blue; MNase – Red triangles, NEBNext Adaptors – Yellow, Barcoding oligonucleotides - Green

Twelve time-points were taken throughout a single respiratory oscillation, and cells from each time-point were subjected to cross-linking, zymolyase digestion, and micrococcal nuclease (MNase) digestion (Figure 2-1). At each time-point 5ml of YMC culture was added to a flask containing 43ml of 1X PBS (137mM Sodium chloride, 2.7mM Potassium chloride, 10 mM Disodium hydrogen phosphate, 1.8 mM Potassium dihydrogen phosphate), 1.4ml of freshly added 37% formaldehyde and crosslinked for 10 minute at room temperature with mild agitation. The OD_{600} of the saturated culture is ~10. Diluting these cells ten-fold brings the density back towards more standard conditions for the crosslinking. The cross-linking was subsequently quenched with 5ml of 2.5M glycine. Quenching was allowed to proceed for 5 minutes with mild shaking at room temperature. Cells were subsequently spun down in 50ml

tubes in Sorvall Legend RT+ centrifuge at 3500rpm for 3 minutes, washed with 50ml sterile ddH_20, and frozen at -80˚ until all twelve samples had been collected.

Cell pellets were then thawed on ice, transferred to 1.5ml eppendorf tubes, and resuspended in 950ul of Zymolyase Digestion Buffer (ZDB)(Table 2-2). 50ul of freshly prepared Zymolyase solution (10mg/ml Zymolyase 20T in ZDB buffer) was then added to each sample and digestion proceeded for 45 minutes at 37˚C. Tubes were periodically inverted by hand throughout the course of the Zymolyase digestion to maintain homogeneity. Spheroplasts were then pelleted in the microcentrifuge and washed 1ml of ZDB. Pellets were then gently resuspended 1ml of Spheroplast Digestion Buffer (SDB)(Table 2-2) and again pelleted in the microcentrifuge. The pellets were then gently resuspended in 0.5ml of SDB and 50 units of MNase, and left at room temperature for 3 minutes. Nuclease digestion stopped by the addition of 50ul of 0.5M EGTA, which chelates the calcium required by the enzyme.

To remove RNA from each sample 10ul of 10mg/ml RNaseI was added and RNA degradation was allowed to proceed for 30 minutes at 37˚C. Subsequently, 10ul of 10mg/ml Protinase K was added to each sample and incubated at 42˚C for >3 hours. To reverse the formaldehyde crosslinks, the samples were incubated at 65˚C for >6 hours.

500ul of phenol:chloroform:isoamyl alcohol (25:24:1, pH 7.0) was then added to each sample. The samples were then vortexed and spun down at high speed in a

tabletop centrifuge for 5 minutes. The phenol extraction was repeated a second time, and supernatants were then ethanol precipitated with 1250ul of 100% ethanol and 10ul of 3M sodium acetate. Pellets were precipitated by spinning the samples at high speed in the tabletop centrifuge at 4˚C for 1 hour. The pellets were then washed with 70% ethanol and spun down for 5 minutes at room temperature. The 70% ethanol was then removed and pellets were allowed to air dry for 5 minutes at room temperature. Once the residual ethanol had evaporated the pellets were resuspended in 100ul TE buffer (10mM Tris, 1mM EDTA, pH 8) and incubated at 37˚C for an hour to facilitate the DNA going into solution. DNA concentration of each sample was determined by using a GE NanoVue spectrophotometer.

Table 2-2 – Buffers for generation of spheroplasts and digestion of chromatin with MNase

ZDB	50mM Tris Cl pH 7.5, 1M Sorbitol, 10mM b-Mercaptoethanol
SDB	1M Sorbitol, 50 mM NaCl, 10 mM Tris pH 8, 5 mM MgCl2, 1 mM CaCl2, 1 mM b-Mercaptoethanol, 0.075% NP40.

2.4 Preparation of DNA Sequencing Libraries

To ensure that nucleosomal fragments had blunt ends, the MNase digested DNA was sequentially treated with T4 polynucleotide kinase (PNK) and T4 DNA Polymerase. 500ng from each sample was incubated with 10U of PNK in a reaction containing 1X T4 DNA Ligase Buffer (50mM Tris-HCl, 10mM $MgCl_2$, 1mM ATP, 10mM DTT, pH 7.5), and 1mM dNTPs for 30 minutes at 37˚C (Total volume = 20ul). 3U of T4 DNA Polymerase was then added to each sample to blunt residual overhangs from MNase digestion and incubation was allowed to proceed for 15 minutes at 12˚C.

Subsequently, 1ul of 0.5M EDTA was added to inhibit the activity of T4 DNA Polymerase and the reaction was terminated by incubation at 75˚C for 20 minutes. 1.8 volumes of 'homebrew Magna beads' (1M Tris-HCl pH 8.0, 1mM EDTA pH 8, 1M NaCl, 18% PEG-8000, 0.1% Sera-Mag SpeedBeads [Thermo Scientific])(Rohland and Reich 2012) were added to each reaction to purify the nucleosomal DNA and remove the T4 PNK and T4 DNA Polymerase. DNA was resuspended in 15ul of TE (10mM Tris, 1mM EDTA, pH 8) and dA tailed with Taq DNA polymerase (Catalog #: M0273S).

The dA tailing reactions included 1X Taq Buffer, 1mM dNTPs, and 5U of Taq DNA Polymerase (Total volume = 20ul), and were incubated at 72˚C for 30 minutes. Reactions were then again cleaned with 1.8 volumes of 'homebrew Magna beads' (1M Tris-HCl pH 8.0, 1mM EDTA pH 8, 1M NaCl, 18% PEG-8000, 0.1% Sera-Mag SpeedBeads [Thermo Scientific]) and resuspended in 17.5ul TE (10mM Tris, 1mM EDTA, pH 8).

To the dA tailed products were then ligated dT tailed hairpin adaptors purchased from NEB (NEBNext® Multiplex Oligos for Illumina® [Index Primers Set 1, Catalog #: E7335S]) (Figure 2-1). These adaptors are designed for use on Illumina platforms. Ligation reactions included the 17.5ul of blunt-end nucleosomal DNA, 1X T4 Ligase Buffer (50mM Tris-HCl, 10mM $MgCl_2$, 1mM ATP, 10mM DTT, pH 7.5), and 400U of T4 DNA Ligase (Total volume = 25ul) and were allowed to proceed at room temperature for 1 hour. To remove unligated adaptors and T4 DNA Ligase, 1.8 volumes of 'homebrew Magna beads' (1M Tris-HCl pH 8.0, 1mM EDTA pH 8, 1M NaCl, 18% PEG-8000, 0.1% Sera-Mag SpeedBeads [Thermo Scientific]) was used and the adaptor ligated nucleosomal DNA was subsequently resuspended in 25ul of TE (10mM Tris, 1mM EDTA, pH 8). Half of this product (12.5 ul) was then used in a polymerase chain reaction which served to both amplify and barcode each sample.

PCR reactions included the adaptor ligated substrates, 1uM Universal Oligo (5´-AAT GAT ACG GCG ACC ACC GAG ATC TAC ACT CTT TCC CTA CAC GAC GCT CTT CCG ATCT-3´), 1uM Barcode Addition Oligo (Table 2-3), 3U of USER enzyme (NEB Catalog # M5505S), and 1X KAPA Hot Start Polymerase Mix (KAPABiosystems Kit#: KK2602) (Final volume = 50ul). The USER enzyme is a mixture of Uracil DNA glycosylase and Endonuclease VIII, which catalyzes the excision of uracil from the loop of the hairpin adaptors, and subsequently cleaves the phosphodiester backbone at the resulting abasic site, ultimately opening up the hair-pinned adaptor (Figure 2-1) (Adaptor Sequence : 5´-/5Phos/GAT CGG AAG AGC

ACA CGT CTG AAC TCC AGT C/ideoxyU/A CAC TCT TTC CCT ACA CGA CGC TCT TCC GAT CT-3´).

Ligation products were then incubated in the thermocycler for 15 minutes at 37˚C to allow for USER enzyme activity, followed by 1 minute at 95˚C to activate the KAPA Hot Start polymerase. Adaptor ligated nucleosomal DNA was then amplified/barcoded with 10 cycles of PCR (95˚C – 15 seconds; 65˚C – 15 seconds; 68˚ C – 2 minutes).

PCR amplified products were purified with 1.8 volumes of 'homebrew Magna beads' (1M Tris-HCl pH 8.0, 1mM EDTA pH 8, 1M NaCl, 18% PEG-8000, 0.1% Sera-Mag SpeedBeads [Thermo Scientific]) and resuspended in 20ul of TE (10mM Tris, 1mM EDTA, pH 8). Products were then run on a 1.4% agarose gel and monosomal bands were excised and gel purified with the Qiagen QIAquick Gel Extraction Kit (Cat. No. 28706) as per manufacturer's instructions. Samples were then submitted for sequencing on the Illumina HiSeq platform by the Sloan Kettering Integrated Genomics Operations core facility.

Table 2-3 – Barcode Oligonucleotide Sequences Utilized for MNase-Seq Library Generation

Barcode Index Number/Sample Number	Oligo Sequence	Barcode Sequence
1/1	CAAGCAGAAGACGGCATACGAGATCGTGATGTGACTGG AGTTCAGACGTGTGCTCTTCCGATC-s-T	CGTGA
2/2	CAAGCAGAAGACGGCATACGAGATACATCGGTGACTGG AGTTCAGACGTGTGCTCTTCCGATC-s-T	ACATCG
3/3	CAAGCAGAAGACGGCATACGAGATGCCTAAGTGACTGG AGTTCAGACGTGTGCTCTTCCGATC-s-T	GCCTAA
4/4	CAAGCAGAAGACGGCATACGAGATTGGTCAGTGACTGG AGTTCAGACGTGTGCTCTTCCGATC-s-T	TGGTCA
5/5	CAAGCAGAAGACGGCATACGAGATCACTGTGTGACTGG AGTTCAGACGTGTGCTCTTCCGATC-s-T	CACTGT
6/6	CAAGCAGAAGACGGCATACGAGATATTGGCGTGACTGG AGTTCAGACGTGTGCTCTTCCGATC-s-T	ATTGGC
7/7	CAAGCAGAAGACGGCATACGAGATGATCTGGTGACTGG AGTTCAGACGTGTGCTCTTCCGATC-s-T	GATCTG
8/8	CAAGCAGAAGACGGCATACGAGATTCAAGTGTGACTGG AGTTCAGACGTGTGCTCTTCCGATC-s-T	TCAAGT
9/9	CAAGCAGAAGACGGCATACGAGATCTGATCGTGACTGG AGTTCAGACGTGTGCTCTTCCGATC-s-T	CTGATC
10/10	CAAGCAGAAGACGGCATACGAGATAAGCTAGTGACTGG AGTTCAGACGTGTGCTCTTCCGATC-s-T	AAGCTA
11/11	CAAGCAGAAGACGGCATACGAGATGTAGCCGTGACTGG AGTTCAGACGTGTGCTCTTCCGATC-s-T	GTAGCC
12/12	CAAGCAGAAGACGGCATACGAGATTACAAGGTGACTGG AGTTCAGACGTGTGCTCTTCCGATC-s-T	TACAAG

2.5 RNA-seq Library Preparation

RNA from each time-point was extracted by utilizing the hot phenol method, and libraries were generated with the NEBNext Ultra RNA Library Prep Kit for

Illumina as per manufacturer's instructions (Catalog #E7530L) (Schmitt et al. 1990). Samples were barcoded (Table 2-4) and submitted for sequencing on the Illumina HiSeq platform by the Sloan Kettering Integraged Genomics Operations core facility.

Table 2-4 – Barcode Oligonucleotide Sequences Utilized for RNA-Seq Library Generation

Barcode Index Number/Sample Number	Oligo Sequence	Barcode Sequence
13/1	CAAGCAGAAGACGGCATACGAGATTGTTGACTGTGACT GGAGTTCAGACGTGTGCTCTTCCGATC-s-T	AGTCAA
14/2	CAAGCAGAAGACGGCATACGAGATACGGAACTGTGAC TGGAGTTCAGACGTGTGCTCTTCCGATC-s-T	AGTTCC
15/3	CAAGCAGAAGACGGCATACGAGATTCTGACATGTGACT GGAGTTCAGACGTGTGCTCTTCCGATC-s-T	ATGTCA
16/4	CAAGCAGAAGACGGCATACGAGATGGACGGGTGACTG GAGTTCAGACGTGTGCTCTTCCGATC-s-T	CCGTCC
18/5	CAAGCAGAAGACGGCATACGAGATGTGCGGACGTGAC TGGAGTTCAGACGTGTGCTCTTCCGATC-s-T	GTCCGC
19/6	CAAGCAGAAGACGGCATACGAGATCGTTTCACGTGACT GGAGTTCAGACGTGTGCTCTTCCGATC-s-T	GTGAAA
20/7	CAAGCAGAAGACGGCATACGAGATAAGGCCACGTGAC TGGAGTTCAGACGTGTGCTCTTCCGATC-s-T	GTGGCC
21/8	CAAGCAGAAGACGGCATACGAGATTCCGAAACGTGAC TGGAGTTCAGACGTGTGCTCTTCCGATC-s-T	GTTTCG
22/9	CAAGCAGAAGACGGCATACGAGATTACGTACGGTGAC TGGAGTTCAGACGTGTGCTCTTCCGATC-s-T	CGTACG
23/10	CAAGCAGAAGACGGCATACGAGATATCCACTCGTGACT GGAGTTCAGACGTGTGCTCTTCCGATC-s-T	GAGTGG
25/11	CAAGCAGAAGACGGCATACGAGATATATCAGTGTGACT GGAGTTCAGACGTGTGCTCTTCCGATC-s-T	ACTGAT
27/12	CAAGCAGAAGACGGCATACGAGATAAAGGAATGTGAC TGGAGTTCAGACGTGTGCTCTTCCGATC-s-T	ATTCCT

2.6 Mapping and Processing of MNase-Seq and RNA-seq Reads

The raw FASTQ paired-end reads were mapped back to the *S. cerevisiae* genome (version R64-2-1 2014_11_18) utilizing the Bowtie2 software to generate files in the SAM format (Langmead and Salzberg 2012). The data was filtered for uniquely mapping reads only at this stage. SAM files were then converted into BAM files with SAMtools, and the resulting BAM files were then processed with BEDtools to generate files in the BED format (Li et al. 2009; Quinlan and Hall 2010). MNase-seq data was filtered for reads of length greater than 124bp and less than 176bp, and subsequently processed with the 'improved Nucleosome Positioning from Sequencing' (iNPS) algorithm (version 1.2.0), which identifies peaks of nucleosome occupancy from the individual reads (Chen et al. 2014). RNA-seq data was utilized to calculate RPKM (Reads per Kilobase per Million) for each open reading frame.

2.7 Generation of *snf2*Δ Deletion Strain

Oligonucleotides with homology to the 50bp directly upstream of start codon, and 50bp of homology directly downstream of the stop codon of *SNF2* was used to amplify and target the G418 resistance cassette using pUG6 as the template in a PCR (Table 2-5).

High efficiency LiAc transformations were performed as described below. 50ml of cells were grown in YPD and harvested at an OD_{600} of 0.7. Cells were then washed in 1ml of 100mm LiAc, and subsequently resuspended in 0.5ml of 100ml LiAc. 50ul of this resuspension was then aliquoted to a fresh tube, where the cells

were spun down at high speed for 10 seconds in a tabletop centrifuge and the supernatant removed. To these pelleted cells 240ul of 50% PEG 8000, 36ul of 1M LiAc, 10ul of 10mg/ml denatured salmon sperm DNA, 50ul of deletion PCR product, and 24ul of H_20 were added sequentially. This mixture was then vortexted for 30-60 seconds and incubated at 42˚C for 45 minutes. These cells were then plated on non-selective YPD plates and allowed to grow overnight. Following one day of growth, cells were replica-plated to selective plates and allowed to grow for three days at 30˚C. Colonies grown on selective media were transferred to a second selective media plate. Single colonies from the second round of selection were then grown in YPD (Yeast extract 10g/L, Bacto peptone 20g/L, 2% Dextrose), genomic DNA was prepared from these samples via phenol extraction and they were checked for integration of the markers at the SNF2 locus by PCR using SNF2 Test and G418 Test oligonucleotides (Table 2-5).

Table 2-5 – Oligonucleotide Sequences Utilized for SNF2 deletion

SNF2 KO Forward	ATGAACATACCACAGCGTCAATTTAGCAACGAAGAGGTCAACCGCTGCTATTTAAGagctgaagcttcgtacgc
SNF2 KO Reverse	TGTTTGTCTACGTATAAACGAATAAGTACTTATATTGCTTTAGGAAGGTAgcataggccactagtggatctg
SNF2 Test	CTTCCTCGCACATTTCTGCTTCTGCTTCC
G418 Test	CTCGAAACGTGAGTCTTTTCCTT

Chapter 3 - Remodeling of Promoter Chromatin At Promoters Governs Expression During the Yeast Metabolic Cycle*

3.1 Summary

Nucleosome repositioning at gene promoters is a fundamental aspect of the regulation of gene expression. Yet the extent to which nucleosome repositioning is utilized within eukaryotic genomes is poorly understood. While many genome-wide maps of nucleosome positions in budding yeast have been published, the majority of these studies sample asynchronous populations of logarithmically growing cells (Lee et al. 2007; Whitehouse et al. 2007; Field et al. 2008; Mavrich et al. 2008; Shivaswamy et al. 2008). Utilizing these experimental conditions, low frequency shifts or subtle in the population will be lost, or potentially disregarded as "noise". In fact, many nucleosomes in *S. cerevisiae* have been designated as being "fuzzy", due to an inability to precisely map them (Jiang and Pugh 2009a). The precise positions of promoter nucleosomes are of great interest to us, in particular, as a shift of several base pairs can potentially have profound effects on transcriptional output by either allowing or preventing access to transcription factor binding sites.

Budding yeast maintains many ATP-dependent chromatin remodeling factors such as SWI/SNF, ISWI, Chd1, RSC, Swr1, and Ino80, and the activities of these factors are often focused on promoter nucleosomes (Whitehouse and Tsukiyama 2006;

* Published previously in modified form: Nocetti N, Whitehouse I. (2016). Nucleosome Repositioning Underlies Dynamic Gene Expression. *Genes Dev*. 30(6)660-672

Whitehouse et al. 2007; Hartley and Madhani 2009; Tirosh et al. 2010; Gkikopoulos et al. 2011; Yen et al. 2012; Parnell et al. 2015). SWI/SNF, ISWI, Chd1, Isw2 and Ino80 maintain the ability to slide nucleosomes along template DNA (Whitehouse et al. 1999; Zofall et al. 2006; Udugama et al. 2011; Lieleg et al. 2015), while RSC functions to evict nucleosomes from chromatin (Lorch et al. 2006). Swr1 functions to actively replace histone H2A with the Htz1 histone variant (Krogan et al. 2003; Kobor et al. 2004), while Ino80 maintains the ability to perform the reverse reaction in a second activity (Papamichos-Chronakis et al. 2011).

The typical experimental approach for attributing remodeling events at a given promoter to a specific remodeling factor often involves deleting the remodeling factor and assaying for differences in nucleosome positioning in its absence. This type of experiment is often supplemented with ChIP to determine whether or not the remodeling factor in question is in fact present at the locus under wildtype conditions (Whitehouse et al. 2007; Yen et al. 2012). While these types of experiments can be very powerful in determining the roles of various remodeling factors, and defining their target sets of genes, they are not without caveats. First, individual nucleosomes may be subject to remodeling by multiple different remodeling factors. Many remodeling factors exhibit significant redundancy, as is the case for the trio of ISWI, Chd1, and Isw2, and the duo of Ino80 and SWI/SNF. (Barbaric et al. 2007; Gkikopoulos et al. 2011). Therefore, one might not observe a significant alteration in nucleosome positioning in the absence of a single of these factors, though in an unperturbed system the factor in question could play a significant role in establishing

or maintaining nucleosome positions. Additionally, remodeling factors can act antagonistically, as is the case for RSC and ISWI (Parnell et al. 2015). Hence, inactivating a single remodeler can potentially enhance the activity of another, further confounding the interpretation of the results.

With respect to using deletion strains to study the contribution of chromatin remodeling on gene expression, deletion of chromatin remodeling factors will often have pleiotropic effects on transcription and the determining whether an effect is direct or indirect can be difficult, particularly when performing genome-wide analyses. As noted earlier, mutations impairing the ability of SWI/SNF to remodel chromatin lead to both widespread transcriptional activation and repression at various loci (Figure 1-5).

To examine the interplay between nucleosome positioning dynamics and cycles of transcriptional activation and repression we sought a system in which deletion or mutation of ATP-dependent remodeling factors would not be required. Additionally, the system would exhibit significant transcriptional dynamics, and be highly synchronized such that subtle shifts in nucleosome shifts would become quantifiable; two qualities a logarithmically growing culture lacks. Presented in this chapter is a comprehensive analysis of nucleosome positions as budding yeast transit through the Yeast Metabolic Cycle (YMC), a system that demonstrates all of the aforementioned criteria.

The data show that extensive nucleosome repositioning occurs at thousands of promoters as genes are activated and repressed through metabolic oscillations. During activation, nucleosomes are positioned to allow sites of general transcription factor binding and transcription initiation to become accessible. We find that the extent of nucleosome shifting is generally related to DNA sequence properties and presence of TAF1 at a promoter. Nucleosome positions at TAF1-enriched (TFIID) promoters (Rhee and Pugh 2012) are generally fixed throughout the course of the YMC, though exceptions to this can be identified. Conversely, TAF1-depleted (SAGA) promoters exhibit highly dynamic promoter chromatin, with access to general transcription factor binding sites being predictive of transcriptional output.

Further, we find that a class of genes required for growth experience acute nucleosome shifting as cells begin to respire. Significantly, our data suggest that the ATP-dependent chromatin-remodeling factor SWI/SNF plays a fundamental role in nucleosome repositioning and the expression of growth genes. We also find that histone H2A variant, Htz1, accumulation is anti-correlated with promoters exhibiting the most significant nucleosome positioning dynamics. Additionally, nucleosome organization changes extensively in concert with phases of the cell cycle, with large, regularly spaced nucleosome arrays being established in mitosis. Collectively the data and analysis provide a framework for understanding nucleosome dynamics in relation to fundamental DNA dependent transactions.

3.2 Results

3.2.1 - +1 Nucleosome Dynamics Correlate Highly With Transcriptional Output

To investigate the role of nucleosome remodeling in regulating transcription dynamics through metabolic oscillations we established the YMC according to previously described methods (Tu et al. 2005). We observed cycles with a ~3.2 hour period length, and harvested samples in 10, 20, or 40 minute intervals. Cells from twelve time points were formaldehyde cross-linked, spheroplasted and then chromatin was digested with Micrococcal nuclease (MNase) (Figure 3-1, Figure 3-2). We then isolated mononucleosme sized DNA from each of the samples was to generate barcoded paired-end libraries for sequencing on the Illumina HiSeq platform. Paired-end reads between 125-175bp were then processed with the iNPS software, a peak-calling algorithm, to annotate nucleosomes in each time point (Chen et al. 2014). Additionally, barcoded RNA-seq libraries were generated from the same time points utilized to generate the MNase libraries. The resulting RNA-seq data was processed with a k-means clustering algorithm (Cluster 3.0; k = 4; 1,000 Runs), and we were able to observe three superclusters of expression corresponding to the Ox, RB, and RC clusters initially described by Tu et al (Tu et al. 2005) (Figure 3-3).

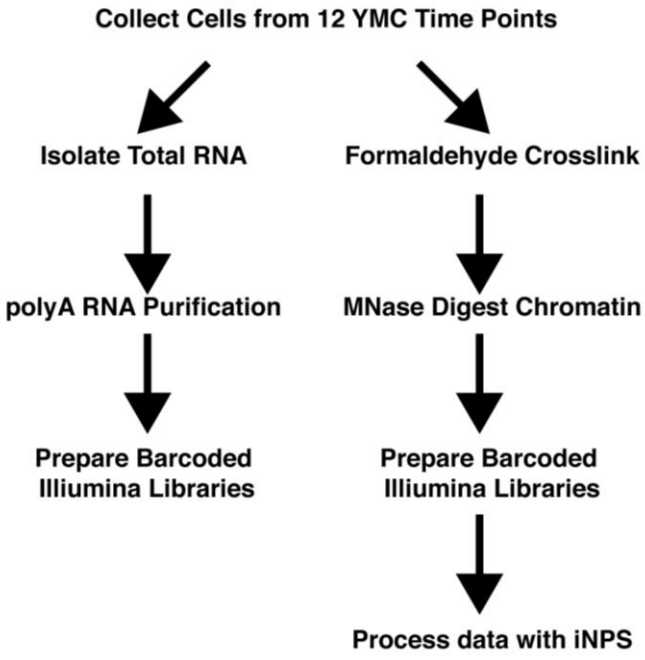

Figure 3-1 – Outline for Raw Data Generation

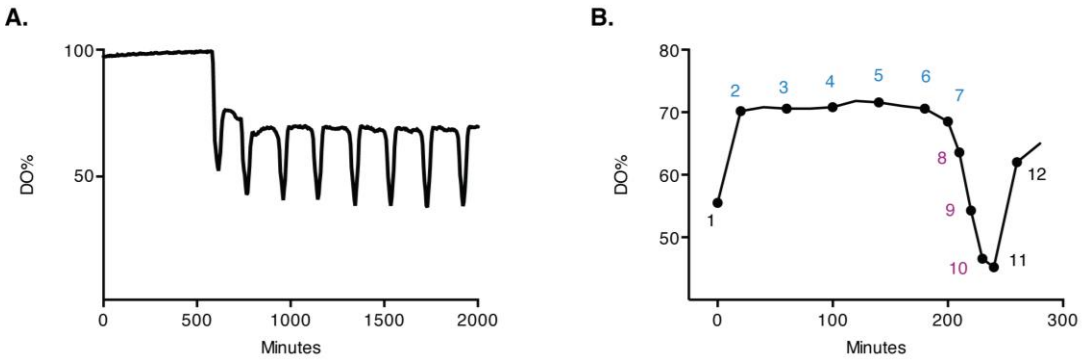

Figure 3–2-A. DO% trace illustrating robust metabolic oscillations. **B.** DO% trace of the cycle sampled for MNase-seq and RNA-seq. Samples 1, 11, and 12 (black text) represent the RB phase. Samples 2-7 (blue text) represent the RC phase. Samples 8-10 (purple text) represent the Ox phase.

Upon analyzing the MNase-seq data from the twelve time points, we found instances highly dynamic chromatin architecture at many promoters. For example, at the *TEA1* locus, we observe significant movement of the +1 nucleosome as the cycles progresses (Figure 3-4). *TEA1* encodes a zinc cluster transcriptional activator involved in Ty element transcription (Gray and Fassler 1996). At time points when *TEA1* exhibits basal levels of transcription, (e.g. time point 1) the +1 nucleosome appears to completely occlude the mapped binding site for TFIIB mapped by ChIP-exo (Rhee and Pugh 2012) and the TSS (Pelechano et al. 2013). The nucleosome then gradually slides towards its furthest downstream at time point 9 - coincident with the Ox phase.

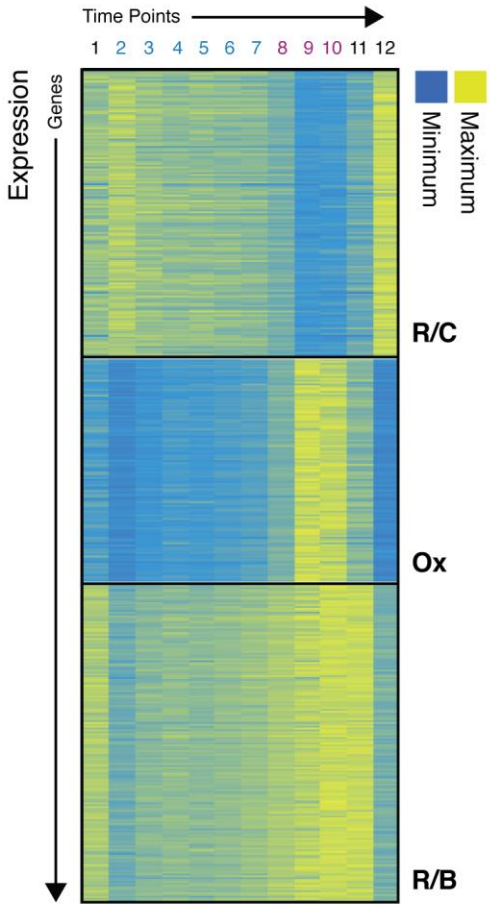

Figure 3-3 – Distinct Waves of Transcription During the YMC

K-means clustering of normalized RNA-seq data from time points taken through the YMC reveals three waves of transcription corresponding to the R/C, Ox, and R/B phases. The time point with the maximum RPKM value for each gene is set to 1 and all other time points are represented as a fraction of that value. Genes are arranged vertically and time points are arranged horizontally.

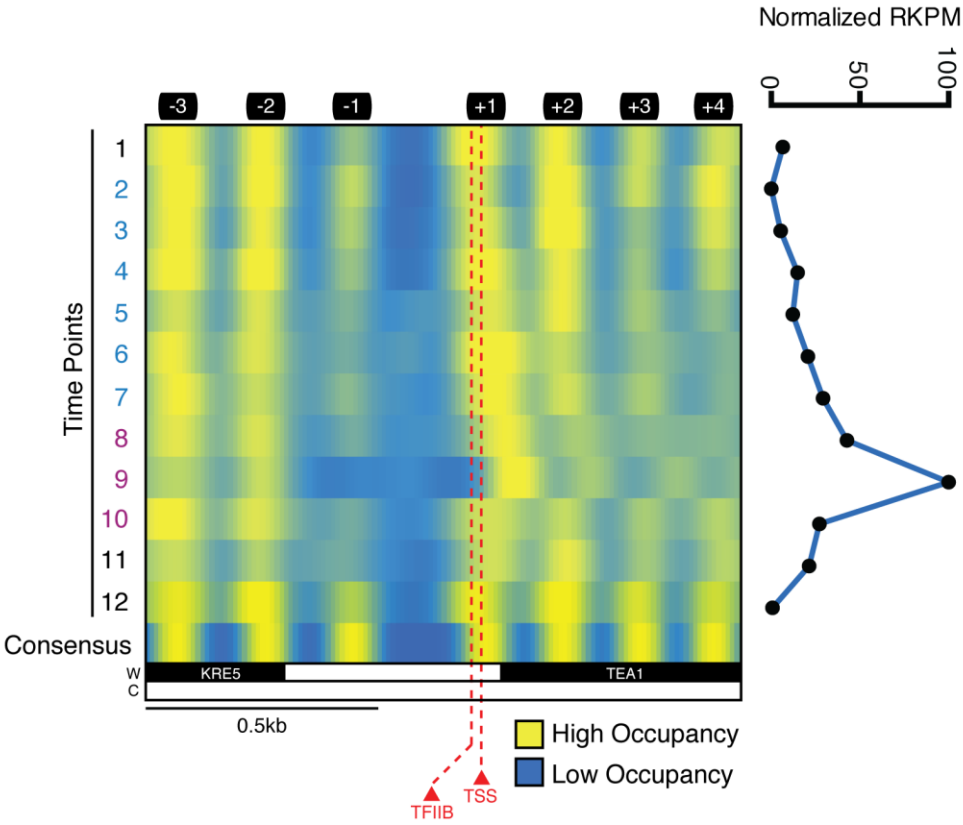

Figure 3-4 - Promoter Chromatin Dynamics at the TEA1 locus

Heat-map illustrating the positions of nucleosomes at the TEA1 locus through the YMC. Time points are arranged vertically, and consensus nucleosome positions are shown in the bottom row (Jiang and Pugh 2009a). Positions of the TSS (Pelechano et al. 2013) and TFIIB binding site (Rhee and Pugh 2012) are denoted with dotted red lines. Normalized RPKM values corresponding to each time point are shown in the right panel. Maximum transcriptional output is represented as an RPKM value of 100.

Strikingly, this shift is accompanied by a spike in transcription at time point 9, as evidenced by RPKM (Reads per Kb per Million) values derived from the RNA-seq data. Both the TSS and TFIIB binding site at this locus become accessible upon the downstream shift of the +1 nucleosome, suggesting that occlusion of these sites is responsible for transcriptional repression of *TEA1* (Figure 3-4). This is the first evidence that *TEA1* promoter chromatin is subjected to dynamic remodeling.

The positioning of the +1 nucleosome is widely recognized to play an influential role in the regulation of transcriptional activity (Wu and Winston 1997; Steger et al. 2003; Whitehouse and Tsukiyama 2006; Lorch et al. 2011; Rando and Winston 2012). In order to characterize the degree to which +1 nucleosomes are repositioned through the metabolic cycle, we determined the positions of +1 nucleosomes at all twelve time points. +1 nucleosomes were defined as the first nucleosome dyad encountered in 100bp windows ranging from 20bp upstream of the TSS to 80bp downstream of the TSS. Genes for which we were unable to assign +1 nucleosomes were excluded from subsequent analysis. Promoters were then ranked by the variability in positioning of their +1 nucleosome by taking the standard deviation of dyad positions (Figure 3-5). Strikingly, we find that +1 nucleosomes shift by >50bp at many promoters (Figure 3-5 A,B). By plotting the dyads of the furthest upstream and downstream +1 nucleosomes against the TSS of 350 genes with the greatest variability, we find that dyads typically occlude the transcription start sites at their most upstream positions, in keeping with what we observed at the TEA1 locus (Figure 3-5 A,B). We term this class of promoters 'Dynamic' (Figure 3-5 B). At the 350 promoters where we observe the smallest shift in +1 positioning (in some cases no change in position at all), which we refer to as 'Static', the dyads are generally found ~50bp downstream of the TSS.

Based on the observation that positioning of the +1 nucleosome strongly predicted the transcriptional activity of TEA1, we assumed that the shift of the most dynamic nucleosomes would be correlated to the transcriptional activity of their associated genes. To investigate this, we analyzed RNA-seq data from each time-point; each gene was assigned an RPKM and the RPKM values for each gene were normalized to a maximum value of 1. In general, we find a clear correlation between Dynamic +1 nucleosomes and genes whose RNA expression exhibits the greatest dynamic range and RNA expression values are highest when nucleosomes are furthest downstream of the TSS (Figure 3-5 A,D). Correspondingly, expression from promoters which exhibit more stable +1 nucleosomes positions does not vary significantly when nucleosomes adopt upstream or downstream positions (Figure 3-5 A,C,D).

To ensure that we had achieved uniform digestion of promoter chromatin among the twelve time points, we plotted the upstream edge of each read, oriented with respect to its associated gene, against the length of that read. This analysis reveals no significant degree of variation in digestion among the samples that would confound our findings (Figure 3-6).

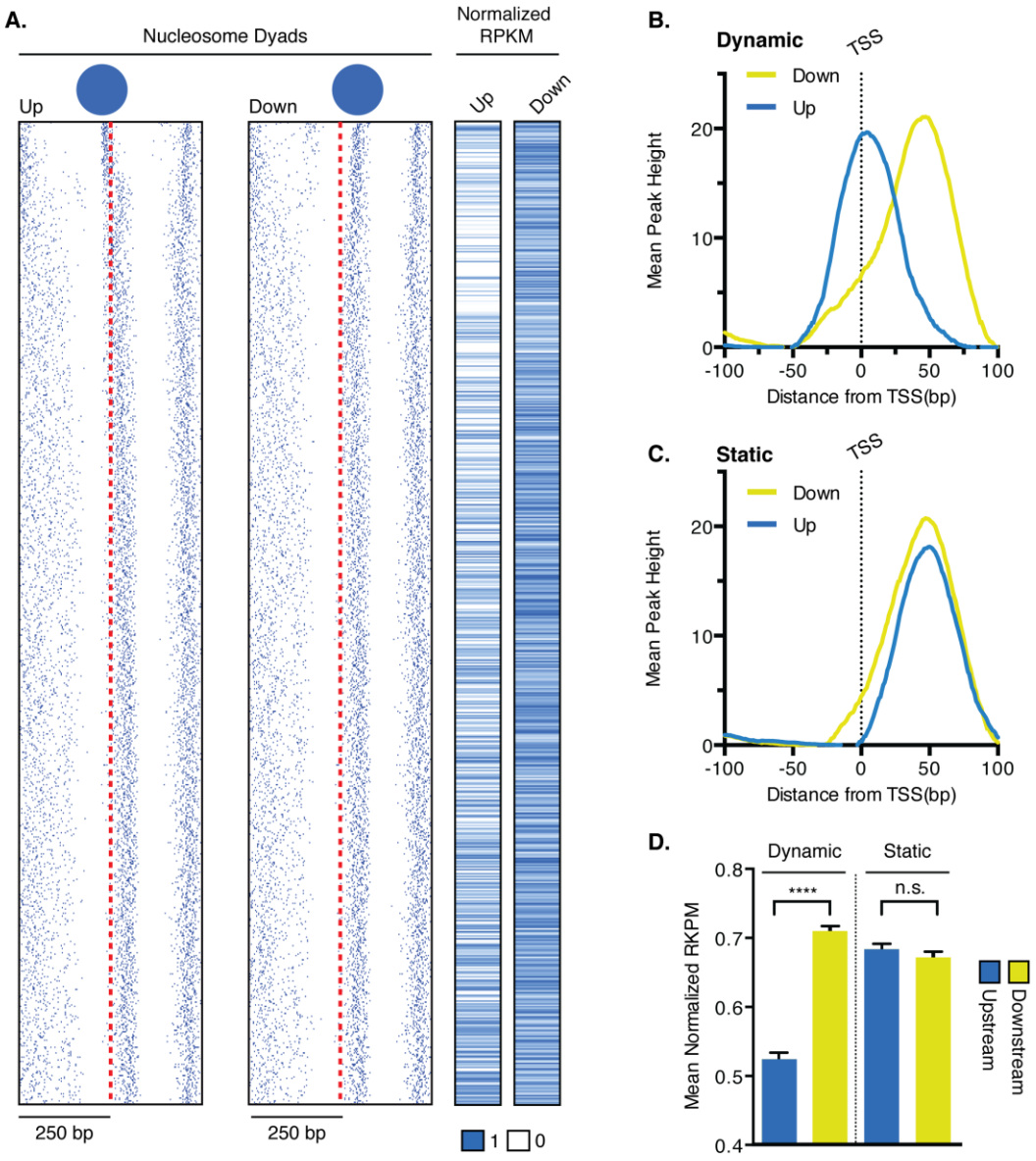

Figure 3-5 – Promoters Ranked by +1 Nucleosome Shift

A. Nucleosome dyads when +1 nucleosomes occupy their furthest upstream (Up) and downstream (Down) positions relative to TSSs (Left two panels). Heat-maps of normalized RKPM values when +1 nucleosomes adopt their furthest upstream and downstream positions (right two panels). **B-C.** Dyads of +1 nucleosomes at promoters classified as Dynamic (**B**) and Static (**C**). **D.** Normalized expression data corresponding to Dynamic and Static positions when nucleosomes occupy upstream (Blue) and downstream (yellow) positions.

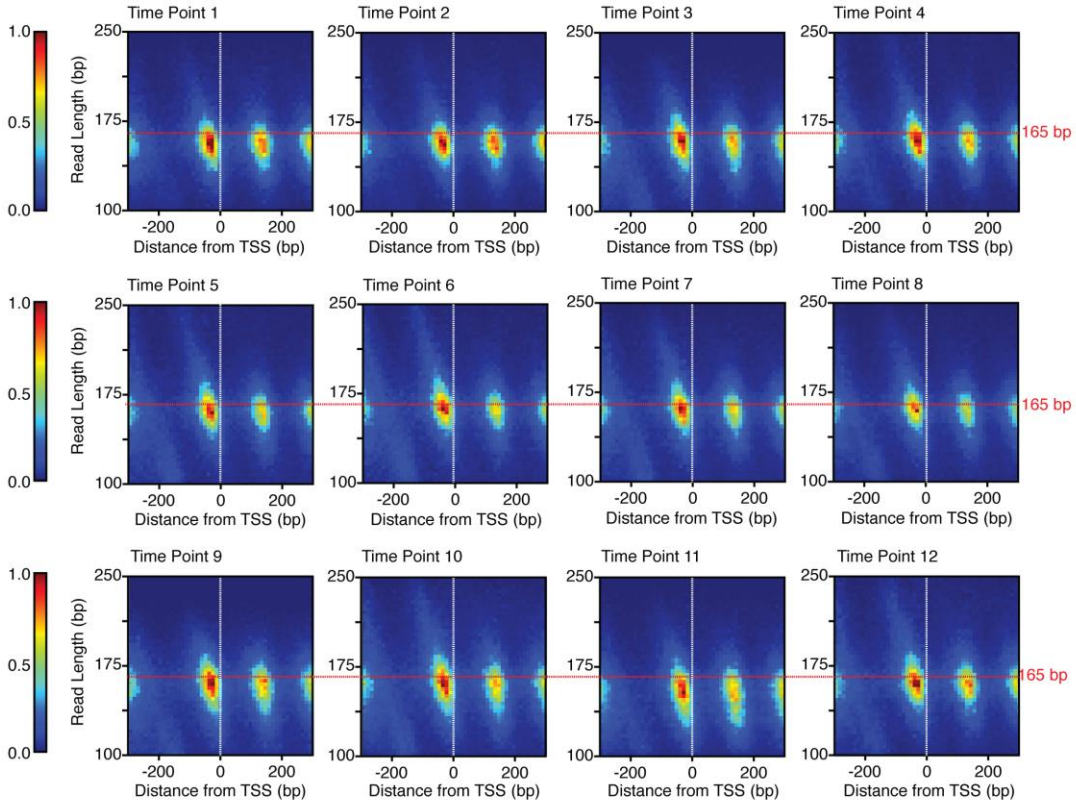

Figure 3-6 – Analysis of MNase cut site and Read Length at Promoters

3.2.2 Dynamic +1 Nucleosomes Are Biased Towards Genes Belonging to the Ox Cluster

Having established a two extreme promoter types with respect to nucleosome repositioning, Dynamic and Static, we investigated whether either type is enriched for genes belonging to the RB, RC, or Ox phases. To do this we calculated the Log_2(Observed/Expected) ratio for Static and Dynamic promoters belonging to each metabolic category. Dynamic promoters are markedly enriched for Ox genes, while Static promoters bear an enrichment for the genes maximally expressed in the RB

phase (Figure 3-7 A). This finding led us to more specifically investigate the relationship between the positioning of +1 nucleosomes and the expression of Ox genes.

Isolating only the Ox cluster, we observe a pronounced correspondence between repositioning of the +1 nucleosome and the burst of maximal transcriptional output (Figure 3-7 B). Both maximal expression and downstream positioning of nucleosomes occurs at time point 9, while nucleosomes shift furthest upstream at time point 12, when the Ox cluster is transcriptionally repressed. While we do observe movement of +1 nucleosomes of promoters outside of the Ox cluster, the uniform behavior of Ox related genes is unique.

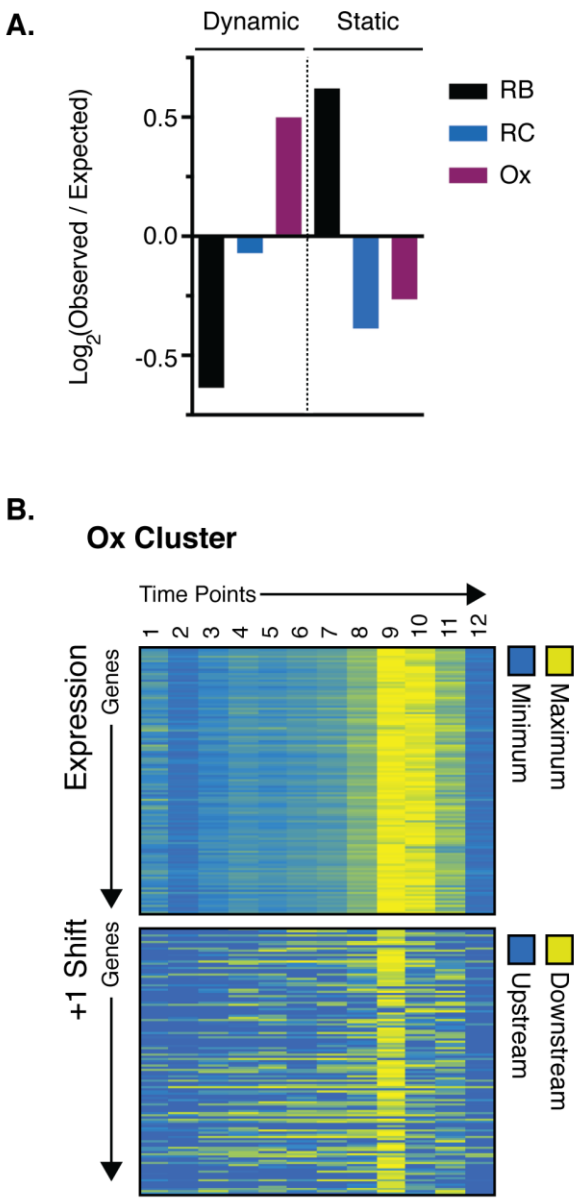

Figure 3-7 – +1 Nucleosome Shifting of Ox Cluster

A. Log2 of observed over expected ratios indicating the overlap of each transcriptional cluster (R/B, R/C, and Ox) with promoter nucleosome classes (Dynamic and Static). **B.** Heat-map of normalized expression of the Ox cluster through the metabolic cycle (top panel). Heat-map of normalized +1 nucleosome shifts of Ox associated genes (bottom panel). Genes are arranged in the same order in both heat-maps.

3.2.3 - SAGA Promoters Exhibit Highly Dynamic Promoter Architecture Corresponding to Transcriptional Activity

Promoters in *S. cerevisiae* broadly belong to one of two categories: those regulated by SAGA or TFIID (Huisinga and Pugh 2004; Rhee and Pugh 2012). SAGA promoters are highly dynamic in both expression and chromatin structure, whereas TFIID promoters exhibit less dynamic levels of expression chromatin reconfiguration (Rando and Winston 2012). Further, each of these classes exhibits a unique relationship between GTFs and +1 nucleosomes, as demonstrated by study utilizing ChIP-exo (Rhee and Pugh 2012). GTFs at TFIID promoters are found a fixed distance upstream of the +1 nucleosome; by contrast, the same GTFs are typically bound throughout the body of the +1 nucleosome at SAGA promoters. These observations suggest that there may be competition between nucleosomes and GTFs for binding at SAGA promoters, as was proposed by the authors (Rhee and Pugh 2012).

We find that genes belonging to the three YMC classes defined by Tu et al. which exhibit metabolic cycling, are typically TAF1-depleted (SAGA) promoters, while minimally-cycling genes are enriched for TFIID (Figure 3-8). In keeping with the known association of SAGA regulated promoters with dynamic chromatin structure and robust gene expression states, we find that Dynamic promoters are often depleted for TAF-1 and therefore likely regulated by SAGA (Figure 3-8 B). Next, we probed the relationship between GTF binding, nucleosome repositioning and gene transcription. The RNA transcript levels of each gene were ranked from maximum (i) to minimum (xii) +1 nucleosomes were plotted in relation to mapped TFIIB binding

sites (Rhee and Pugh 2012) for either SAGA (TAF-1 depleted) or TFIID (TAF-1 enriched) promoters (Figure 3-9). The +1 nucleosomes of TFIID promoters remain in the same position independent of transcriptional activity. In contrast, when SAGA genes are at their lowest expression level, +1 nucleosomes frequently occupy (an likely occlude) TFIIB binding sites; yet, when maximally induced, +1 nucleosome configuration at SAGA promoters is almost indistinguishable from TFIID promoters (Figure 3-9). Thus, transcriptional repression of SAGA regulated genes is likely the result of the +1 nucleosome preventing assembly of the PIC, which is relieved by the nucleosome repositioning downstream to allow for transcriptional activation.

Additionally, we utilized the non-normalized RPKM data to examine the average dynamic range of expression associated with TAF1-Depleted and TAF1-Enriched promoters through the YMC. This analysis was performed for the three transcriptional superclusters, as well as non-cycling promoters, separately. We find that TAF1-Depleteted promoters are much more highly expressed than their TAF1-Enriched counterparts or promoters for which no TAF1 designation has been assigned. Further the average range of expression is the widest for TAF1-Enriched promoters belonging to each the Ox, RB, and RC clusters (Figure 3-10).

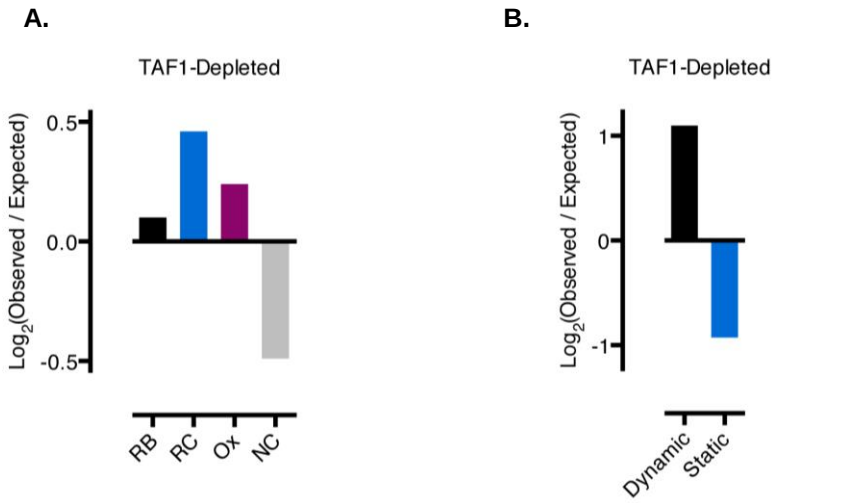

Figure 3-8 – Enrichment of YMC Transcript Clusters for TAF1-Depleted Promoters

A. Log2 of Observed/Expected ratio of TAF1-Depeleted promoters belonging to RB, RC, Ox, and non-cycling (NC) clusters. **B**. Log2 of Observed/Expected ratio of Dynamic and Static promoters among TAF1-Depleted promoters.

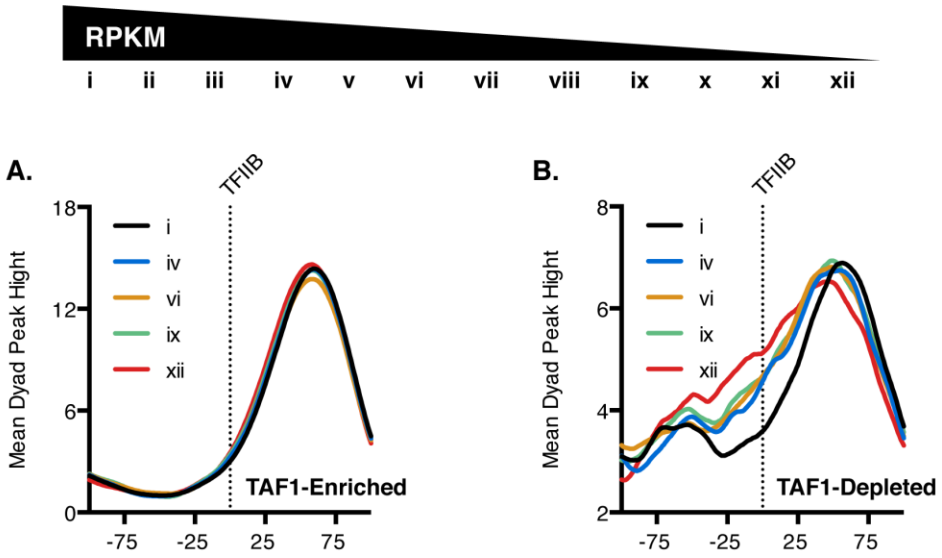

Figure 3-9 – Nucleosome Positioning With Respect to Transcriptional Output

A. Nucleosome dyad positions at TAF1-Enriched (TFIID) promoters at various levels of transcriptional activity. i – Maximal Expression ; xii – Minimal Expression. **B.** Nucleosome dyad positions at TAF1-Depleted (SAGA) promoters at various levels of transcriptional activity. Descending RPKM values associated with roman numeral illustrated above.

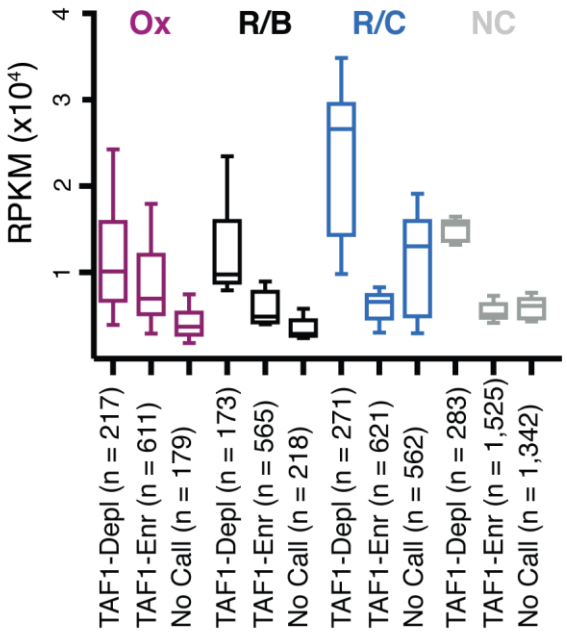

Figure 3-10 – Average Dynamic Ranges of Transcriptional Output Associated with TAF1-Enriched and Depleted Promoters

3.2.4 - DNA sequence elements correlated with Dynamic and Static Promoters

Nucleosome positioning *in vivo* is dictated by a complex interplay between ATP dependent chromatin remodeling enzymes, DNA sequence and DNA binding proteins (Zhang et al. 2009; Gkikopoulos et al. 2011; Zhang et al. 2011). Given that DNA sequence is a very strong determinant of the NDR, we investigated whether the nucleosome repositioning is related to the intrinsic propensity of the DNA sequence to favor or disfavor nucleosomes. We examined the predicted nucleosome occupancies as calculated by Kaplan et al (Kaplan et al. 2009) and plotted predicted occupancy relative to the TSS at the Dynamic or Static classes of promoters. This analysis

revealed a clear bias in promoter DNA composition: Dynamic promoters exhibit a severe dip in predicted occupancy upstream of the TSS (Figure 3-11 A). To examine if this feature was only to be found at dynamic promoters, we ranked genes according the degree of +1 shift and then segmented the predicted occupancy into quintiles. As Figure 3-9 illustrates, stretches of promoter DNA with lowest intrinsic nucleosome affinity are found upstream of the TSS at high shifting promoters, but this signal gradually transitions downstream of the TSS at static promoters (Figure 3-11 B). Thus, the degree of the +1 nucleosome shift, the use of SAGA or TFIID and the dynamic range of gene expression, all bear a clear relation to properties of the underlying DNA sequence relative to the TSS.

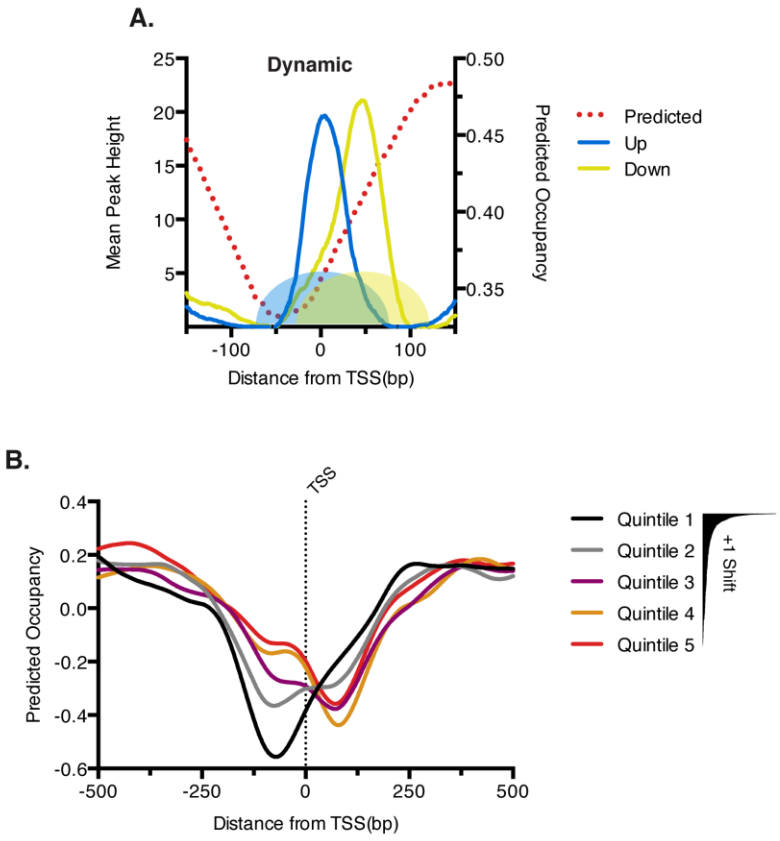

Figure 3-11 – Analysis Intrinsic Affinity of Promoter DNA for Nucleosomes and Nucleosome Positioning in the YMC

A. Furthest upstream and downstream positions of +1 nucleosome positions of Dynamic promoters are shown. Also shown is the mean predicted occupancy of promoter DNA at these loci (Segal et al. 2006). **B.** Promoters were segregated into quintiles based on the standard deviation of +1 positions.

3.2.5 - Differences in Nucleotide Content at Static and Dynamic Promoters

Sequence determinants other than transcription factor binding sites have also been shown to influence the strength of a promoter (Lubliner et al. 2013; Lubliner et al. 2015). Recently, T-richness was shown to be highly predictive of maximal promoter activity. This was shown to be true for promoters exhibiting both inducible and constitutive expression. High levels of T-richness upstream of the TSS correlate with high maximal transcriptional output, presumably due to effects on rate-limiting steps downstream of RNAPII recruitment. Further, at constitutively expressed T-rich promoters, predicted nucleosome occupancy based on intrinsic DNA affinity is in good agreement with observed *in vivo* occupancy. However, there is a significant discrepancy between predicted and observed nucleosome occupancy at T-rich inducible promoters (Lubliner et al. 2013). This suggests that although recruitment of RNAPII is regulated primarily by chromatin architecture, the subsequent events involved in transcription initiation are highly context dependent.

Examining mean nucleotide content at Dynamic promoters, we find that these loci are slightly A-rich around TSSs, with a stretch of T-rich sequence further upstream. This profile most closely resembles promoters with medium E_{max} (maximal activity level) scores (Lubliner et al. 2013) (Figure 3-12 A,B). Mean nucleotide content at Static promoters exhibits no significant stretches of A or T-richness, and more closely resembles promoters with low E_{max} score (Figure 3-12 C,D). Accordingly, we find that the average max expression level of Dynamic promoters is greater than that of Static promoters (Figure 3-12 E). However, neither promoter class

exhibits a dip in GC content downstream of the TSS, as is characteristic of promoters with the highest maximal activity levels.

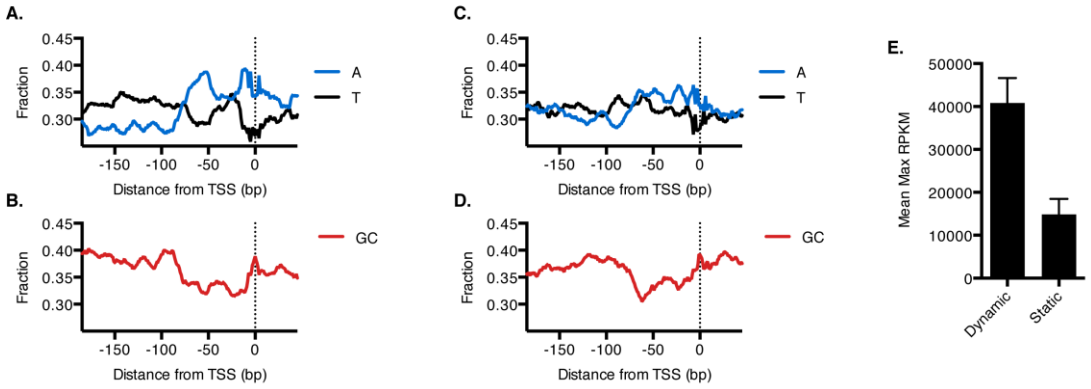

Figure 3-12 – Nucleotide Content at Dynamic and Static Promoters

A-B. A-richness (**A**) T-richness (**A**), and GC-richness (**B**) of Dynamic Promoters. **C-D.** A-richness (**C**), T-richness (**C**), and GC-richness (**D**) of Static promoters. **E.** Average of Maximum RKPM values of Dynamic and Static promoters. Error bars represent the SEM.

3.2.6 - Role of Chromatin Remodeling Factors and Htz1 in Governing +1 Shifts

The periodic patterns of gene expression of the YMC are uncovered by the culture conditions; yet, periodic gene expression programs are an intrinsic property of cellular growth (Silverman et al. 2010). Although populations of yeast cells cultivated in batch display no apparent gene expression synchrony, individual cells within a population can be observed to follow the periodic gene expression programs revealed by the YMC (Silverman et al. 2010). Therefore, experiments to map the occupancy of histone modifications and chromatin remodeling enzymes performed in batch cultures will report average occupancy across the phases of the YMC.

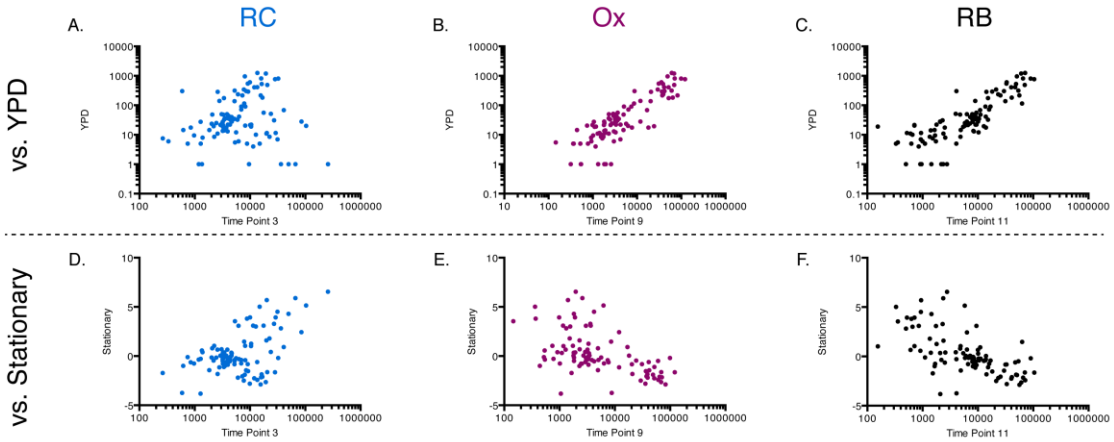

Figure 3-13 – Comparison of Transcriptional Landscape of Logarithmically Growing and Stationary Yeast with of Phases of the YMC

A-C. Comparison of expression of 75 sentinel genes (Tu et al. 2005) belonging to each transcriptional supercluster, R/C (**A**), Ox (**B**), and RB (**C**) compared to logarithmically growing yeast in YPD media (Nagalakshmi et al. 2008). **D-F**. Comparison of expression of 75 sentinel genes (Tu et al. 2005) belonging to each transcriptional supercluster, R/C (**D**), Ox (**E**), and RB (**F**) compared to stationary phase yeast (Gasch et al. 2000).

To understand whether ChIP data from asynchronous cultures would be informative for our analysis of nucleosome repositioning during the YMC, we compared the expression of a subset of periodic genes with the expression of the same gene set in an asynchronous log-phase culture. This analysis revealed that log-phase cultures are more closely correlated with the Ox and R/B phases (Figure 3-13), which is as logical as these cell populations are in rapid growth. Since we find that the majority of nucleosome repositioning occurs during the OX phase.

First, we utilized recently published data from Weiner et al., which contains high-resolution genome-wide location maps of the histone variant Htz1 and numerous histone modifications. Strikingly, we observe clear anti-correlation between Htz1 occupancy and the shift of the +1 nucleosome (Figure 3-14); consistent with this,

'Static' promoters exhibit significantly more H4K5ac, H4K8Ac, and H4K12ac than their 'Dynamic' counterparts (Figure 3-14). These findings are in excellent agreement with previous findings as H4K5/8/12ac have been shown to facilitate the incorporation of Htz1 into chromatin by Swr1 (Altaf et al. 2010; Ranjan et al. 2013) and Htz1 was shown previously to be enriched at TFIID regulated genes (Zhang et al. 2005). Other PTMs display similar levels of enrichment at both classes of promoters.

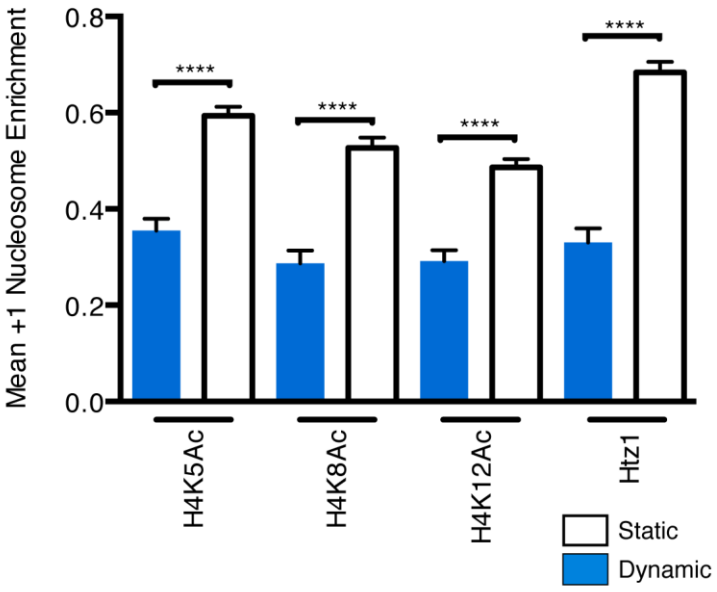

Figure 3-14 – Enrichment of Htz1 and Histone H4 Acetylation at Static +1 Nucleosomes

Enrichment of H4K5Ac, H4K8Ac, H4K12Ac, and Htz1 (Weiner et al. 2015) at Static (white) and Dynamic (blue) +1 Nucleosomes.

To examine which chromatin remodeling factors might be responsible for remodeling +1 nucleosomes through the YMC we utilized data from Yen et al, in which promoters were classified as being bound by components of remodeling complexes Ino80 (Arp5, Ino80) Isw1a (Ioc3), Isw1b, (Ioc4,) Isw1, Isw2, RSC (Rsc8) and SWI/SNF (Snf2) as assayed by ChIP (Yen et al. 2012). We calculated the shifts of

+1 nucleosomes for promoters both bound and not bound by each factor (Figure 3-15). We observe no significant difference in the degree of +1 shifts for promoters bound by Arp5, Ioc3, Ioc4, Rsc8, indicating that these factors are likely not involved in dynamic remodelling of +1 nucleosomes through metabolic cycles.

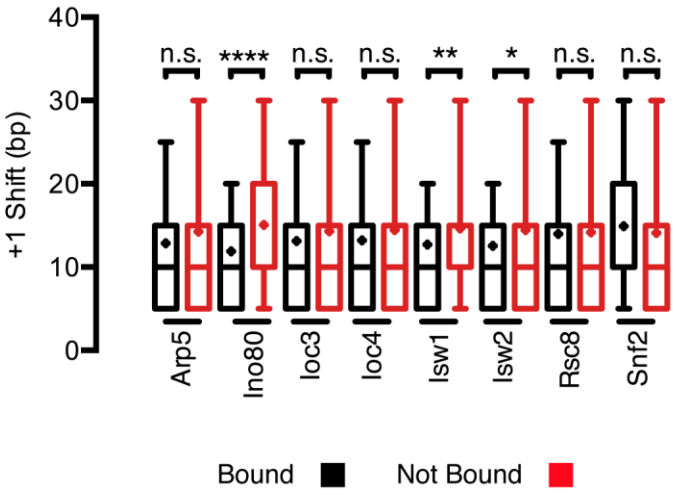

Figure 3-15 – Shifts of +1 Nucleosomes Bound By Various Remodeling Factors in YPD

Differences in furthest upstream and downstream positioning of +1 Nucleosomes determined to be bound (black) or unbound (red) by Arp5, Ino80, Ioc3, Ioc4, Isw1, Isw2, Rsc8, Snf2 (Yen et al. 2012). Significance is determined by the Kolmogorov-Smirnov test.

We find that Isw1 and Isw2 are enriched at Static promoters and that +1 nucleosomes at promoters bound by these factors exhibit significantly less movement than +1 nucleosomes without these factors by the Kolmogrov-Smirnov test (Figure 3-13). Similarly, we find that Ino80 bound promoters are predominantly classified as Static, and that this enrichment is statistically significant. We posit that the enrichment of Ino80 at Static promoters is related to its involvement in the complex in the biology of Htz1 (Papamichos-Chronakis et al. 2011)

3.2.7 - Role of SWI/SNF in Ox gene cluster

Upon analyzing the enrichment of Snf2, the catalytic subunit of SWI/SNF, as determined by Yen et al. (in YPD) we observed a trend of enrichment at Dynamic promoters, but this trend was of limited significance (Figure 3-15). The activity of SWI/SNF is known to be modulated by the nutrient conditions of the growth media (Sudarsanam et al. 2000) thus we utilized a ChiP data from Parnell et al. (Parnell et al. 2015) who performed ChIP of Snf2 in minimal media that more closely matches the nutrient conditions in the YMC, in which cells can be assumed to be undergoing asynchronous metabolic oscillations.

Examining Snf2-enriched promoters under these conditions we observe that Snf2 bound promoters display a highly significant increase in +1 shift distances, indicating that Snf2 is likely involved in mediating the chromatin remodeling events at these loci (Figure 3-16).

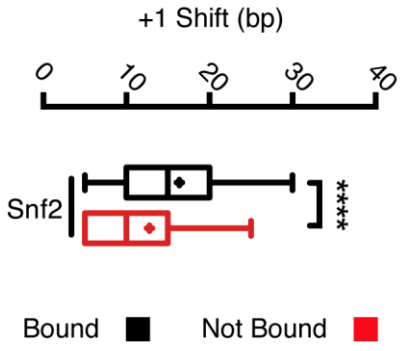

Figure 3-16 - Shifts of +1 Nucleosomes Bound By Snf2 in Minimal Media

Differences between furthest upstream and downstream positions of +1 nucleosomes bound by Snf2 in minimal media (Parnell et al. 2015). Significance is determined by the Kolmogorov-Smirnov test.

This discrepancy among the analysis with respect to the two data sets could be due to two (not mutually exclusive) reasons. The simplest reason is the coverage from the data procured by Yen et al. does not offer high enough coverage to distinguish many sites of Snf2 enrichment from background levels (Yen et al. 2012).

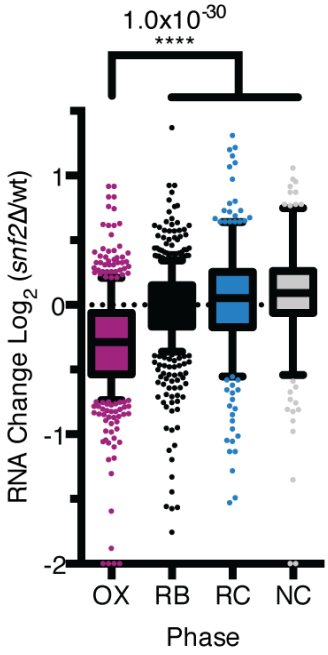

Figure 3-17 – Effect of snf2Δ on the YMC Transcriptional Super Clusters

Fold change in transcription in *snf2*Δ compared to wildtype on Ox, RB, RC, and non-cycling (NC) clusters. Transcript data from Sudarsanam et al.

Further, as shown above, the transcriptional landscape of cells cultured in YPD closely resembles the Ox/RB phase from the YMC, with little to no correlation with the RC phase (Figure 3-13). While asynchronous cells grown in minimal media are have been shown to individually undergo metabolic oscillations (Silverman et al. 2010), this is unlikely to be the case for cells grown in nutrient replete conditions, such as YPD. These cells appear to be locked in an active respiratory state in which they are

constantly consuming glucose and oxygen, and regularly dividing. The nucleosome shift we observe associated with Ox cluster genes appears to be coincident with the transition from RC to Ox. If YPD grown cells do not enter the RC phase there can be no transition from RC to Ox, and thus the requirement for remodeling by Snf2 may not be required for activation of the Ox cluster in YPD and hence not observed.

There is evidence that the maintenance of transcriptional activity at genes activated by the SAGA pathway is subsequently achieved by the TFIID pathway (Lee et al. 2000; Ghosh and Pugh 2011). Thus activation and maintenance of transcription are two separable activities, and the SAGA and TFIID pathways can work together to contribute to the transcriptional output of individual loci. Based on this observation we propose that transcription of the Ox cluster is likely dominated by the TFIID pathway in YPD, as these genes would be expected to be constitutively transcribed under these conditions. Conversely, under minimal media conditions the Ox cluster is transcribed with bursts, with respect to the YMC, and each burst of expression is expected to involve SAGA, Gcn5, and SWI/SNF. Under this paradigm it is not surprising that Snf2 ChiP signal is much more robust when interrogated under minimal media conditions.

Given that ‘Dynamic” nucleosomes are strongly enriched for genes expressed during the Ox phase (Figure 3-7) we next asked whether SWI/SNF may play a central role in the regulation genes necessary for growth. When examined under standard growth conditions, deletion of SNF2 has pleotropic effects on gene

expression. However, when evaluated with respect to the YMC, analysis of transcript abundance in *snf2*Δ mutant cells reveals that the vast majority of genes in the Ox cluster require Snf2 for maximal expression (Figures 3-17, 3-18). Further, peaks of Snf2 binding are highly enriched in the Ox cluster (Figure 3-18)(Parnell et al. 2015). Thus, SWI/SNF appears to be a specific regulator of growth genes, consistent with this, we not been able to achieve metabolic cycling in *snf2*Δ yeast.

Histone acetylation by Gcn5, the acetyltransferase component of SAGA, is important for regulating the activity of SWI/SNF at promoters (Hassan et al. 2001; Chandy et al. 2006; Cai et al. 2011). Kuang et al., have recently shown Gcn5, H3K9ac and H3K14ac occupancy are coincident with Ox gene expression, and we have plotted their data organized with the same gene organization as ours (Figure 3-18 E-G)(Kuang et al. 2014). Acetylation of histone H3 at residues 9 and 14, and binding of Gcn5 are maximal at Ox promoters, and peak temporally when these genes are being actively transcribed. Collectively, the data demonstrate that nucleosome repositioning and gene expression at Dynamic promoters belonging to the Ox class are regulated by the SWI/SNF complex.

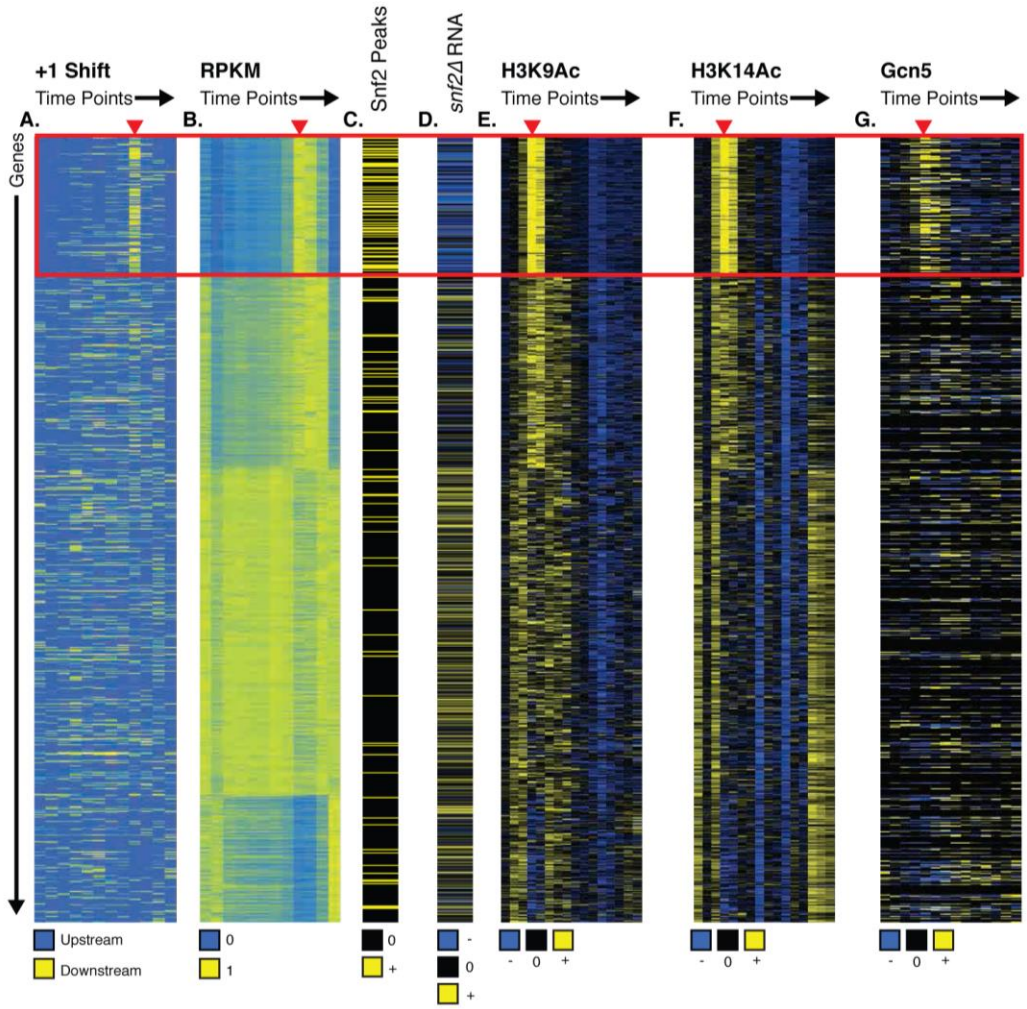

Figure 3-18 – Confluence of SWI/SNF Activity, Histone Acetylation, and Gcn5 Binding Activates the Ox Cluster

Red triangles indicate initiation of the Ox phase. **A.** Normalized shift associated with +1 nucleosomes. **B.** Normalized transcriptional output as measured by RPKM. **C.** *In vivo* Snf2 occupancy in minimal media. (Parnell et al. 2015) **D.** Fold change in transcript abundance in *snf2*Δ relative to wildtype. **E-F.** Acetylation of H3 at residues 9 (**E**) and 14 (**F**). **G.** Binding of Gcn5 histone acetyltransferase.

3.2.8 - Examining Nucleosome Shifts at Ribosomal Protein and Ribosomal Biogenesis Promoters with Respect to Transcription

Despite our finding that SAGA genes exhibit +1 nucleosome movement according to transcriptional output, and TFIID regulated genes generally do not (Figure 3-18), numerous TFIID regulated genes belong to the Ox cluster which experiences clear nucleosome repositioning upon gene activation (Figure 3-6). Amongst these TFIID regulated/Ox promoters are many Ribosomal Protein (RP) and Ribosomal Biosynthesis (Ribi) genes (Jorgensen et al. 2004; Kuang et al. 2014). Thus we specifically analyzed the relationship between +1 position and transcriptional output at RP and Ribi genes (Figure 3-19). This analysis revealed that nucleosomes can indeed be repositioned in concert with gene activation at TAF1-enriched genes, though this behavior is much more prevalent at promoters defined as TAF1-depleted. Thus, nucleosome remodeling occurs broadly at SAGA promoters and additionally at a subset of TFIID promoters, where the position of the +1 nucleosome can either inhibit or promote general transcription factor binding.

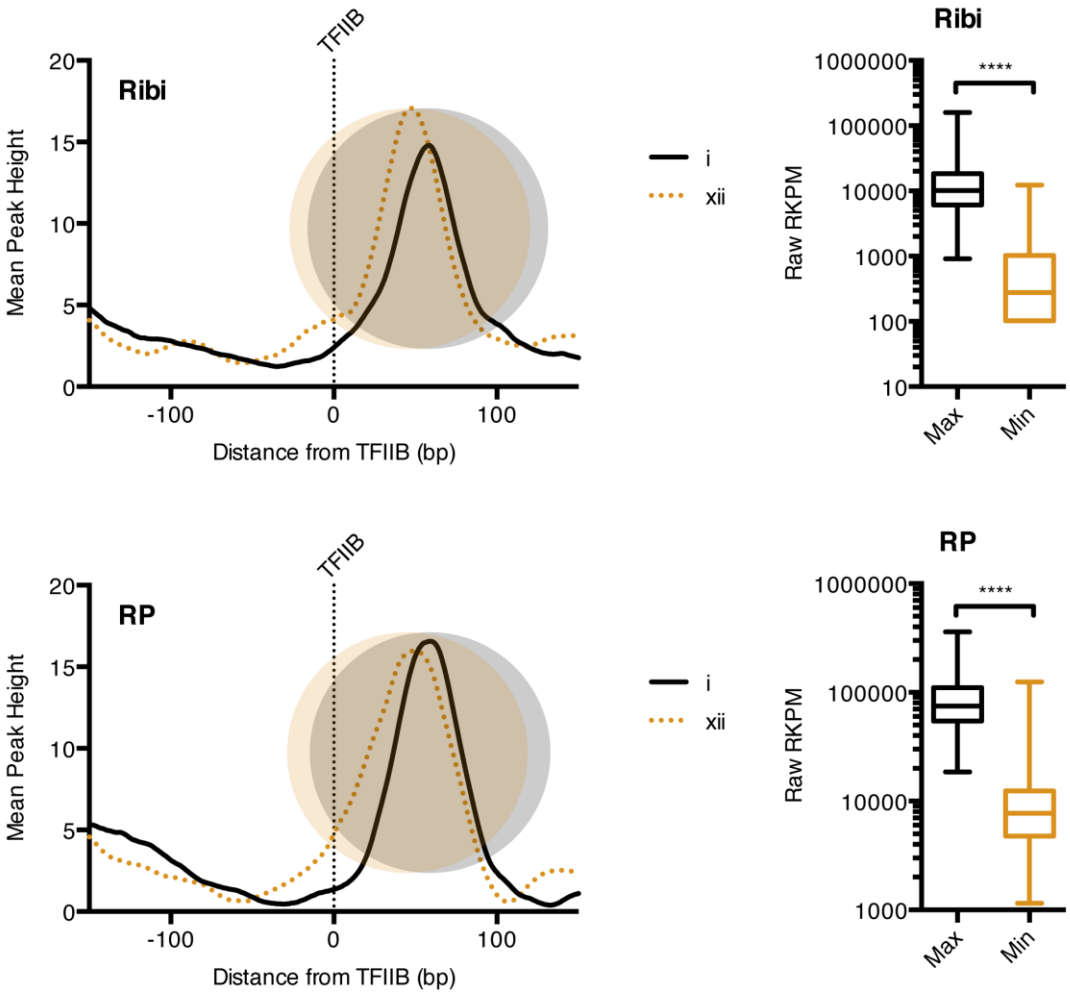

Figure 3-19 – +1 Nucleosome Dynamics at Ribosomal Biogenesis and Ribosomal Protein Promoters

Positions of +1 nucleosomes at ribosomal biogenesis (Ribi) genes when transcription is maximal (i) an minimal (xii) (top left), and the difference in maximal and minimal levels of expression of the same subset of genes (top right). The same analysis was performed for ribosomal protein (RP) genes (bottom right and left).

3.2.9 - Variation of Nucleosome Number and Internucleosome Distances Through Metabolic Oscillations

In addition to nucleosome repositioning, we observed a variation in the number of nucleosome calls as cell progressed through the YMC. While the length of reads from each sample is highly similar, the number of nucleosomes detected increases as

the culture transitions out of the R/B phase, peaks in early R/C and then decreases into OX (Figure 3-20). Time point 6 was excluded due to low read count.

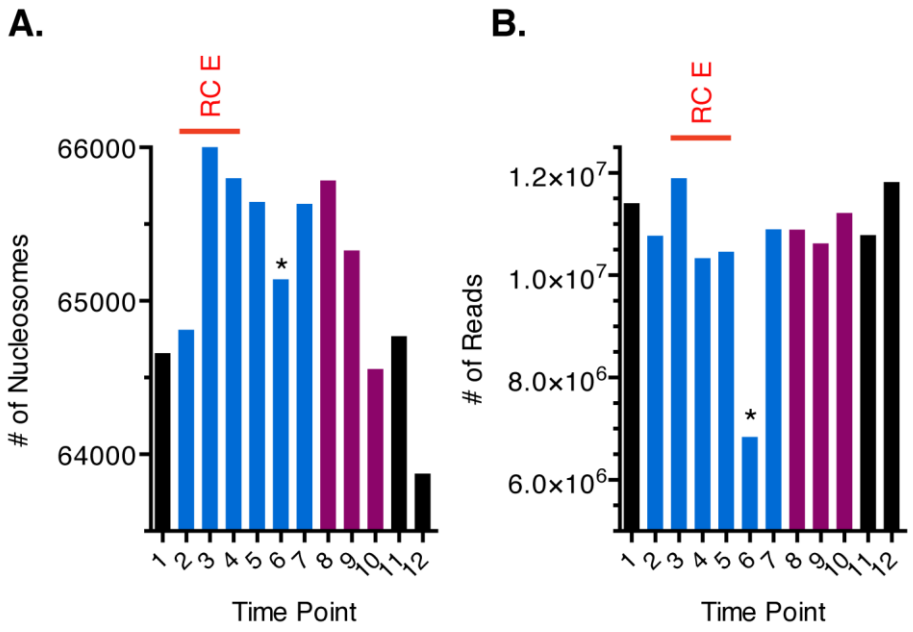

Figure 3-20 – Total Nucleosome Number Varies Through the YMC

A. The total number of nucleosome calls increases as cells transition from RB to RC, and decreases as cells transition from Ox to RB. The early stage of the RC phase is marked as RC E. **B.** The total number of sequencing reads from each sample is highly similar, with the exception of time point 6. This indicates that the differences in nucleosome calls among the samples is not an artifact of inadequate sampling.

Examining individual loci, we are able to identify many regions that acquire nucleosomes in the RC phase, exemplified by the HCA4 promoter (Figure 3-21).

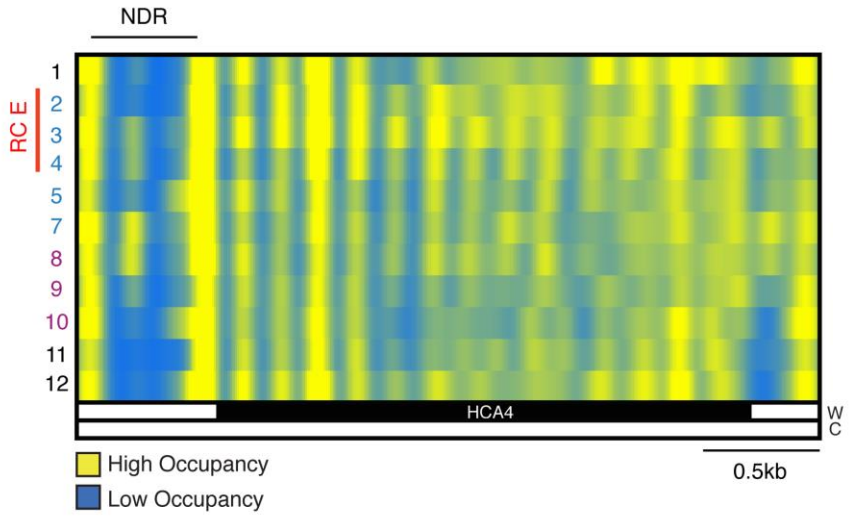

Figure 3-21 – Transient Nucleosome Occupancy in the HCA4 promoter

Heat-map of nucleosome positions across the HCA4 gene through the metabolic cycle. Nucleosome occupancy in the NDR appears in time point 3 and subsequently increases in intensity before disappearing in time point 11.

Unlike nucleosome repositioning, we find no evidence that transcriptional activity is related to occupancy within the NDR during the RC phase (Figure 3-22), forcing us to consider if they were perhaps involved in other aspects of chromatin biology.

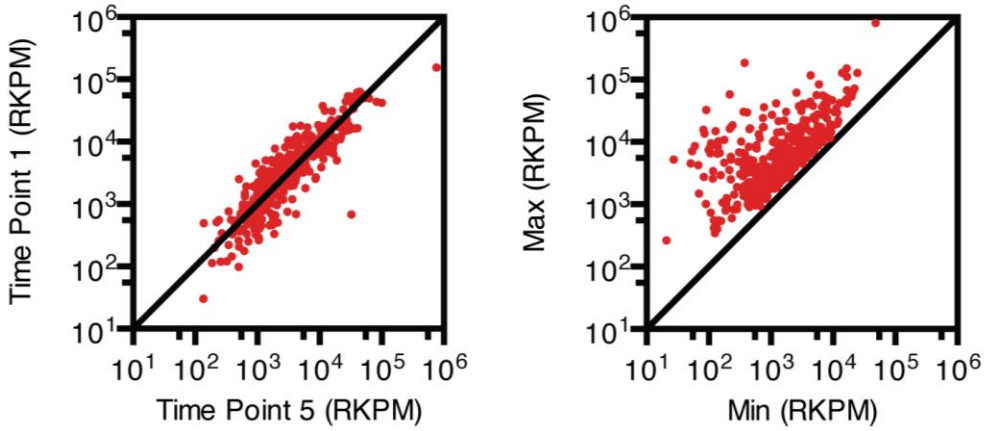

Figure 3-22 – Transient Promoter Occupancy is Not Correlated to Gene Expression

Genes exhibiting transient promoter occupancy in time point 5, are shown. RKPM values from time point 1 (RB) are plotted against values from time point 5 (RC). (left panel). Values corresponding to the Maximum and Minimum for the same subset of genes (right panel).

Next we considered whether sites of transient occupancy in promoters may be indicative of global chromatin reconfiguration which likely occurs as cells enter the quiescent-like RC phase (Pinon 1978; McKnight et al. 2015; Rutledge et al. 2015). Also, the transcriptional landscape of yeast in the RC phase is highly correlated to that of yeast grown to saturation and devoid of a carbon source (Figure 3-13). It has recently been demonstrated that promoters in *S. cerevisiae* can function as boundary elements which separate CIDs (chromosomally interacting domains), typically comprised of ~5 genes (Hsieh et al. 2015). Interestingly, we find that ~70% of the 737 promoters which contain transient nucleosomes in RC, function as CID boundaries in rich media ($p = 2.2X10^{-168}$) which raises the prospect that CID boundaries are extensively reconfigured as cells enter RC (Figure 3-23).

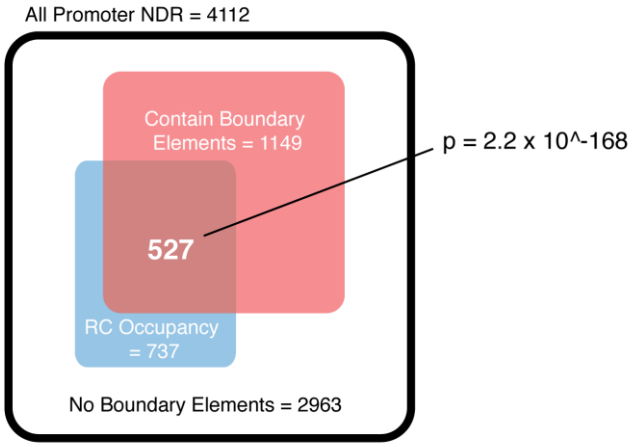

Figure 3-23 – Transiently Occupied Promoters are Likely to Function as CID Boundaries

Venn diagram indicating the overlap between NDRs occupied in RC and NDRs containing CID boundaries. Significance was calculated by the Hypergeometric distribution.

Outside of gene promoters we found many other regions which became occupied during the RC phase, to understand the how chromatin is being reconfigured we considered two models: firstly, the incorporation of extra nucleosomes may be indicative of tighter spacing and a global reduction in nucleosome repeat length; secondly; the number of nucleosomes may actually change little, but our ability to unambiguously map nucleosomes may alter as nucleosome positioning may become more consistent in different phases of the YMC. To distinguish these possibilities – which are not mutually exclusive – we calculated the inter-nucleosomal distances genome-wide for each time point.

We find that dyad-to-dyad nucleosome spacing of 160-170 base pairs peaks early in the RC phase (RC E)(Figure 3-24). Accordingly, internucleosome distances corresponding to NDRs (200+ bp) are least common in the early stages of the RC phase, coincident with the time points in which we detect the most nucleosomes

(Figure 3-20). This suggests that the observed alteration in nucleosome calls is – in part – due to NFR filling.

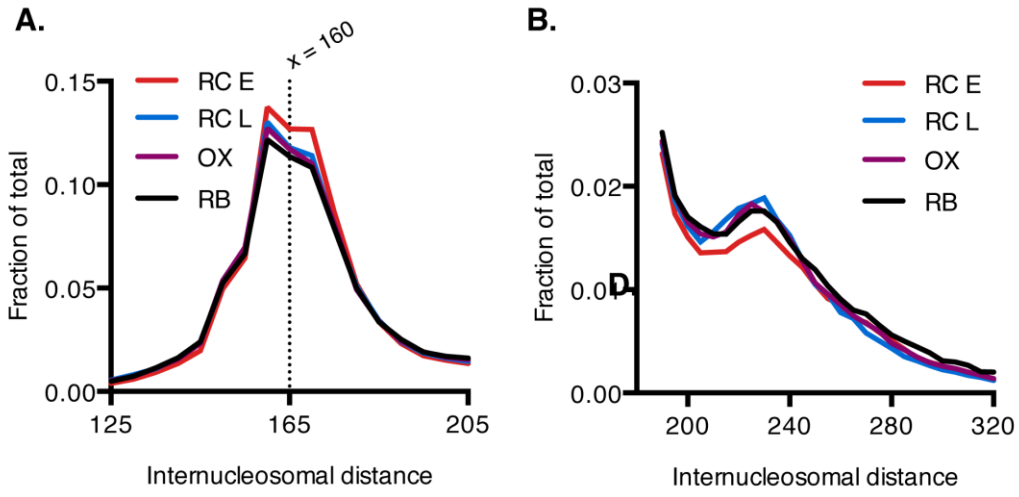

Figure 3-24 – Internucleosome Distances Within Each Metabolic Phase

Dyad-to-dyad distance between each nucleosome and its downstream neighbor was calculated for each metabolic phase: early RC (RC E), late in the RC (RC L), Ox and RB. **A**. Internucleosome distances in the 125-205bp range. **B**. Internucleosome distances in the 180-320 range.

Next, we considered whether nucleosomes generally become more consistently positioned in the RC phase. A study examining intragenic chromatin structure uncovered two classes of nucleosome ordering among genes (Vaillant et al. 2010). In the first class, nucleosomes are organized in a 'crystal-like' array in which intragenic nucleosomes are regularly spaced and their number is tightly constrained by gene length. A second class of genes exhibit 'bi-stable' organization in that they appear to capable of adopting states of high and low compaction. We decided to test if intragenic nucleosome compaction varied among genes through metabolic oscillations, and if variation in chromatin compaction contributed to the observed increase in nucleosome calls. To calculate 'crystallinity' within genes we determined the

internucleosome distances found within the range of the TSS and TTS for a given gene, as defined as the distance between a given dyad and its downstream neighbor. We then calculated the standard deviation (SD) among the internucleosome distances associated with a given gene (Figure 3-25).

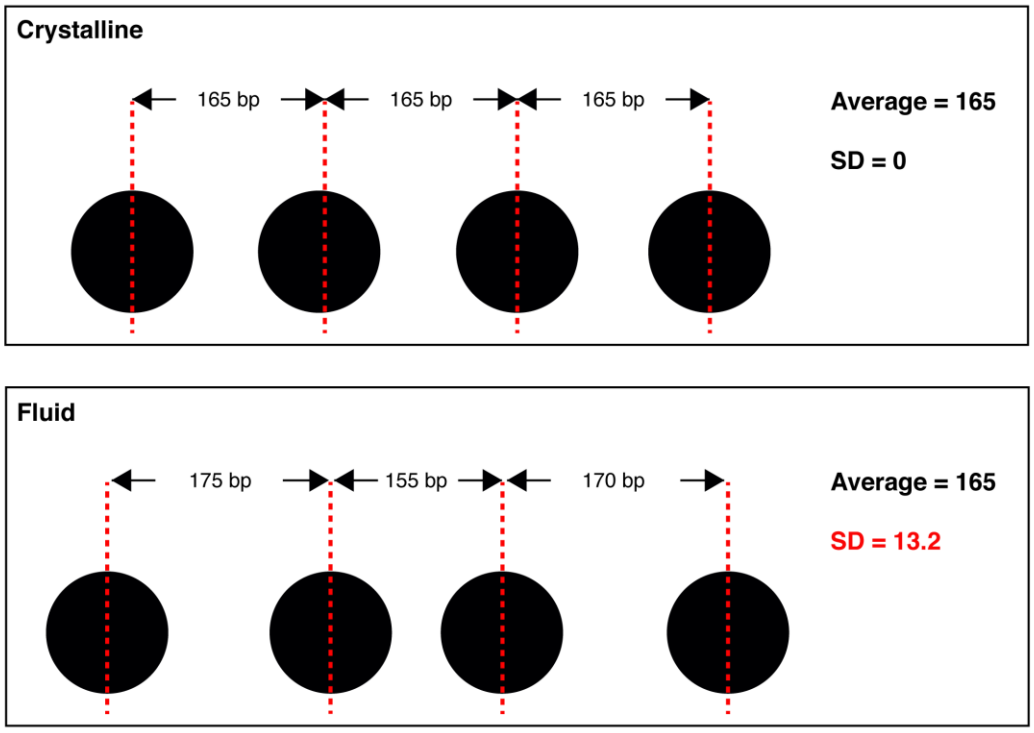

Figure 3-25 – Illustration of Crystalline and Fluid Nucleosome Organization

Crystallinity is defined as even spacing among nucleosomes within a transcribed unit. Highly crystalline transcribed units exhibit a small standard deviation with respect to spacing between nucleosomes. Transcription units with inconsistent nucleosome spacing exhibit a larger standard deviation values, and are referred to as Fluid.

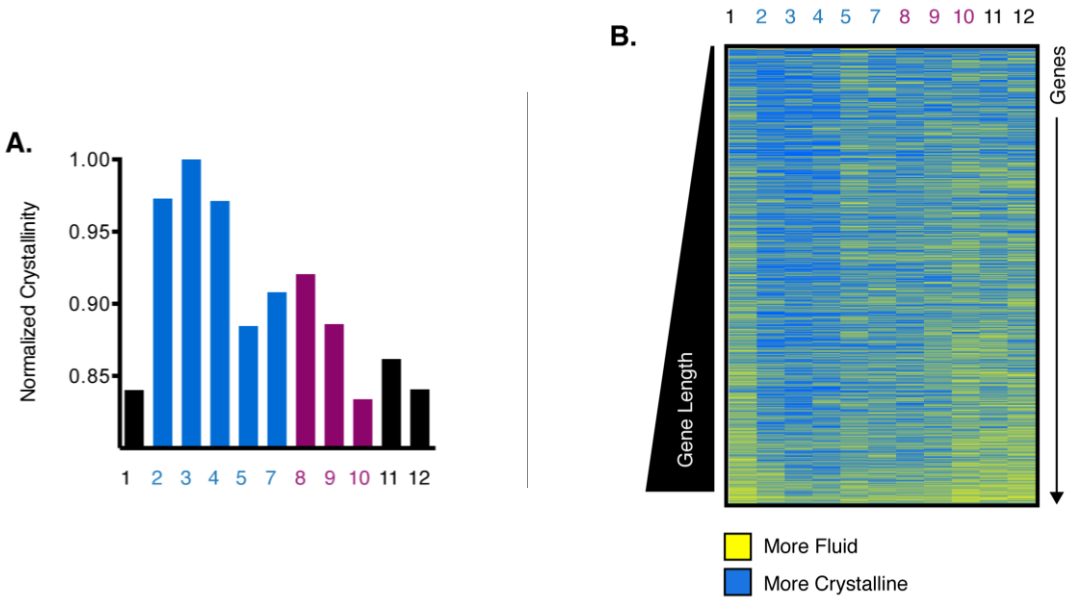

Figure 3-26 – Crystallinity Peaks in RC

A. Crystallinity across genes is calculated as 1/(Standard Deviation of Nucleosome Positions). The crystallinity of all genes was averaged within each time point. The twelve resulting values were normalized and plotted. **B.** Crystallinity of individual genes organized by gene length is shown as a heat-map.

Crystallinity was calculated for each gene at all time points, and genes were ranked by length (Figure 3-26). We normalized the data across time points such that the time point with the highest (SD) for each gene is set to a value of 1. Time points with the most variation among internucleosome distances are considered the most 'fluid', while those with consistent spacing of nucleosomes are considered to be 'crystalline'. The intragenic nucleosome organization at the vast majority of genes becomes most 'crystalline' as the culture enters the RC phase, when the number of observed nucleosomes is highest, and subsequently relaxes through progression to the Ox and RB phases (Figure 3-26).

To examine the relationship intragenic nucleosome organization and transcription, we organized our quantification of crystallinity by the transcriptional clusters derived from the RNA-seq data (Figure 3-27). Globally, the strongest predictor of chromatin order remains the phase to which the time point belongs. However, we do observe an distinct increase in fluidity of nucleosome organization corresponding to transcription of the Ox and RB clusters, which was to be perhaps to be expected as these genes are likely to be transcribed with more 'burst-like' kinetics due to the relatively short lengths of these phases relative to the RC cluster.

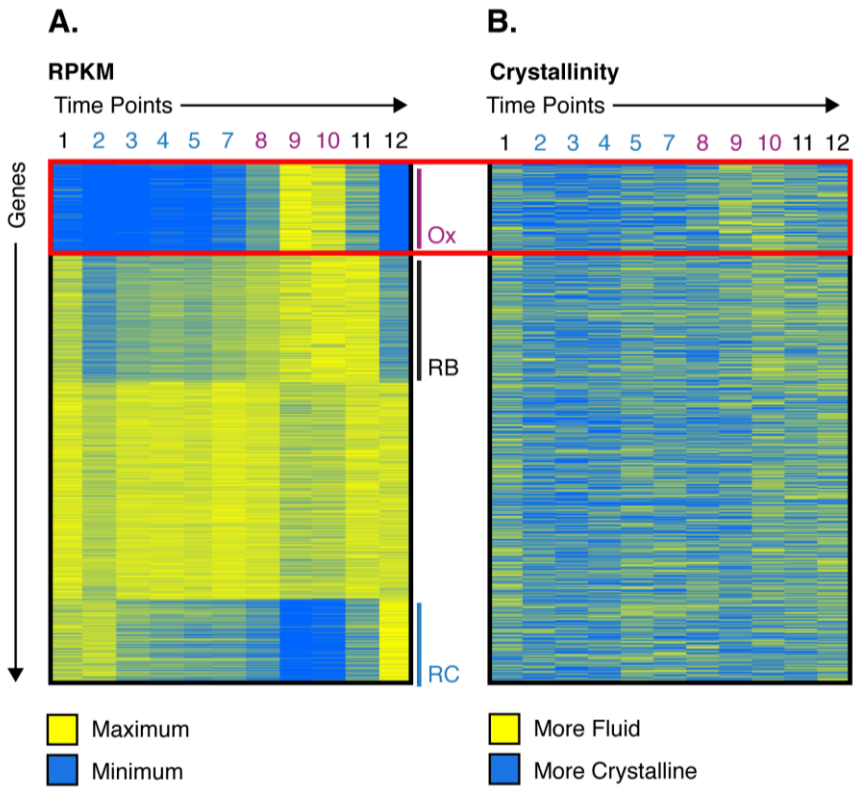

Figure 3-27 – Nucleosome Order and Transcription

Ox phase is highlighted with a red box. **A.** Normalized RPKM values associated with genes through the YMC. **B.** Normalized crystallinity associated with genes through metabolic oscillation.

To examine nucleosome periodicity across the genome, without respect to gene length, we divided each chromosome into 5kb bins and calculated nucleosome order within each bin. This analysis confirmed that nucleosomes are generally more "crystalline" across all chromosomes in the RC phase of the cycle (Figure 3-28 A). Further, closer inspection reveals that the alteration in nucleosome order largely corresponds to distinct phases in the cell cycle (Figure 3-28 B). Entry into mitosis (high Clb2) is coincident with the peak in nucleosome organization in time point 3, this persists through the remainder of the RC phase but diminishes as cells pass START (high Cln3) and then enter S phase (High Clb5) in time point 9. Thus, this straightforward assay has revealed that nucleosome organization is significantly altered through the YMC: chromatin is least ordered during S phase - when DNA replication occurs; but most ordered during mitosis, when chromosomes are condensed.

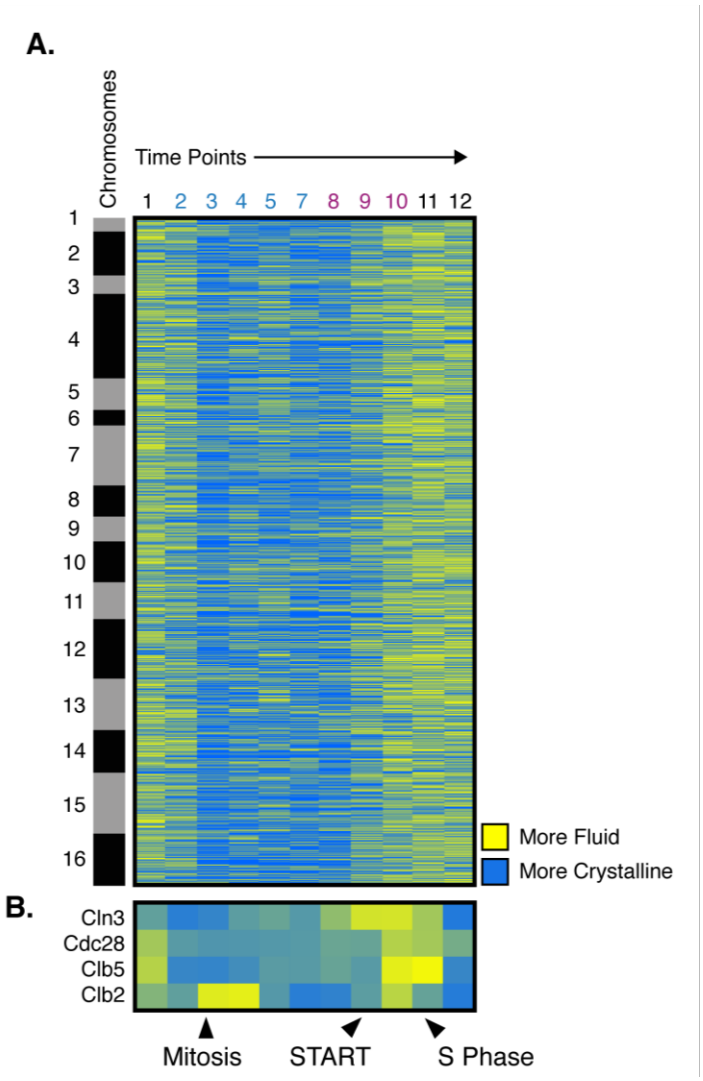

Figure 3-28 – Ordering of Nucleosomes Through the YMC

A. The yeast genome was divided in to 5kb bins and the crystallinity within each bin was calculated. Bins along each chromosome are arranged vertically, and time points are arranged horizontally. **B.** Expression of cell cycle factors Cln3 (START), Cdc28 (S-phase), Clb5 (S-phase), and Clb2 (Mitosis).

3.3 – Discussion

In examining nucleosome dynamics through metabolic oscillations we have demonstrated that nucleosome repositioning occurs at many promoters and is highly coordinated with gene transcription. Repositioning of +1 nucleosomes is predictive of the use of accessibility of transcription factors, the incorporation of the histone variant Htz1 and the magnitude of the transcriptional output. Nucleosome repositioning occurs predominantly at a subset of genes highly expressed during the Ox phase of the YMC, which is intimately coupled with growth. During activation nucleosomes are repositioned downstream, which permits binding of GTFs and assembly of the RNAPII holoenzyme. Further, the data blur the lines between SAGA and TFIID promoters in the case of RP and Ribi genes, suggesting that these designations can potentially vary with regard to experimental conditions. Importantly, we find that changes in promoter chromatin are closely linked to the activity of the SWI/SNF complex, which places ATP-dependent chromatin remodeling as a key regulator of growth. Finally, we reveal that chromosomes undergo a significant alteration in nucleosome arrangement as cells progress through cell cycle.

3.3.1 - Remodeling Factors and the Plasticity of SAGA Promoters

We find that by ranking the degree of repositioning of the +1 nucleosome we can uncover many of the general principals of gene regulation. Promoters with the most dynamic nucleosomes are SAGA enriched, are acutely expressed and display the

greatest dynamic range of transcription. These promoters are bound and modified by Gcn5 and are regulated by SWI/SNF. In contrast, TFIID promoters, by and large, display minimal nucleosome repositioning and exhibit a lower dynamic range of expression. TFIID promoters are commonly enriched for Htz11, H4 K5/8/12ac and bound by Ino80. While these findings are in generally keeping with current models of gene regulation by co-activators, these findings also question the general notion that TFIID regulated "housekeeping" genes are responsible for the regulation of growth, and SAGA regulated genes are dynamically controlled "Stress response genes". Examination of genes massively induced in the Ox cluster (growth genes), reveals dynamic nucleosome repositioning, acute transcriptional activation – and repression – and regulation by both Gcn5 and SWI/SNF, which are hallmarks of SAGA. Yet many of the genes within this cluster i.e. ribosomal protein genes and other genes associated with growth, are classically described as TFIID dependent, housekeeping genes. This apparent discrepancy likely highlights that use of SAGA or TFIID at a given promoter is somewhat plastic and influenced by a variety of intrinsic and extrinsic factors such as growth conditions and availability of nutrients. Indeed, SAGA and TFIID have been shown to act sequentially (Lee et al. 2000; Ghosh and Pugh 2011) and many gene promoters, including ribosomal protein genes, are enriched for both SAGA and TFIID (Ohtsuki et al. 2010). Moreover expression of a large fraction of all yeast genes were found to be regulated by either complex (Lee et al. 2000; Huisinga and Pugh 2004). Thus Ox genes may initially utilize SAGA and chromatin based reconfiguration for rapid activation, followed by TFIID-mediated sustained transcription in YPD.

The requirement for SWI/SNF for the activation of growth genes in the Ox cluster may be particularly necessary when cells are cultivated in media that is limiting in nutrients. Interestingly, we show that Snf2 is enriched at growth genes when cells are cultured in minimal media, but we found that this enrichment is less apparent when data from rich media is used (Figures 3-15, 3-16).

In the case of the YMC, cells transition through distinct phases sequentially. Importantly, the acute Ox phase is preceded by a comparatively lengthy R/C phase; here, gene transcription is limited and this phase displays many hallmarks of quiescence (Shi et al. 2010). The remarkably rapid conversion from R/C to growth has been shown to be triggered by Acetyl CoA levels, rising and peaking in Ox phase (Cai et al. 2011; Kuang et al. 2014), and we find that genes activated during this transition experience significant remodeling of promoter nucleosomes by SWI/SNF (Figure 3-29). Thus, under YMC growth conditions, SAGA and SWI/SNF may be required for the rapid conversion of a "quiescent" chromatin organization into a state conducive with gene expression. Cells cultured in rich media presumably only transiently inactivate the Ox cluster and therefore this class of genes may be less reliant on SWI/SNF and SAGA under those conditions.

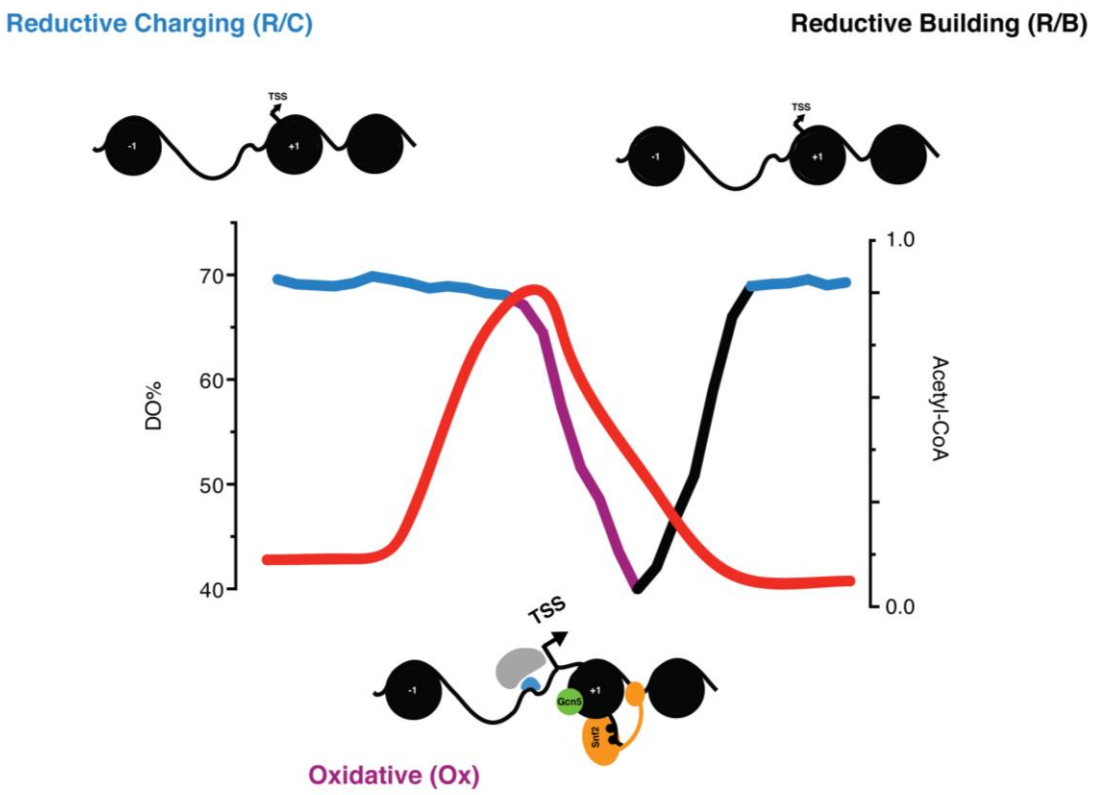

Figure 3-29 – Model Diagramming How the Spike in Acetyl-CoA levels Could Trigger Expression of the Ox Cluster

A trace of DO% through a single metabolic oscillation (left axis). Hypothetical trace of intracellular Acetyl-CoA concentration (right axis) with peak levels occurring in the Ox phase as previously demonstrated (Cai et al. 2011). Schematized are the position of +1 nucleosomes relative to transcription start sites, and the occupancy of SWI/SNF, Gcn5, and RNAPII during the different phases of the YMC.

Histone acetylation, nucleosome remodeling, and gene transcription of the Ox cluster occurs with a short timeframe, which shows that robust mechanisms for activation and repression are utilized. Gcn5 is intimately involved in the regulation of Ox genes (Cai et al. 2011; Kuang et al. 2014), and it is noteworthy that histone acetylation by Gcn5 stimulates the binding and nucleosome remodeling (Chandy et al. 2006; Chatterjee et al. 2011) by SWI/SNF. Additionally, SWI/SNF is also known to

be recruited by acidic transcriptional activators (Neely et al. 1999; Yudkovsky et al. 1999; Neely et al. 2002). While the identity of specific transcription activators for Ox cluster genes is unknown, ribosomal protein genes, at which Snf2 is strongly enriched, are activated by Ifh1, which contains a potent acidic transcriptional activation domain (Schawalder et al. 2004). Interestingly, the function of both SWI/SNF and Ifh1 are negatively regulated by acetylation mediated by Gcn5 (Kim et al. 2010b; Downey et al. 2013), thus non-nucleosomal protein acetylation potentially also has a role in regulating the expression of Ox genes.

3.3.3 – Context Dependence of 'Housekeeping Gene' Designation for RP and Ribi Promoters

A ubiquitous feature of all genes – regardless of GTF usage – is that the dyad of the +1 nucleosome lies ~60bp downstream of TFIIB binding site upon maximal activation (Figure 3-6). This organization is conducive to transcription as TFIIB would bind close to the edge of the +1 nucleosome in a region known to be highly accessible (Anderson et al. 2002). TFIID regulated genes are typically assumed to be "housekeeping", however our findings call that designation into question. Studies classifying RP and Ribi promoters as being "housekeeping" were performed in rich media, and we know that the transcriptional landscape of cultures grown in YPD very closely resembles expression in the Oxidative phase (Figure 3-13), a temporally small part of the YMC. Thus, the observed constitutive expression of these "housekeeping" genes is likely an artifact of the culture conditions.

3.3.3 - Enrichment of Htz1 at Static Promoters

We find that repositioning of the +1 nucleosome is anti-correlated with the presence of the histone variant Htz1. These ‘static’ promoters are also enriched for Ino80, H4K5ac, H4K8ac, and H4K12ac and are likely regulated by TFIID (Raisner et al. 2005; Zhang et al. 2005). While the range of expression for genes associated with ‘Static’ promoters is not as broad as those associated with ‘Dynamic’ promoters, many genes belonging to the ‘Static’ class are periodically transcribed with respect to the metabolic cycle. Previously Htz1 has been shown to be enriched at inactive genes and is displaced upon gene activation, leading to the hypothesis that H2A.Z poises genes for transcriptional initiation (Zhang et al. 2005). Thus, Htz1 incorporation and removal may be involved in governing bursts of transcription from these promoters during the YMC. Thus, periodic transcription is perhaps broadly governed by different mechanisms at SAGA and TFIID promoters, with chromatin remodeling by SWI/SNF being a major determinant at SAGA promoters, and Htz1 incorporation influencing transcriptional activity at TFIID promoters.

3.3.4 - YMC and global chromatin organization

We find that chromatin is globally altered as cells progress through the YMC. We find two key events, which occur as cells transition through the RC phase: first, we find that many nucleosome-depleted regions become occupied; second, we find that nucleosomes become more consistently spaced. The increased occupancy of NDRs appear to occur predominantly at previously described boundary elements, which is likely indicative of global chromosome restructuring that occurs in RC. While our data is most consistent with extra nucleosomes being deposited within the NDRs, it remains entirely possible that other protein complexes occupy and protect these regions from MNase digestion during the RC phase. We also find that nucleosome positioning becomes more consistent in RC, which is likely conducive to the generation of compact chromatin structures. This feature may be related to the profound chromosomal rearrangements observed in quiescent yeast cells. Interestingly, entry into the RC phase is coordinated with mitosis at which time chromosomes are highly compact. Thus, the decrease in variance of nucleosome spacing we observe in early RC, may be reflective of the formation of mitotic chromosome structures which may persist through much of the RC phase. In this regard it is noteworthy that the commitment to enter the cell cycle is made at mitotic exit (Spencer et al. 2013), thus cells entering quiescence may maintain compact "mitotic" chromosomes, rather than establish the complex decondensed organization found in G1.

3.3.5 - Parallels Between YMC Regulation and Cancer

Here we have shown that transcription of genes belonging to the Ox cluster is highly sensitive to remodeling of promoter chromatin. Ox genes are involved with cellular processes that promote cell growth, such as ribosome biogenesis, a process that is often targeted by cancer therapies (Burger et al. 2010; Cai and Tu 2012). Further, we implicate SWI/SNF component, Snf2, as likely being responsible for remodeling events at these promoters. In the absence of human SWI/SNF homologs, Swi5 and Brg1, many human promoters exhibit altered chromatin architecture, and levels of gene expression change accordingly (Tolstorukov et al. 2013). We have demonstrated that SWI/SNF is involved in mediating the transition from R/C to Ox, thus overexpression of SWI/SNF or hypermorphic alleles of SWI/SNF components could potentially lead to permanently "Ox-like" environment, in which growth signals persist indefinitely. Such a state would be highly prone to transformation, and in fact SWI/SNF homologs BRG and BRM are overexpressed in many breast cancers and melanomas (Lin et al. 2010; Wu et al. 2015). Further, knockdown BRG1 has been shown to inhibit cell proliferation in both cases (Lin et al. 2010; Wu et al. 2015). Future work examining the role of SWI/SNF in mediating the transition of R/C to Ox may therefore be crucial in advancing the understanding of how BRG and BRM can function as a proto-oncogenes.

3.3.6 – Future Avenues of Study

While the RNA-seq protocol we used to measure gene expression proved to be very powerful, it is not without caveats. Firstly, the protocol is not strand specific, meaning that anti-sense transcription of non-coding RNA could potentially confound our measurements. Further, the protocol is not specific for nascent RNA. Given that transcripts in *S. cerevisiae* exhibit unique half-lives, it would be ideal to measure transcriptional activity on the chromatin, as opposed to measuring bulk levels of cellular RNA. This is particularly true when examining the role of chromatin remodeling as it pertains to the regulation of transcriptional output. In fact, we observe transcript levels persisting near the maximum following the shift of +1 nucleosomes to their upstream sites at many genes (Figure 3-18). Transcript levels at these genes do eventually decay, but a tighter relationship between chromatin remodeling and transcriptional output could be observed if we were to focus our analysis on nascent initiating transcripts. NET-seq, a protocol designed to capture the 3' ends of nascent transcripts has been used to great effect in *S. cerevisiae* (Churchman and Weissman 2012). The protocol requires the C-terminal tagging of Rpb3, the largest subunit of RNAPII, with a 3XFLAG epitope, which allows the polymerase to be efficiently immunoprecipitated. RNA co-purified with the polymerase is isolated and prepared for high-throughput sequencing. It is unlikely that addition of the 3XFLAG epitope would interfere with metabolic oscillations, and thus implementation of this technique in the context of the YMC should be feasible.

Though the bulk of this chapter has focused on how ATP-dependent remodeling controls transcriptional output at Dynamic promoters, that is not to say that chromatin remodelling factors do not play a role at Static promoters. In fact, ATP-dependent remodelers Isw1, Isw2, and Ino80 are significantly enriched at promoters that exhibit no shifting of the +1 nucleosome through metabolic oscillations (Figure 3-15). Interestingly, +1 nucleosomes at these promoters tend to occupy highly thermodynamically unfavorable positions. Thus, the role of chromatin remodeling factors at these loci might be to maintain precise positioning of +1 nucleosomes despite changes in metabolic state or transcriptional activity. This hypothesis could be difficult to study, however, given that these factors likely exhibit redundancy with one another (Gkikopoulos et al. 2011). Further, it would not be at all surprising if deletion of multiple of these factors prevented the culture from cycling synchronously. The best way to initiate the investigation of Isw1, Isw2, and Ino80 at Static promoters in the context of the YMC is likely to epitope tag each factor and perform chromatin immunoprecipitation from samples taken at multiple time points and quantitate the abundance of these factors at each promoter as the cycle progresses. Based on the results of this experiment we would be able to determine whether all three factors are constitutively bound to Static during the YMC, or if there is exchange among the three factors as metabolic conditions fluctuate.

Chapter 4 - Introduction : Transcription Start Site Selection and Cryptic Transcription

4.1 - Rate Limiting Steps of Transcription Initiation Function As Points of Regulation

Throughout biology there are instances of each of the rate-limiting steps of transcription (Figure 1-2) functioning as a point of regulation. For instance, promoter clearing appears to be the key rate-limiting step to producing coding transcripts at the PHO5, ADY2, and ADH2 loci (Korber et al. 2006; Adkins et al. 2007). Chromatin remodeling at these loci is a prerequisite for expression as the default chromatin state occludes transcription factor binding sites, and prevents the assembly of a PIC. Further, promoter clearing appears to factor heavily in the recruitment of GTFs and RNAPII to genomic DNA as these proteins are known to exhibit opportunistic and promiscuous binding to intragenic segments of the genome in the absence of nucleosome deposition factors, resulting in the generation of non-coding transcripts (Kaplan et al. 2003).

Further, the rate-limiting steps following RNAPII recruitment have been demonstrated to be regulatable in many instances. The immune response requires that lymphocytes undergo a rapid response from a quiescent state to an activated state (Kouzine et al. 2013). This switch is characterized by an extremely rapid induction of expression of genes transcribed only in the activated state. Interestingly, RNAPII is present at these promoters even in the quiescent state when these loci are

transcriptionally silent, thus recruitment of RNAPII is not rate-limiting for these promoters. The abrupt initiation of transcription is due to increased expression of TFIIH factors, XPB and XPD helicases, subsequently triggering widespread promoter melting, thereby allowing for the release of paused polymerases (Kouzine et al. 2013).

Not only can polymerase lie dormant at promoters as the closed complex, RNAPII has been shown to be present at promoters in an inactive open complex state as well. The first demonstration of RNAPII pausing following the unwinding of promoter DNA comes from studies of the hsp70 promoter of *D. melanogaster*. The hsp70 promoter is a highly inducible promoter that is activated upon a temperature shift from 25˚C to 37˚C (Lindquist 1986). Rougvie and Lis discovered that RNAPII is bound to the hsp70 promoter in the uninduced state, and that the polymerase is paused in the open complex following the transcription of several nucleotides (Rougvie and Lis 1988).

Additionally, transcription start site selection has been shown to be a regulated step at the *S. cerevisiae* IMD2 and URA2 promoters, two genes involved in guanosine triphosphate (GTP) and uracil triphosphate (UTP) biosynthesis, respectively (Kuehner and Brow 2008; Thiebaut et al. 2008). When GTP and UTP levels are high, transcription at these promoters initiates from upstream TSSs generating a short non-coding transcript, and when levels of GTP/UTP are sufficiently low enough to require the activity of *IMD2*/*URA2* transcription initiation shifts to downstream TSS and produces full-length transcripts (Davis and Ares 2006; Jenks et al. 2008; Kuehner and

Brow 2008). Thus, rate-limiting steps involved in the initiation of transcription are frequently exploited as a mechanisms of regulation.

4.2 - Promoter Scanning and Start Site Selection

Once RNAPII has made the transition from the closed complex to the open complex it can then scan the downstream DNA for an appropriate TSS, prior to initiation transcription (Giardina and Lis 1993). TSS in wildtype *S. cerevisiae* are highly coincident with +1 nucleosomes, and are found between ~30 and 150 bases downstream of the initial site of RNAP recruitment (Hampsey 1998; Whitehouse et al. 2007; Corden 2008; Jiang and Pugh 2009a; Jiang and Pugh 2009b). Many components of the RNAPII are involved in maintaining the precision of TSS selection, and the contribution of individual factors in TSS selection can vary amongst promoters.

TFIIF, composed of subunits Tfg1, Tfg2, and Tfg3, associates with RNAPII near the active site of the enzyme. Tfg1 and Tfg2 play critical roles in guiding RNAPII to an appropriate TSS. Missense alleles of Tfg1 and Tfg2 genes lead to transcription initiation up to 26 nucleotides upstream of the canonical TSS at the *ADH1* promoter and other loci (Ghazy et al. 2004; Khaperskyy et al. 2008). Conversely, a temperature sensitive allele of general transcription factor TFIIB, *sua7-1*, shifts transcription initiation downstream of the canonical *ADH1* TSS at the non-permissive temperature (Pinto et al. 1994).

RPB9 was discovered in a suppressor screen for cold sensitivity conferred by the *sua7-1* (Sun et al. 1996). In addition to restoring growth at 16˚C, *rpb9*Δ was also shown to correct the downstream start site shift observed in *sua7-1*, focusing initiation back on the canonical TSS. In an otherwise wildtype background, *rpb9*Δ was shown to shift transcription initiation ~20 base pairs upstream of the normal *ADH1* TSS. TFIIF associates with the polymerase much less efficiently in the absence of Rpb9, potentially explaining why *rpb9*Δ and the mutant alleles of *TFG1* and *TFG2* phenocopy one another (Ziegler et al. 2003).

Mechanistic insights into how Rpb9 and TFIIF affect start site selection initially came from crystallographic studies of RNAPII, and the observation that *rpb9*Δ and mutations in the active site of RNAPII raise similarly impair transcription fidelity (Walmacq et al. 2009). Rpb9 binds to the surface of the polymerase, however, based on various crystal structures of RNAPII, it was proposed that Rpb9 could make transient contacts with the trigger loop (TL) domain of RNAPII. The TL domain is capable of isomerizing between a closed conformation, in which it participates in the essential chemistry of RNA synthesis at the active center of the enzyme, and an open conformation, where it is found along the surface of RNAPII where it is not involved in catalytic activity (Wang et al. 2006). Rpb9 is believed to interact with the open conformation of the TL. The kinetics of the conformational changes associated with the open-closed transition have significant effects on the rates of RNA synthesis and misincorporation of NTPs (Wang et al. 2006; Kaplan et al. 2012). Mutation of a residue on the TL, Rpo21-E1103G, induces a 3-fold increase in NTP misincorporation

in vivo, and a 10-fold increase *in vitro*, as a result of the destabilization of the open conformation of the TL (Kireeva et al. 2008). *rpb9*Δ similarly disrupts the TL in the open conformation and increases the rate of NTP misincorporation (Nesser et al. 2006; Walmacq et al. 2009). Further, genetic analysis of *rpb9*Δ and *RPO21*-E1103G mutations has revealed a synthetic lethal interaction (Walmacq et al. 2009).

4.3 - Cryptic Transcription in *S. cerevisiae*

Transcription of non-coding regions of the genome is prevalent in eukaryotes. In *S. cerevisiae*, many non-coding transcripts are rapidly recognized and ultimately degraded by the RNA exosome complex (Wyers et al. 2005; Davis and Ares 2006; Vanacova and Stefl 2007). The nuclear exosome is an eleven-member ribonuclease complex that functions in processing of ribosomal RNAs, tRNAs, and snRNAs, as well as quality control of mRNA transcripts. The nuclear form of the exosome is defined by the inclusion of Rrp6, a distributive 3'->5' exonuclease, which is absent from the exosome in the cytosol (Vanacova and Stefl 2007; Wasmuth et al. 2014). While viable, the deletion of *RRP6* does slow the growth-rate of *S. cerevisiae*, and leads to the stabilization of cryptic transcripts emanating from intragenic regions (Wyers et al. 2005; Davis and Ares 2006; Neil et al. 2009; Xu et al. 2009).

Though transcribed by RNAPII, transcripts degraded by the nuclear exosome are subject to a unique 3' end processing pathway involving termination by the Nrd1-Nab3-Sen1 (NNS) complex and polyadenylation by the Trf/Air/Mtr4 (TRAMP) complex (Steinmetz et al. 2001; Vasiljeva et al. 2008). TRAMP can be assembled in a

variety of ways, containing one of two non-canonical poly(A) polymerases, Trf4 and Trf5, and one of two RNA binding proteins Air1 or Air2, in addition to RNA helicase, Mtr4 (Wyers et al. 2005).

One of the original investigations of cryptic transcription in budding yeast revealed a non-coding RNA upstream of the *IMD2* locus, these 'promoter-associated transcripts' were shown to regulate *IMD2* expression in response to GTP levels, and initiate from unique upstream TSSs (Davis and Ares 2006; Jenks et al. 2008; Kuehner and Brow 2008). While non-coding transcripts initiating from upstream TSS have been implicated in gene regulation, characterization of this phenomenon genome-wide has not been performed.

4.4 – The RNAPII CTD

The RNAPII C-terminal domain (CTD) contains a heptad repeat of YSPTSPS (Corden et al. 1985). In *S. cerevisiae* the CTD is comprised of 26 repeats, while *S. pombe* maintains 29 repeats of the heptad and humans maintain 52 repeats (Schwer and Shuman 2011). Serine residues 2,5, and 7, tyrosine 1, and threonine 4 are all subject to phosphorylation and dephosphorylation by various kinases and phosphatases, while proline residues can undergo isomerization (Dahmus 1996; Singh et al. 2009; Kim et al. 2010a; Mayer et al. 2010; Hsin et al. 2011).

The phosphorlylation state of the CTD is highly predictive of polymerase activity, and serine 5 phosphorylation (S5P) is primarly associated with the 5' ends of

genes as this posttranslational modification is involved in recruiting the factors necessary for generating 5' methylguanosine caps on nascent transcripts (McCracken et al. 1997; Ho et al. 1998). Levels of the S5P modification decrease as RNAPII elongates and traverses the gene body (Mayer et al. 2010). Conversely, serine 2 phosphorylation (S2P) accumulates at 3' ends of genes and is associated with factors involved in canonical transcription termination (Kim et al. 2010a; Mayer et al. 2010)(Figure 6-14). The phosphorylation state of the RNAP CTD can also play a role in recruiting the Nrd1-Nab3-Sen1 complex, as the Nab3 subunit of the complex exhibits a significant affinity for S5P (Vasiljeva et al. 2008). Consequently, Nrd1-Nab3-Sen1 is enriched at the 5' end of many genes where levels of serine 5 phosphorylation are high (Kim et al. 2010a), though the role of the Nrd1-Nab3-Sen1 complex in the processing of coding transcripts, if any, is unknown. Interestingly, the

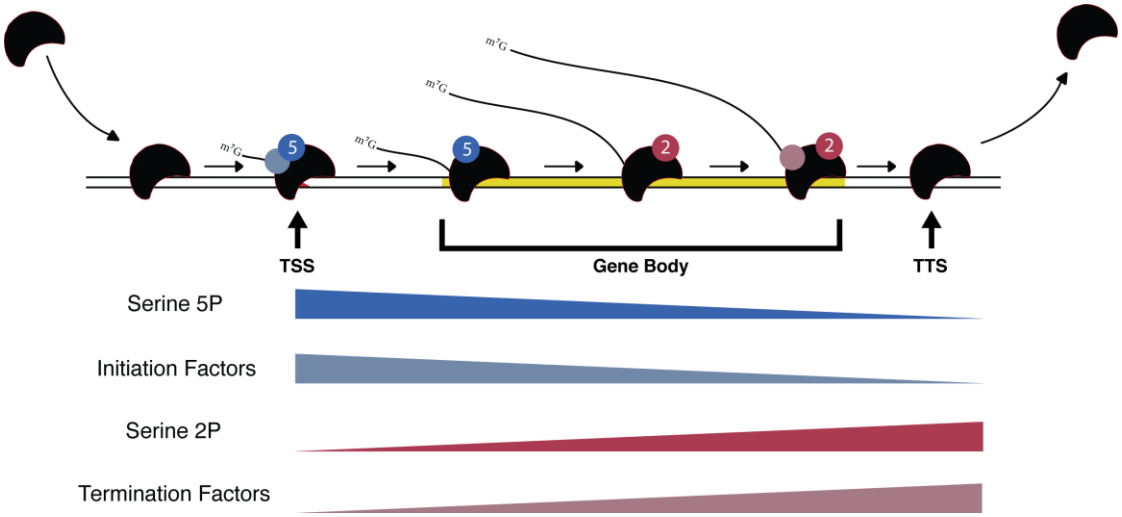

Figure 4-1– Simplified Illustration of the CTD Phosphorylation Cycle

Phosphorylation of serine 5 of the heptad repeat and transcription initiation factors accumulate at gene 5' ends and decrease in abundance as RNAPII enters the gene body. Conversely, serine 2 phosphorylation increases as RNAPII nears the 3' end of the gene, and maximal levels of serine 2 phosphorylation coincide with the binding of transcription termination factors.

Nrd1-Nab3-Sen1 also displays a tendency to co-occupy regions of high levels of S7P, though the significance of this observation is also unclear (Kim et al. 2010a).

The observed transition from high levels of S5P to S2P enrichment as RNAPII traverses transcriptional units is orchestrated by an ensemble of CTD kinases and phosphatases. The S5P posttranslational modification is the result of Kin28/Cdk7 kinase activity, and this mark is erased by the Rtr1 phosphatase (Mosley et al. 2009). Phosphorylation of serine 2 of the CTD heptad is the result of Ctk1 and Bur1/Bur2 activity (Qiu et al. 2009). While Kin28/Cdk7 also phosphorylate the CTD at serine 7 *in vitro* (Akhtar et al. 2009), dephosphorylation of this residue is achieved by Ssu72, not Rtr1 (Zhang et al. 2012). Mutation of the serine 7 residue to alanine causes defects in snRNA gene expression in mammalian cells (Egloff et al. 2007). The Ssu72 phosphatase plays a crucial role in the termination of non-coding RNAPII transcripts in *S. cerevisiae*, and impairment of of Ssu72 catalytic activity results in the extension of the 3'ends of these RNAs (Dichtl et al. 2002; Zhang et al. 2012).

Chapter 5 - Materials and Methods : Transcription Start Site Selection and Cryptic Transcription

5. 1 - Generation of deletion strains

To examine the roles of *RPB9* and *RRP6* in maintaining accurate TSS selection and degradation of non-coding transcripts, respectively, deletion mutants of each gene were generated. *RPB9* was disrupted with the G418 cassette (pUG6), and *RRP6* was disrupted with the NAT marker (pAG25), and both mutations were made in the wildtype S288C background. Oligonucleotides with homology to the 50bp directly upstream of start codon, and 50bp of homology directly downstream of the stop codon of each gene were used to amplify and target the cassettes. The template for the *rpb9*Δ::G418 PCR product was pUG6, and the template for the *rrp6*Δ::NAT PCR product was pAG25 (Table 5-1).

Table 5-1 – Oligonucleotides Used to Delete RRP6 and RPB9

RRP6 KO Forward	CGTTATGACTTCTGAAAATCCGGATGTACTTTTATCTAGGGTGATAAATGTGGagctgaagcttcgtacgc
RRP6 KO Forward	ATAATCACCTTTTAAATGACAGATTCTTACCTTTGGCGGCAGGCCTCCTCgcataggccactagtggatctg
RRP6 Test	CCCAAAAATATGAGGGCATCGG
NAT Test	TGTCGTCAAGAGTGGTACCCAT
RPB9 KO Forward	ATGACTACGTTTAGATTTTGTCGTGACTGCAACAATATGTTGTACCCTCGagctgaagcttcgtacgc
RPB9 KO Forward	CATTTTCTCTCCCTCTGTCATTAATTTTGAAAGTTCGTTGAGCACTCATGgcataggccactagtggatctg
RPB9 Test	GCCCCACGACGGCCATAACCACGAACAGCACC
G418 Test	CTCGAAACGTGAGTCTTTTCCTT

High efficiency LiAc transformations were performed as follows. 50ml of cells were grown in YPD and harvested at an OD_{600} of 0.7. Cells were then washed in 1ml of 100mm LiAc, and subsequently resuspended in 0.5ml of 100ml LiAc. 50ul of this resuspension was then aliquoted to a fresh tube, where the cells were pelleted and the supernatant removed. To these pelleted cells 240ul of 50% PEG 8000, 36ul of 1M LiAc, 10ul of 10mg/ml salmon sperm DNA, 50ul of deletion PCR product, and 24ul of H_20 were added in that sequence. This mixture was then vigorously vortexted for 30-60 seconds and incubated at 42˚C for 45 minutes. These cells were then plated on non-selective YPD plates and allowed to grow overnight. Following one day of growth, cells were replicated to selective plates containing either G418 (200mg/L) or NAT (0.1mg/ml) and allowed to grow for three days. Colonies grown on selective media were transferred to a second selective media plate. Singles colonies from the second round of selection were then grown in YPD, genomic DNA was prepared from these samples and they were checked for integration of the markers at the loci in question by PCR.

The *rpb9*Δ::G418 was created in a mating type a background, while the *rrp6*Δ::NAT mutant was generated in a mating type α background. To generate the double mutant the two were mated together and the resulting diploids were subsequently sporulated and subjected to tetrad dissection. Double mutant haploids were selected for based on their viability on media containing both drugs, G418 and NAT.

5.2 - Sporulation and Dissection of Tetrads

Diploid yeast were struck out on YPD plates and allowed to grow overnight. A single colony of yeast was then transferred to a plate containing a suboptimal carbon source, and also lacking a nitrogen source to induce sporulation. Sporulation was allowed to proceed for 4-7 days at 30˚C, and plates were sealed with parafilm to prevent desiccation of the media. Tetrads were scraped from the plate and resuspended in 1M sorbitol with 0.5mg/ml zymolyase 20T to weaken the integrity of the asci holding the individual spores together. Asci digestion was allowed to proceed for 5 minutes at room temperature and tetrads were gently plated on to a fresh YPD plate. Tetrads were dissected with a Nikon Eclipse 50i dissection microscope.

5.3 - Generation of Point Mutants

I generated a novel method of creating site-specific point mutants in *S. cerevisiae* to make these strains that uses PCR stitching. The oligonucleotide set to generated the first PCR product contains a 71 nucleotide oligonucleotide with the desired point mutation flanked by 50bp of surrounding homology to the yeast genome upstream, and another 20 bases of homology downstream. The second oligo used to generate this PCR product has homology to the 50 bases downstream of the cleavage and polyadenylation site of the transcript corresponding to the gene I am attempting to mutate at its 5’ end. The 3’ end of this oligo has homology selectable drug marker resistance cassette (Table 5-2).

The second PCR product utilizes one oligonucleotide with only homology to the G418 resistance cassette being amplified, and a second oligonucleotide with homology to the G418 resistance cassette at its 5' end, and 50 bases of homology to the yeast locus to which it is being targeted.

Table 5-2 – Oligonucleotides utilized to generate PCR products for the introduction of point mutations

RPO21-E1103G Forward (PCR 1)	ACCAGCCACACAAATGACCCTTAACACCTTCCATTTTGCTGGTGTTGC TTCCAAAAAAGTTACTTCTGGTGTCCCCCGTTTAAAGGGAATTTTGAA TGTGGCC
RPO21-E1103G Reverse (PCR 1)	GCAGCGTACGAAGCTTCAGCTATTCCCTATCCCTACCATAATGCTATG AAAAAT
RPO21-E1103G Forward (PCR 2)	AGCTGAAGCTTCGTACGCTGC
RPO21-E1103G Reverse (PCR 2)	CTAGCGCCGTTGGTTTTCCCAATGCTCTGCGGATATAAATTAGTTACT TGCGCATAGGCCACTAGTGGATCT
RPO21-H1085Q Forward (PCR 1)	TCTGTTGTTCACCCTGGTGAAATGGTTGGTGTTCTAGCAGCCCAATCC ATTGGTGAACCAGCCACACAAATGACCCTTAACACCTTCCAATTTGCT GGTG
RPO21-H1085Q Reverse (PCR 1)	GCAGCGTACGAAGCTTCAGCTATTCCCTATCCCTACCATAATGCTATG AAAAAT
RPO21-H1085Q Forward (PCR 2)	AGCTGAAGCTTCGTACGCTGC
RPO21-H1085Q Reverse (PCR 2)	CTAGCGCCGTTGGTTTTCCCAATGCTCTGCGGATATAAATTAGTTACT TGCGCATAGGCCACTAGTGGATCT
SSU72-R129A Forward (PCR 1)	CTTGTGAAGAGAGATGTTTTGATGCCGTTTGTGAAGATTTGATGAATG CAGGTGGGAAATTAAACAAAAT
SSU72-R129A Reverse (PCR 1)	GCAGCGTACGAAGCTTCAGCTTATTACGTTTCTTGTTGCGGCTCTCT
SSU72-R129A Forward (PCR 2)	AGCTGAAGCTTCGTACGCTGC
SSU72-R129A Reverse (PCR 2)	ACAGTGTGTTGTATATCAAGCTTCTTGATAAAAAAATAGCTATGTGGA CAACAAGCAAATAATGTGCTTACGCATAGGCCACTAGTGGATCT
RPO21 Test	GTTCTGTTGTTCACCCTGGTGAAA
SSU72 Test	GGCAAGAAAGTACAAAAGTCTTCGACTTCG
G418 Test	CTCGAAACGTGAGTCTTTTCCTT
HYG Test	AAGTACTCGCCGATAGTGGAAA

These two products are then stitched together in a third PCR reaction, and this final PCR product is gel excised and used in a transformation reaction described above

(Figure 5-1). Cells in which the PCR was correctly targeted and successfully inserted will then contain the mutation at the desired site and a G418 resistance cassette downstream of the mutated gene. In effect the point mutation has been 'tagged' with G418 resistance. Colonies that survived two rounds of selection on drug containing media were then sequenced at the loci in question to verify the mutation. In order to examine the effects these mutation had on the production of cryptic RNAs strains harboring these mutations were crossed to the *rrp6*Δ strain mentioned above.

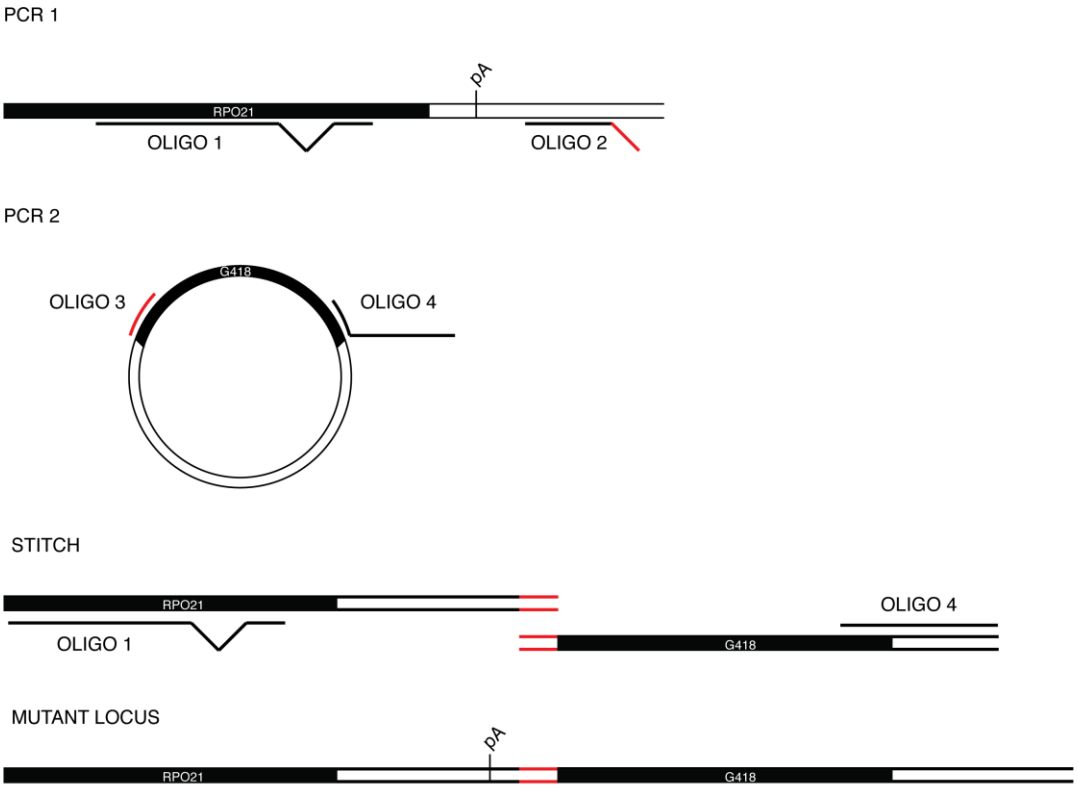

Figure 5-1 – Outline of the Method

PCR 1 - Oligo 1 maintains homology to the locus, with a mismatch where the desired mutation will be made. Oligo contains homology to the sequence downstream of the poly(A) signal, and a flap to anneal to PCR 2. Oligo 3 anneals to a plasmid containing a drug resistance cassette. Oligo 4 anneals to the same plasmid, and contains a flap with 50bp of homology to the locus to be targeted. PCR1 and PCR2 are then stitched together in a third PCR reaction and the stitched product is transformed into the desired genetic background.

5.4 – Preparation of RNA

RNA was prepared via the hot phenol method (Schmitt et al. 1990). Briefly, were 50 ml of cells harvested during logarithmic growth, pelleted, and washed with 50ml ddH_20. Pellets were transferred to 1.7ml eppendorf tubes and placed on ice. To each pellet 300ul of acid phenol (pH 4.5), 300ul of AE Buffer (50mM sodium acetate

(pH 5.2), 10mM EDTA (pH 8.0)), and 60ul of 10% SDS. Tubes containing this mixture were vigorously vortexed for 60-120 seconds and incubated at 65˚ for 10 minutes or until the phases separated. At this point the tubes were again vortexed for another 60 seconds and phases were again allowed to separate while being incubated at 65˚C. Tubes were then spun down at maximum speed in a tabletop centrifuge for five minutes. The supernatants were then transferred to tubes already containing 300 of fresh acid phenol, briefly vortexed and centrifuged at maximum speed for five minutes. Phenol extractions were repeated until the interface between the aqueous phase and the phenol became clear. RNA was precipitated by transferring the aqueous phase to a tube already containing 900ul of ethanol and 10ul of 3M NaOAc (ph 5.2), and spinning down at maximum speed in a tabletop centrifuge at 4˚C for 30 minutes. RNA pellets were subsequently washed with 80% ethanol to remove salt, and ultimately resuspended in ~50ul of sterilized H_20. RNA concentrations were quantified using 1:50 dilutions on the GE NanuVue.

5.5 - Northern Blotting

30ug of total RNA was run on a 1.1% denaturing formaldehyde agarose gel. To make the gel 1.65g of agarose was dissolved in 110ml of H_20 by microwaving for 2 minutes. One the agarose mixture had cooled to ~65˚, 15ml of 10X MOPS buffer and 25ml of 37% formaldehyde were added. Once the solution was mixed to homogeneity the gel was cast. While the gel solidified, RNA samples were denatured at 65˚C for 5 minutes. Following denaturation 2 volumes of loading buffer was added

to each sample (1ml Loading Buffer : 750ul Formamide, 150ul 10X MOPS Buffer, 75ul 37% Formaldehyde, 25ul H_20, and 1ul 10mg/ml Ethidium Bromide). Gels were run at 85V for 1 hour in 1X MOPS buffer. Gels were then washed three times for 8 minutes with 500ml ddH_20, and subsequently equilibrated with 500ml 10X SSC buffer for 30 minutes.

Following SSC equilibration RNA was transferred to an uncharged GeneScreen nylon matrix via capillary transfer overnight. The RNA was then crosslinked to the membrane in the Spectrolinker XL-1000 UV Crosslinker utilizing the 'Optimal Crosslink' setting. The membrane was then transferred to a hybridization tube and blocked with 25 ml of hybridization buffer (5X SSC, 50% Formamide, 0.1 mg/ml salmon sperm DNA, 5X Denharts Solution, 0.2% SDS) for 30 minutes to several hours at 45˚C.

While the membrane was being blocked, radiolabelled probes targeting the transcript of interest were generated. 25ng of a 300-400bp PCR product with homology to the transcript served as the template for randomly primed synthesis of P32 alpha-dCTP labeled probes generated using the Roche High Prime kit (Table 5-3). Unincorporated label was removed by passing the reaction over G50 spin column to reduce non-specific background signal. The radioactive probe was then denatured at 95˚C for five minutes and subsequently placed on ice. The denatured probe was then added to the hybridization tube containing the membrane and the hybridization buffer, and hybridization was allowed to proceed overnight at 45˚C.

The membrane was then washed twice with low stringency wash buffer (6X SSC, 0.5% SDS) for 5 minutes at 45˚ and once with low stringency wash buffer (0.5X SSC, 0.5% SDS) for 5 minutes at 45˚C. The membrane was then exposed overnight to a phosphor screen and visualized using a GE Typhoon FLA 9500.

Table 5-3 Oligonucleotides used for generation of GCN4 Promoter Northern Probe

GCN4 Northern F	GATCTTCGGGGAATAAAGTGCATG
GCN4 Northern R	GTATAATTCGCTAGTGAAACTGATGG

5.6 - Primer Extension

50pmol of oligonucleotide was radiolabeled using in a 30ul reaction with 2ul of gamma P32 and Polynucleotide Kinase (NEB Catalog #: M0201S). The reaction was allowed to proceed for 30 minutes at 37˚C. Free label was removed from the reaction using a G-50 column.

30ug of total RNA was mixed with 0.15ul of labeled oligonucleotide (Table 5-4) and 2ul of 5X Annealing Mix (25mM Tris-Cl pH 8.3, 375mM KCl, 5mM EDTA) in a total of 10ul. This mix was boiled for 1 minute, briefly centrifuged and annealing of the oligonucleotide to RNA was allowed to proceed for 45 minutes at 48˚C. Following the annealing, 20ul of RT Mix (50mM Tris-Cl pH 8.3, 75mM KCl, 4.5mM $MgCl_2$, 15mM DTT, 0.1mM dNTPs, SuperScript II Reverse Transcriptase 100U) was added to the reaction, and the reaction was incubated at 48˚C for another 30 minutes. 100ul of 100% ethanol was then added to the reaction, as was 3ul of 3M NaOAc, and

this precipitation was spun down at max speed in a tabletop microcentrifuge for 30 minutes at 4˚C. The resulting pellet was subsequently washed with 80% ethanol, and resuspended in 10ul of 10 ug/ml RNase A solution. The pellet was allowed to enter solution and total RNA was degraded by incubating at 37˚C for 30 minutes. Once the pellet has gone into solution, one volume of loading buffer (100% formamide) containing xylene cynanol (0.025% (w/v)) and bromophenol blue (0.025% (w/v)) was added. Extension products were resolved on 6% denaturing polyacrylamide gels run at 20W for 30-45 minutes. The gels were then exposed to a phosphor screen for several hours to overnight depending on intensity of signal, and subsequently visualized using a GE Typhoon FLA 9500.

Table 5-4 – Oligonucleotides used for primer extension

GCN4	GTATAATTCGCTAGTGAAACTGATGG
TPI1	CAACTTCGACATTTTCTGGGATAGAAG
IDH2	AATTGTTGTTCGTTCCCGATCTGTATC

5.7 - Generation and Optimization of a Method to Sequence RNA 5' Ends

To investigate the severity of the effects of *rpb9*Δ and *rrp6*Δ on TSS selection genome-wide we turned to an RNA-seq based approach. Template switch methods have been shown to be effective in mapping the 5' ends of 7-methylguanosine capped transcripts, specifically (Picelli et al. 2013). This is due to the fact that the protocol relies on SuperScript II, which has the ability to utilize the 7-methylguanosine cap as a template in the reverse transcription reaction. As a result, the 3' end of the randomly primed reverse transcription (RT) product is tailed with multiple deoxycytidine

residues. These residues then allow for the annealing of a Template Switch Oligo (TSO) tailed with three ribo-guanosines on its 3' end. Once annealed, the reverse transcription reaction can continue on through the template switch oligo (Figure 5-2). It should be noted that the 3' end of the TSO is methylated, to prevent it from being used as a template by the reverse transcriptase.

Sequences included at the ends of the RT primer and the TSO allow for the RT products to be amplified in a semi-suppressive PCR reaction. The purpose of this reaction is to enrich RT products that resulted from RNA being the substrate, and to suppress products that are the result of random priming from the TSO. When the RT oligo primes off of the TSO it will produce a product < 60 bp. The 3' ends of the RT primer and the TSO are highly complementary, thus the likelihood of the short products annealing to themselves is very high, and the two ends often out-compete the binding of the amplification oligos in the PCR reaction. For longer RT products the odds of the two complimentary ends finding and annealing to each other is reduced, and these products are more likely to be amplified in the PCR. (Figure 5-4).

Our modified protocol is segmented into eight steps: randomly primed reverse transcription, template switch, semi-suppressive PCR, kinasing, dA tailing, hair-pin adaptor ligation, uracil DNA glycosylase/endo VIII treatment, and a round of barcoding PCR (Figure 5-2).

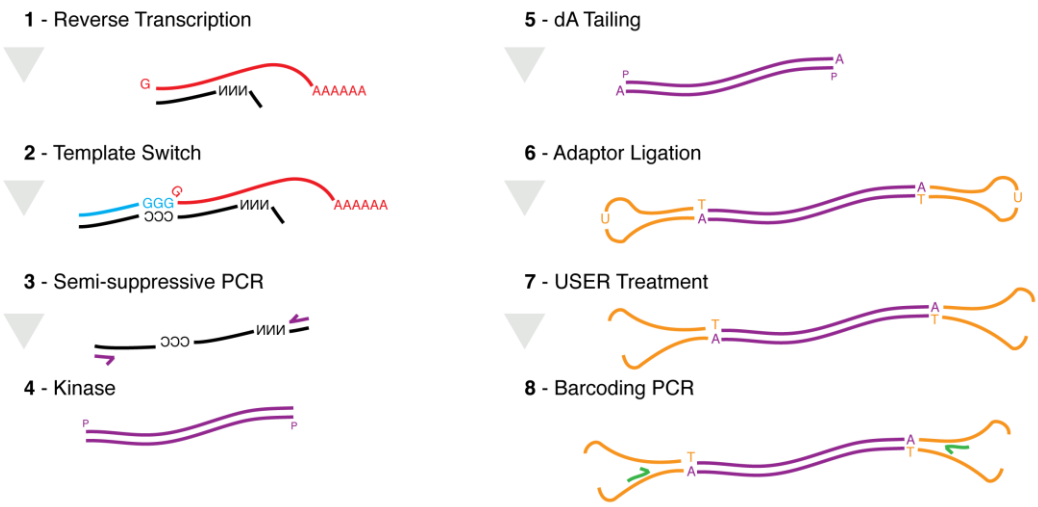

Figure 5-2 – Outline of the 5' RNA-seq Methodology

5.7.1 - Reverse Transcription and Template Switch

Reverse transcription / template switch for each sample was performed in duplicate, in two separate tubes. 100 ug of total RNA, 1ul of 100uM Random Priming Oligo (Table 5-1) and 1ul of 10mM dNTPs were mixed and denatured at 65˚C for 10 minutes. 7ul of RT Mix (1X First Strand Buffer, 10mM $MgCl_2$, 2.5mM DTT, 1M Betaine, 1uM Template Switch Oligo, 5U SUPERse In RNAse Inhibitor, 100U SuperScript II)(Table 5-1) was then added and the reverse transcription was allowed to proceed at 42˚C for 90 minutes, followed by 10 cycles of extension (50˚C - 2 minutes; 2 minutes - 42˚C). Reactions were then terminated at 70˚C for 15 minutes. Duplicates were then pooled and purified with 1.6 volumes of 'homebrew Magna beads' (1M

Tris-HCl pH 8.0, 1mM EDTA pH 8, 1M NaCl, 18% PEG-8000, 0.1% Sera-Mag SpeedBeads [Thermo Scientific]), and resuspended in 40ul TE pH 8.0 (Figure 5-3).

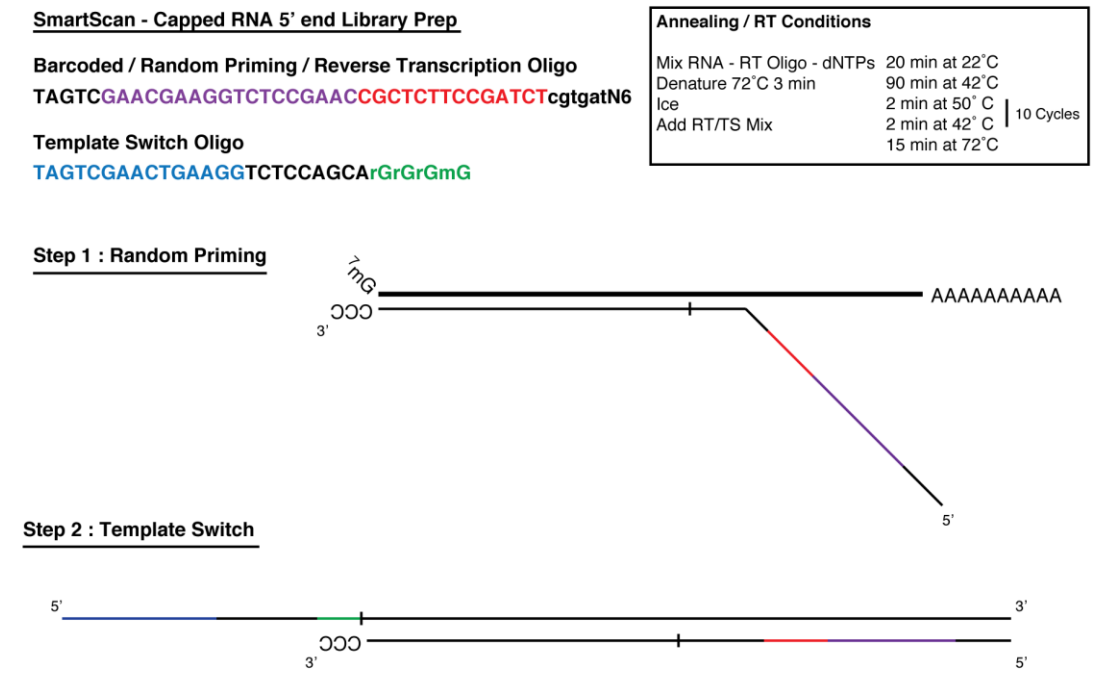

Figure 5-3– Illustration of the Reverse Transcription and Template Switch Steps of the 5' RNA-seq protocol

5.7.2 - Semi-suppressive PCR

Each semi-suppressive PCR reaction was performed in duplicate (Figure 5-4). Reactions consisted of 15ul of RT-TS products, 50 ul of KAPA Hot Start Polymerase, 0.3 ul of each Semi-suppresive oligo (100uM Stock), and 34.4 ul H_20. The PCR reaction was performed as follows:

Stage 1 – 1 cycle – 95˚C, 3 minutes

Stage 2 – 15 Cycles – 95˚C, 15 seconds; 65˚, 15 seconds; 68˚C, 2 minutes

Stage 3 - 4˚C - ∞.

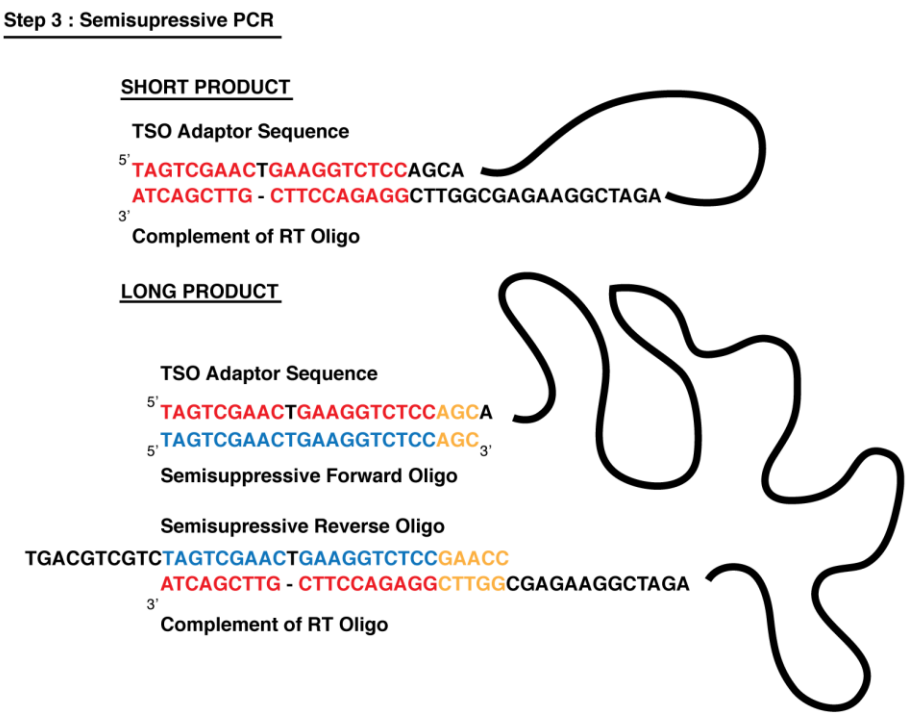

Figure 5-4– Illustration of the semi-suppressive PCR

Semisupressive PCR prevents amplification of small products, including products resulting from random priming utilizing the template switch oligo as a substrate.

Duplicate samples were pooled and purified with 1.8 volumes of 'homebrew Magna beads' (1M Tris-HCl pH 8.0, 1mM EDTA pH 8, 1M NaCl, 18% PEG-8000, 0.1% Sera-Mag SpeedBeads [Thermo Scientific]), and eluted with 30 ul of 1X TE pH 8.0. To optimize the size distribution and the yield of the semi-suppressive PCR products we attempted varying the concentration of the oligos in the PCR, and the amount of Ampure beads used in the purification. We hypothesized that a lower concentration of oligos could result in a library biased towards longer products, and

that higher oligonucleotide concentrations would generate shorter products. We determined that the effect of oligonucleotide concentration on the size distribution of the library (if any) is subtle. However, using 30pmol of each primer, rather than 10pmol, significantly increased the yield of the PCR. Further, using 1.8 volumes of 'homebrew Magna beads' allowed us to retain a larger fraction of semisuppressive PCR products in the 300-500 base pair range, than using 1.5 volumes of beads. Given that many cryptic RNAs exhibit a similar size distribution we decided that it would be best not to deplete the libraries of products in this range and to use 1.8 volumes of beads (Figure 5-5).

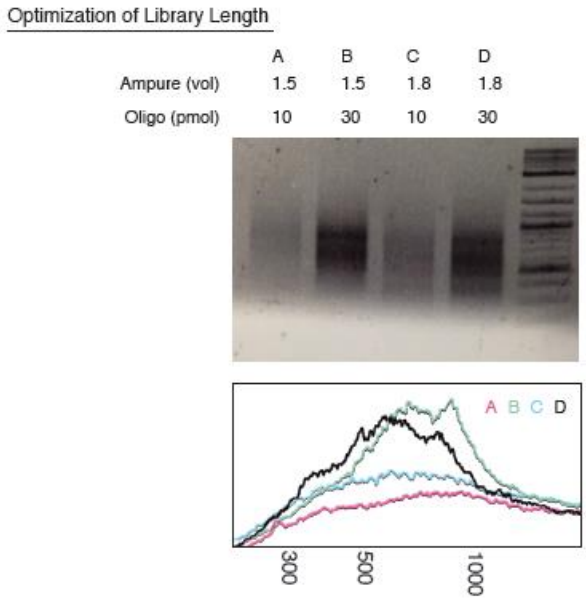

Figure 5-5 – Optimization of semi-suppressive PCR

Different concentrations of oligonucleotides in the PCR, and Ampure beads to clean up the reaction were tested.

Table 5-5 – Oligonucletides Used to Generate RT and Semi-suppressive PCR Products

SET I : Template Switch	TAGTCGAACTGAAGGTCTCCAGCAGrGrGmG
SET I : ss Forward	TAGTCGAACTGAAGGTCTCCAGC
SET I : Random RT	TAGTCGAACGAAGGTCTCCGAACCNNNNNN
SET I : ss Reverse	TGACGTCGTCTAGTCGAACTGAAGGTCTCCGAACC
SET IV : Template Switch	GCTGATCCAGTCCTTGAGAACTAArGrGrGmG
SET IV : ss Forward	GCTGATCCAGTCCTTGAGAACTA
SET IV : Random RT	GCTGATCCATCCTTGAGAATCCAANNNNNN
SET IV : ss Reverse	GTCATGATGAGCTGATCCAGTCCTTGAGAATCCAA

5.7.3 - End Repair, Ligation, and Barcoding/Amplification

PCR products were then treated with 20U T4 Polynucleotide kinase (37˚C for 30 minutes) with T4 DNA Ligase buffer (50mM Tris-HCl, 10mM $MgCl_2$, 1mM ATP, 10mM DTT, pH 7.5) serving as a source of ATP. Kinased PCR products were purified with 1.6 volumes of 'homebrew Magna beads' and eluted in 7ul of 1X TE. 1ul of 10mM dNTPs, 1 ul of 10X Taq DNA Polymerase Buffer (10mM Tris-HCl, 50mM KCl, 1.5mM $MgCl_2$, pH 8.3)(Rohland and Reich 2012) and 1ul Taq DNA Polymerase (5 U/ul) were added to each sample, bringing the reaction volume to 10ul. dA tailing reactions were allowed to proceed at 72˚C for 15 minutes. Reactions were then run on a 1% Agarose gel and products in the 200-700bp were excised and purified with the Qiagen QIAquick Gel Extraction Kit (Cat. No. 28706) as per manufacturer's instructions. Following elution from the column in 50ul of TE (10mM Tris, 1mM EDTA, pH 8) the products were precipitated with 5ul of 3M Sodium acetate and 200ul

of 100% ethanol. Pellets were washed with 200ul of 70% ethanol, and resuspended in 17.5 ul 1X TE (10mM Tris, 1mM EDTA, pH 8).

NEBNext adaptors for Illumina were then ligated onto the kinased, dA tailed products with T4 DNA Ligase at room temperature for 1 hour. The reaction consisted of 17.5ul semi-suppressive PCR products, 2.5ul of NEBNext adaptors (Cat. Nos. E7335S & E7500S), 2.5ul of T4 DNA Ligase (400U/ul), and 2.5ul of 10X T4 DNA ligase buffer (500mM Tris-HCl, 100mM $MgCl_2$, 10mM ATP, 100mM DTT, pH 7.5), for a total volume of 25ul. Ligation products were purified with 1.6 volumes of 'homebrew Magna beads' (40ul), and subsequently eluted with 25ul 1X TE (10mM Tris, 1mM EDTA, pH 8).

To 12.5ul of adaptor-ligated products 1uL of Universal Oligo, 1uL of Barcoded Oligo, 7.5 uL of H_20, 25 ul of 2X KAPA Hot Start Polymerase (KAPABiosystems Kit#: KK2602), and 3uL of NEB USER Enzyme (0.15 U) were added. Unique barcoding sequences were assigned to each genotype (Table 5-6). PCR Amplification conditions were as follows: *Stage 1* – 1 cycle – 37˚C, 15 minutes; 95˚C, 1 minute; *Stage 2* – 10 Cycles – 95˚C, 15 seconds; 65˚, 15 seconds; 68˚C, 2 minutes; *Stage 3* - 4˚C - ∞. Barcoded products were purified with 1.6 volumes of 'homebrew Magna beads' and submitted to the core facility at MSKCC, Integrated Genomics Operation (iGO) for sequencing on the Illumina HiSeq platform. Paired end reads were filtered to exclude reads shorter than 150bp or longer than 500bp. 29 base pairs were trimmed from the 5' end of each filtered read before being aligned to the *S.*

cerevisiae genome (version R64-2-1 2014_11_18) with Bowtie2 software utilizing the 'local' mapping setting (Langmead and Salzberg 2012)(Figure 5-7).

Table 5-6 – Barcode Sequences for Each Indexed Genotype

Genotype	Index Number	Barcode Sequence
Wt	13	AGTCAA
*rrp6*Δ	14	AGTTCC
*rpb9*Δ	15	ATGTCA
*rrp6*Δ*rpb9*Δ	16	CCGTCC

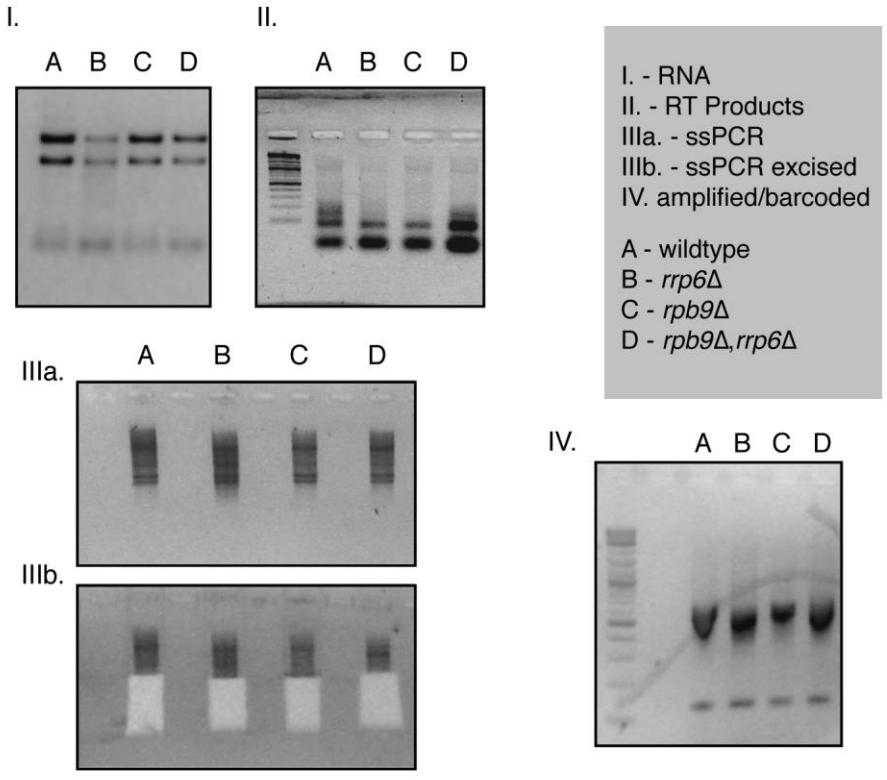

Figure 5-6 – Products Following Each Stage of the Protocol

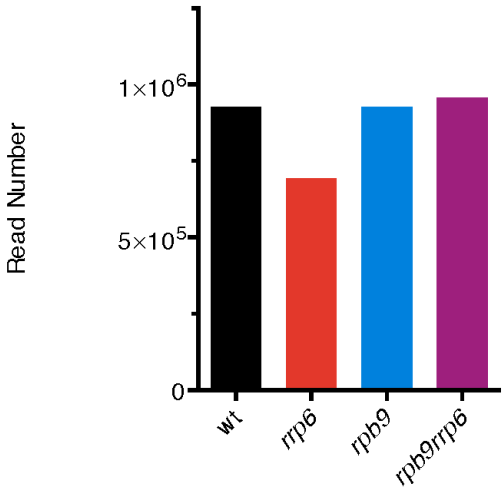

Genotype	Read #
wt	926620
rrp6	694047
rpb9	926643
rpb9rrp6	956878

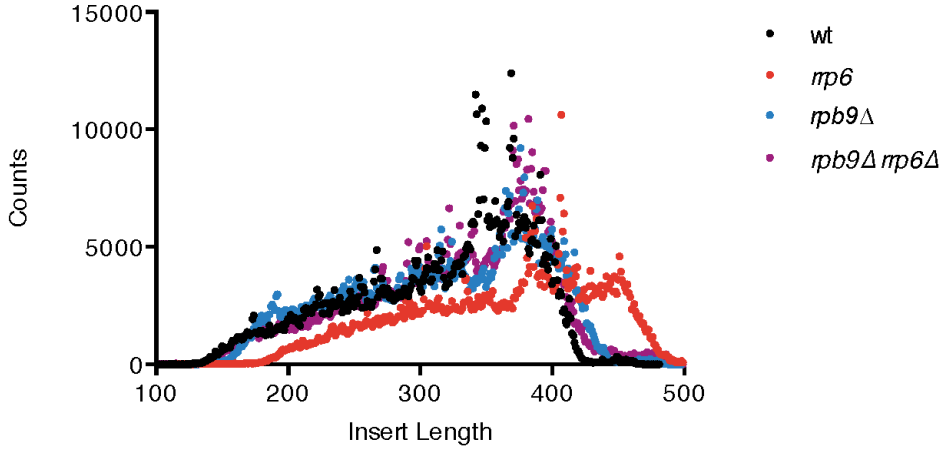

Figure 5-7 – Depth and Size Distribution of RNA-seq Libraries

Chapter 6 - Misregulation of RNAPII Trigger Loop Dynamics Resuslts in Cryptic Transcript Initiation Within NFRs

6.1 Summary

Several studies have previously implicated Rpb9 in transcription start site selection via *in vivo* and *in vitro* approaches (Sun et al. 1996; Hemming and Edwards 2000; Hemming et al. 2000; Ziegler et al. 2003). To date only a single study has performed genome-wide analysis of transcription in an *rpb9*Δ mutant (Hemming et al. 2000). This study found that the transcriptional output of many genes drops significantly in the absence of *RPB9*, and this effect was largely attributed to defective transcription elongation as *rpb9*Δ and *dst1*Δ exhibit synthetic lethality (Hemming and Edwards 2000; Hemming et al. 2000).

Many non-coding transcripts are degraded by the nuclear exosome complex in *S. cerevisiae* (Wyers et al. 2005; Davis and Ares 2006; Neil et al. 2009; Xu et al. 2009). These transcripts are ~200-500 nucleotides in length, and utilize a unique 3' end processing pathway involving the Nrd1-Nab3-Sen1 (NNS) complex, a non-canonical polyA polymerase complex termed TRAMP, and the nuclear exosome (Vasiljeva et al. 2008; Jamonnak et al. 2011). Deletion of non-essential 3'->5' exonuclease, and exosome component, RRP6, stabilizes thousands of cryptic transcripts (Wyers et al. 2005; Davis and Ares 2006; Neil et al. 2009; Xu et al. 2009).

Given the involvement of Rpb9 in transcription start site selection, we considered a model in which the observed decrease in transcriptional output caused by

*rpb9*Δ is result of transcripts initiating from non-canonical start sites and being targeted by the exosome, and not a defect in transcription elongation.

6.2 Results

6.2.1 - Transcripts initiating upstream of canonical start sites are targets of the exosome

To test the hypothesis that alteration of start site selection could induce cryptic initiation, we generated an *rrp6*Δ*rpb9*Δ mutant, and performed primer extension at loci that had previously been shown to be negatively impacted by *rpb9*Δ. (Figure 6-1) (Hemming et al. 2000). While signal corresponding to the mRNA TSS of these transcripts is suppressed in the *rpb9*Δ background, as expected, we found that transcripts initiating further upstream were stabilized in the absence of *RRP6* (Figure 6-1). Further, in the *rrp6*Δ*rpb9*Δ background we find that the Cryptic Transcription Start Site (cTSS) transcripts are generated at the expense of transcripts initiating from the canonical TSS (Fig 1A). Analysis of GCN4 transcripts by northern blot shows that full-length transcripts are lost in favor of short non-coding transcripts when Rpb9 is absent (Figure 6-1 A).

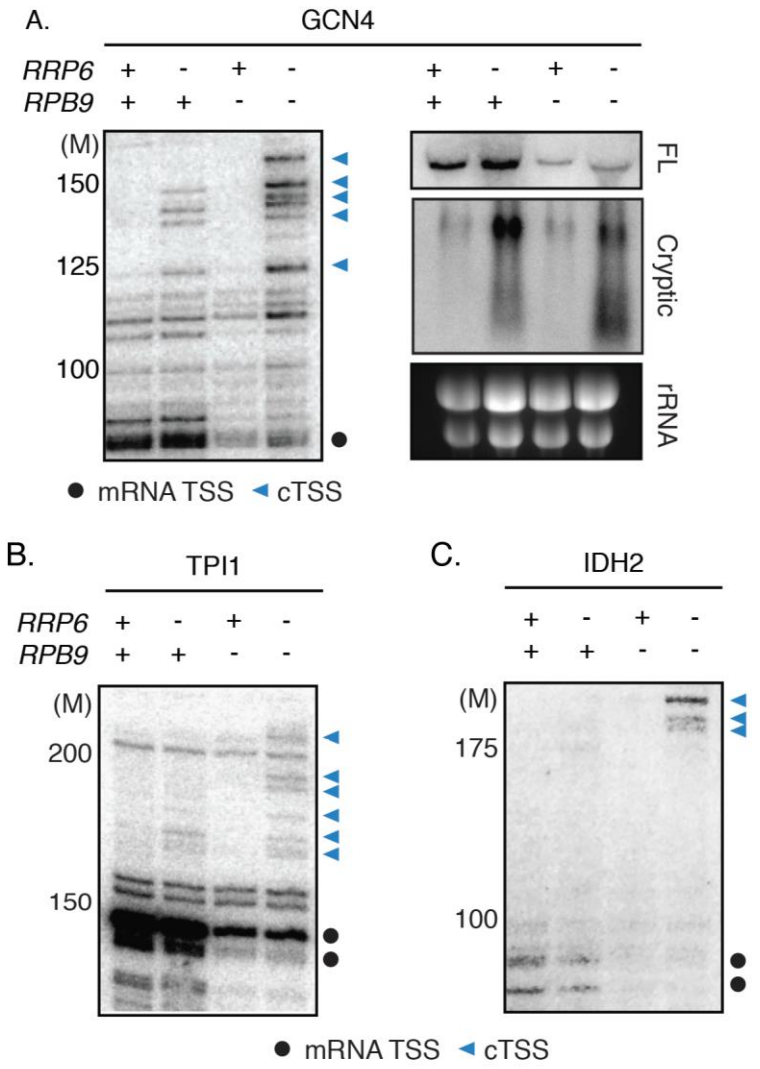

Figure 6-1 – Loss of RPB9 Causes Cryptic Transcription Initiation

A. Primer extension examining 5' end of transcripts at the GCN4 locus (left panel). Black circle denotes mRNA TSS. Blue triangles indicate cryptic start sites. Northern blot of transcripts emanating from the GCN4 locus (right panel). **B-C.** Primer extension of transcripts at the TPI1 (**B**) and IDH2 (**C**) loci.

Interestingly, we observe synthetic sickness between *rpb9*Δ and *rrp6*Δ, indicating that the accumulation of non-coding RNA may be toxic in the double mutant (Figure 6-2).

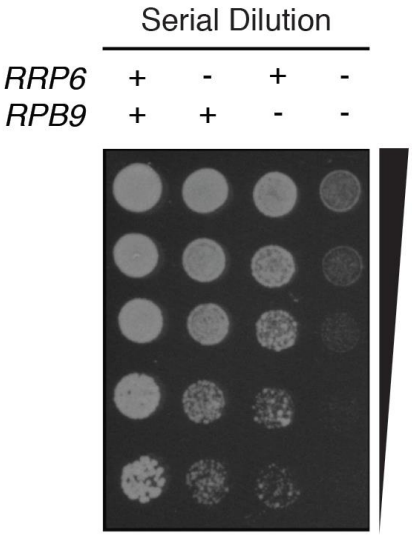

Figure 6-2 – Synthetic Sickness of *rpb9*Δ*rrp6*Δ

Serial dilution of wildtype, rrp6Δ, rpb9Δ, and rpb9Δrrp6Δ strains.

6.2.2 - cTSS Transcripts are Widespread

To ascertain how widespread of an effect *rpb9*Δ has on cryptic initiation we generated genome-wide TSS maps utilizing a modified template-switching based method (Chapter 5.7) in wildtype, *rrp6*Δ, *rpb9*Δ, and *rpb9*Δ*rrp6*Δ backgrounds (Picelli et al. 2013). The RNA-seq was filtered for reads under 300bp, and each sample was normalized based on total read number. Transcription start sites have been extensively mapped in wildtype *S. cerevisiae*, most recently by the isoform profiling method, and the 5' ends of our reads correlate highly with previously annotated TSSs (Figure 6-3) (Pelechano et al. 2013).

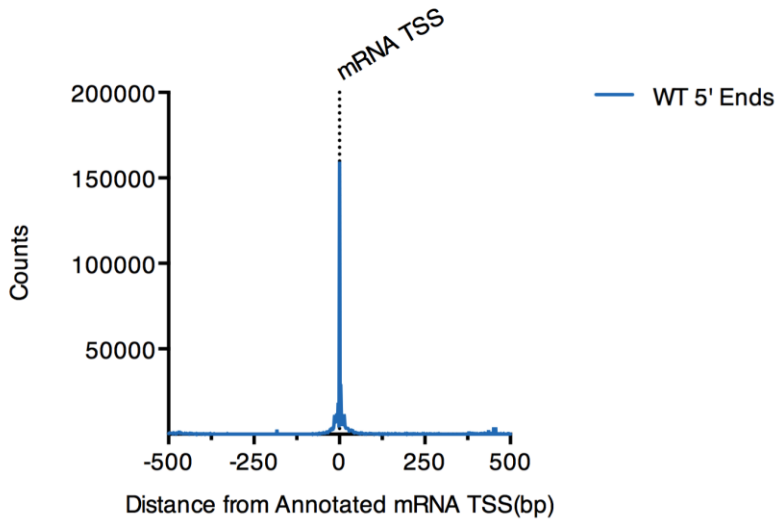

Figure 6-3 – Global Alignment of Mapped 5' Ends to Annotated TSSs

Wildtype 5' ends of transcripts determined in this study compared to previously annotated TSS (Pelechano et al. 2013).

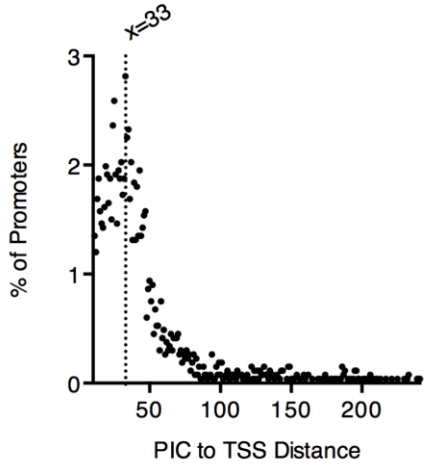

Figure 6-4– Determining the PIC to TSS Distance

PIC to TSS distance (PTD) was calculated for all genes for which a PIC (Rhee and Pugh 2012) and TSS has been determined. A PTD of 33bp is most common.

Additionally, transcription pre-initiation complexes (PIC) have been mapped via ChIP-exo for myriad General Transcription Factors (Rhee and Pugh 2012). Utilizing these two pieces of information we are able to determine how many base pairs RNAPII must scan between the site of PIC assembly and initiation of transcription, we refer to this as the PIC to TSS distance (PTD). *S. cerevisiae* is excellent model for studying start site selection in that transcription does not initiate a fixed distance from the site of PIC formation at each promoter. In higher eukaryotes transcription is believed to initiate ~30 bp downstream of the PIC, while in budding yeast this distance has been observed to be over three times as long at some promoters (Hampsey 1998; Smale and Kadonaga 2003). However, analysis of our data reveals that initiation typically occurs 33 bp downstream of the PIC in budding yeast (Figure 6-4).

We limited analysis of the effects of *rrp6*Δ, *rpb9*Δ, and *rpb9*Δ*rrp6*Δ to the defined PTDs to specifically isolate the 5' ends of transcripts resulting from premature initiation. Additionally, we are able to study the effect of these mutants on transcription initiation from and around canonical mRNA TSSs. Subtracting the number of normalized counts in the wildtype sample from the mutant samples, we find that *rpb9*Δ*rrp6*Δ causes accumulation of cTSS transcripts (Figure 6-5A). Further, this observation is coupled depletion of reads mapped to corresponding to mRNA TSSs (Figure 6-5B). We find that 236 of 2665 promoters for which we can define a PTD exhibit this behavior. Subsequent analysis is focused on this set of promoters. This

observation broadens the interpretation our results observed at the GCN4, TPI1, and IDH2 promoters.

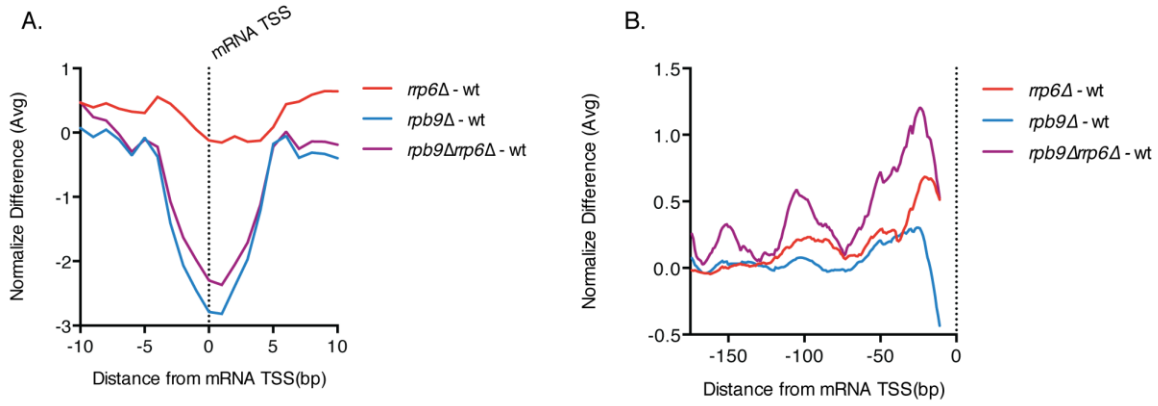

Figure 6-5 – Effect of rrp6Δ and rpb9Δ on the 236 Promoters Exhibiting the Accumulation of cTSS Transcripts

A. Difference between *rrp6*Δ, *rpb9*Δ, and *rpb9*Δ*rrp6*Δ with respect to wildtype around mRNA transcription start sites, 10bp upstream and downstream. **B.** Effect of mutants on transcription initiation upstream of start sites.

We hypothesized that promoters with longer PIC to TSS distances (PTD) might be the most sensitive to *rpb9*Δ, given that each base within the PTD is an opportunity to initiate transcription. Concordantly, we find that RNAPII must scan 56bp on average at promoters exhibiting high numbers of cTSS transcripts. This is significantly higher than the genome average of 39bp (Figure 6-6). Interestingly, the degree to which transcripts are stabilized in the absence of the exosome is inversely correlated to their proximity to the +1 nucleosome. Cryptic transcripts initiating further upstream of the mRNA TSS exhibit a higher fold-change in *rrp6*Δ and *rpb9*Δ*rrp6*Δ mutants when compared to their counterparts in which the exosome is fully active (Figure 6-6). This indicates that the transcripts initiating further away from canonical TSSs are more sensitive to degradation by the nuclear exosome.

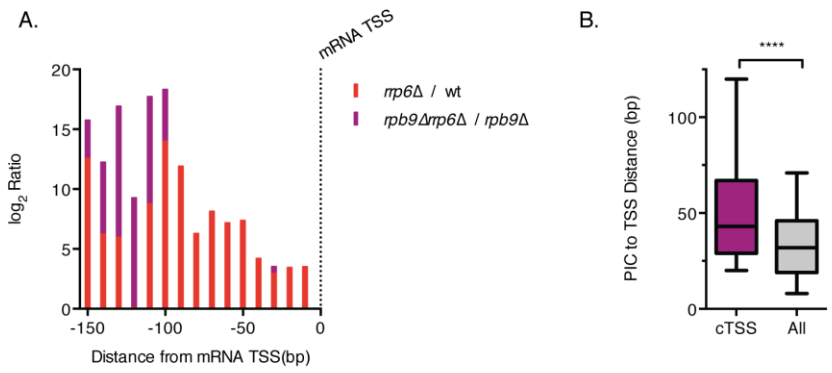

Figure 6-6 – Accumulation of Cryptic Transcripts within PIC to TSS Distances

A. Log2 ratio of *rrp6*Δ/wt (red) and *rpb9*Δ*rrp6*Δ/*rpb9*Δ (purple) is plotted as a function of distance from the TSS. **B.** PIC to TSS distances of cTSS promoters (purple) and all promoters (grey).

6.2.3 - The +1 nucleosome directs the transition from scanning to elongation for mRNA Transcripts

TSSs are highly associated with the +1 nucleosome (Jiang and Pugh 2009b; Hughes et al. 2012), suggesting that promoter scanning is potentially limited to non-nucleosomal promoter DNA, and that transcription may begin once contact with the +1 nucleosome is made. Aligning nucleosomes to cTSS promoters and calculating the $\log_2$ ratio of normalized *rpb9*Δ*rrp6*Δ reads over wildtype we find that cryptic 5' ends are highly enriched immediately upstream of the +1 nucleosome, and that this enrichment is accompanied by a depletion of initiation within the nucleosome (Figure 6-7). This behavior can be observed at the individual loci *NOP16*, *LSB5*, and *RTF1* (Figure 6-8). By examining the start site data in the context of promoter chromatin we have uncovered a potential role in +1 nucleosomes in preventing nascent transcripts from being recognized and terminated by the Nrd1-Nab3-Sen1 complex and ultimately degraded by the nuclear exosome.

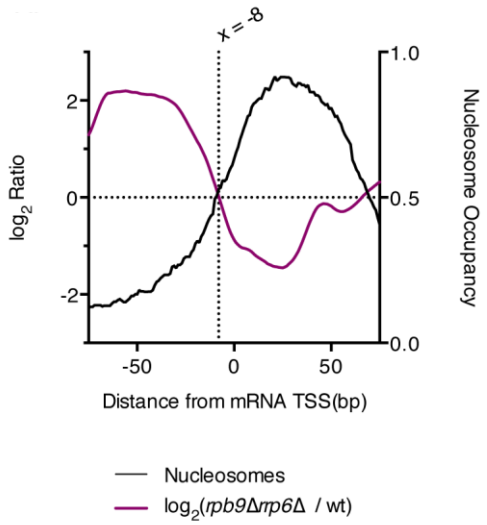

Figure 6-7 – Cryptic Initiation and the +1 Nucleosome

Left axis - Log2 ratio of cryptic 5' ends over wildtype (purple). Right axis – Nucleosome occupancy (Jiang and Pugh 2009a) (black). Cryptic initiation accumulates directly upstream of the +1 nucleosome.

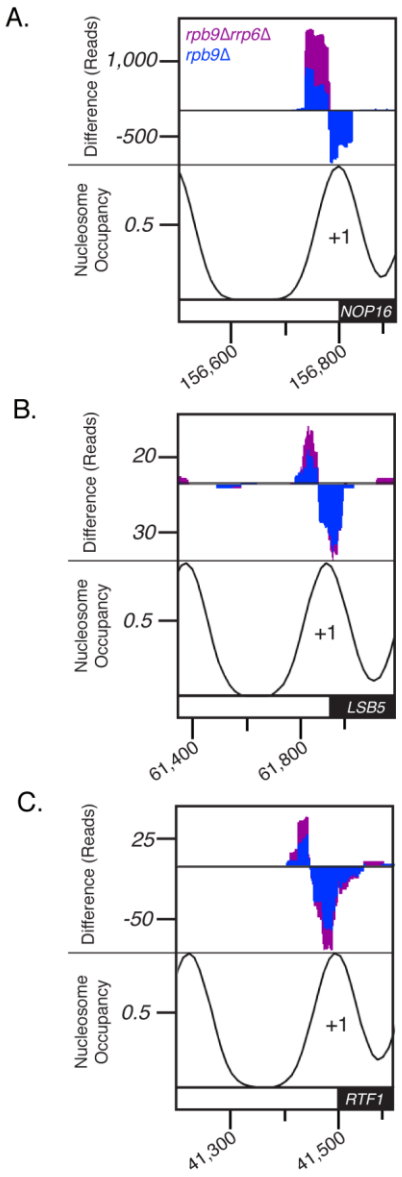

Figure 6-8 – Accumulation of Cryptic Transcripts at Individual Loci

A-C. Difference between *rpb9*Δ (blue) and *rpb9*Δ*rrp6*Δ (purple) against wildtype at the *NOP16* (A), *LSB5* (B) and *RTF1* (C) loci.

6.2.4 - Trigger Loop Dynamics Can Induce or Rescue Transcription from cTSSs

The trigger loop of RNAPII alternates between an "open" and "closed" conformation, wherein the open conformation allows for pairing of NTPs with the template DNA in the active site of the polymerase (Wang et al. 2006; Kaplan et al. 2008; Kaplan et al. 2012). Once an incoming NTP is correctly paired it can be added to the nascent RNA chain only after the transition of the trigger loop to the closed conformation. Mutation of Glu 1103 to Gly (E1103G) destabilizes the open conformation of the trigger loop, and this disruption causes transcription start sites to shift upstream, similar to *rpb9*Δ (Wang et al. 2006; Kaplan et al. 2008; Kaplan et al. 2012). The E1103G mutation creates a more catalytically active form of the enzyme and increases the transcription elongation rate (Kaplan et al. 2012; Larson et al. 2012). Additionally, *RPO21*-E1103G exhibits synthetic lethality with *rpb9*Δ, and it has been proposed that Rpb9 stabilizes the TL in the open complex (Walmacq et al. 2009). Trigger loop residue His 1085 contacts the incoming NTP to be added to the 3'-OH of the nascent RNA (Wang et al. 2006; Kaplan et al. 2012). The histidine interacts with the beta and gamma phosphates of the NTP allowing and is critical for catalysis. While H1085A is lethal in *S. cerevisiae*, H1085Q is viable, despite severely impacting trigger loop dynamics and slowing the rate of transcriptional elongation (Wang et al. 2006; Kaplan et al. 2008; Kaplan et al. 2012).

Given that Rpb9 has been implicated in regulating trigger loop dynamics, we decided to directly test the effect of mutations in the TL on cryptic initiation. We were

able to confirm the previously reported synthetic lethal interaction between *rpb9*Δ and *RPO21*-E1103G (Figure 6-9 C) (Walmacq et al. 2009). Performing primer extension and northern analysis on GCN4 transcripts shows that *RPO21*-E1103G *rrp6*Δ behaves remarkably similarly to *rpb9*Δ*rrp6*Δ, albeit the effect is more subtle (Figure 6-9 A). Concordantly, the synthetic sickness of *RPO21*-E1103G, *rrp6*Δ is less severe than *rpb9*Δ*rrp6*Δ (Figure 6-9 B).

Both *rpb9*Δ and *RPO21*-E1103G destabilize the open conformation of the TL, and enhance the rates of catalysis and elongation (Walmacq et al. 2009; Kaplan et al. 2012). Conversely, *RPO21*-H1085Q has opposing effects on rates of catalysis and elongation (Wang et al. 2006; Kaplan et al. 2012). We decided to test whether this allele of *RPO21* could rescue the *rpb9*Δ start site selection defect, and restore transcription from the canonical mRNA TSS. Analyzing transcripts at the GCN4 locus we find that RPO21-H1085Q does not significantly affect the distribution of transcription start sites relative to wildtype. Importantly, in the context of *rpb9*Δ*rrp6*Δ, *RPO21*-H1085Q suppresses transcription from cTSS start sites, and restores transcription from the downstream canonical start site (Fig 6-9 D).

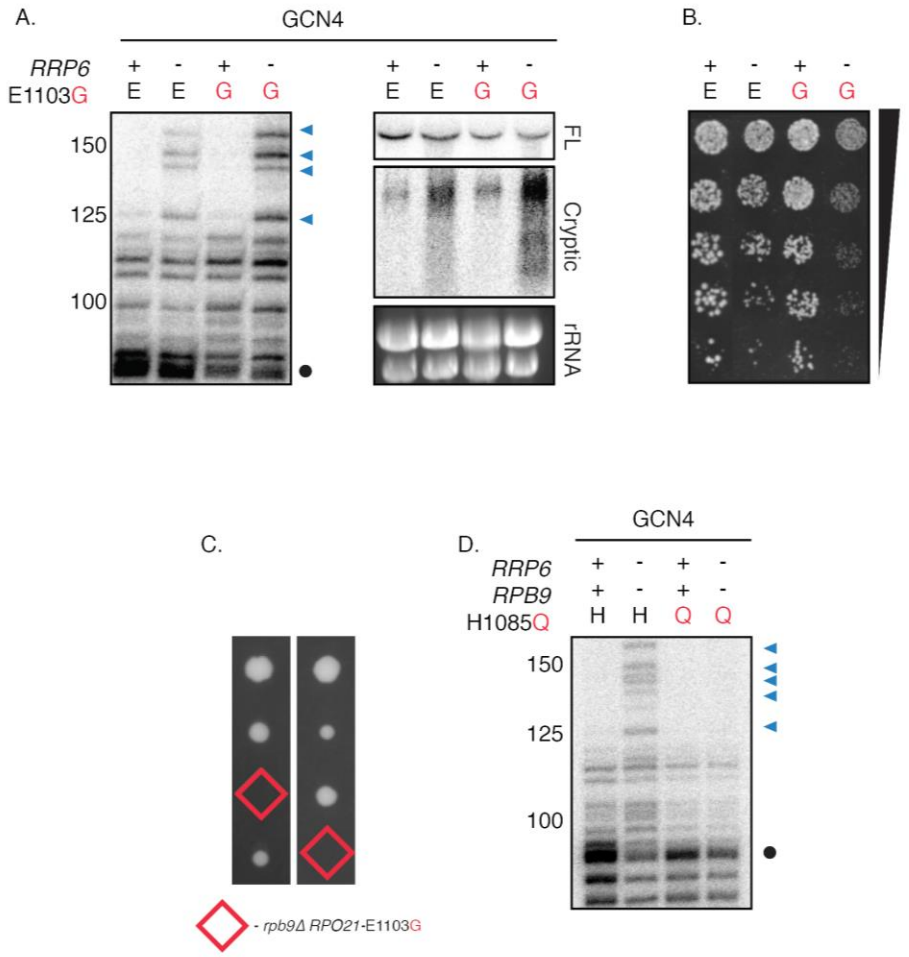

Figure 6-9 – Trigger Loop Mutants Affect Cryptic Initiation

A. Effect of RPO21-E1103G on cryptic initiation by primer extension (left panel) and northern blot (right panel). **B.** Serial dilution of wildtype, *rrp6*Δ, E1103G, and *rrp6*Δ E1103G cells. **C.** Synthetic lethality of *rpb9*Δ *RPO21*-E1103G cells. **D.** H1085Q restores proper TSS choice at GCN4 locus as assayed by primer extension.

6.2.5 - TATA Genes Have Longer Scanning Distances and are more significantly affected by rpb9Δrrp6Δ

Given the documented role that start site selection plays in regulation of *IMD2* and *URA2* (Kuehner and Brow 2008; Thiebaut et al. 2008), we speculated that the

cTSSs observed at many promoters could be involved in the regulation of their associated genes. As mentioned in the previous chapter, promoters in *S. cerevisiae* can be broadly divided into two categories: SAGA and TFIID. Arranging genes by increasing PTD we find that genes with longer PTDs are more likely to exhibit the characteristics of SAGA promoters. Promoters were assigned a "SAGAness" score based on the presence of a consensus TATA-box sequence, or if they qualified as TAF1-depleted (Rhee and Pugh 2012) (Figure 6-11). Reads aligning to mRNA TSS at promoters displaying SAGA characteristics are significantly less abundant in the *rpb9*Δ dataset relative to wildtype. Further, these promoters exhibit an accumulation of 5' end reads in the absence of *RRP6* (Figure 6-11).

Comparing the PTDs of SAGA genes to that of TFIID genes we find that RNAPII must scan almost twice as far on average when transcribing a SAGA classified gene (Avg. PTD_{SAGA} = 57bp, Avg. PTD_{TFIID} = 33bp) (Figure 6-12 A). Concordantly, SAGA genes are much more significantly affected by *rpb9*Δ than genes belonging to the TFIID class. Signal at SAGA TSSs drops precipitously in the absence of RPB9, while cTSS transcription is significantly enhanced (Figure 6-12 C,D).

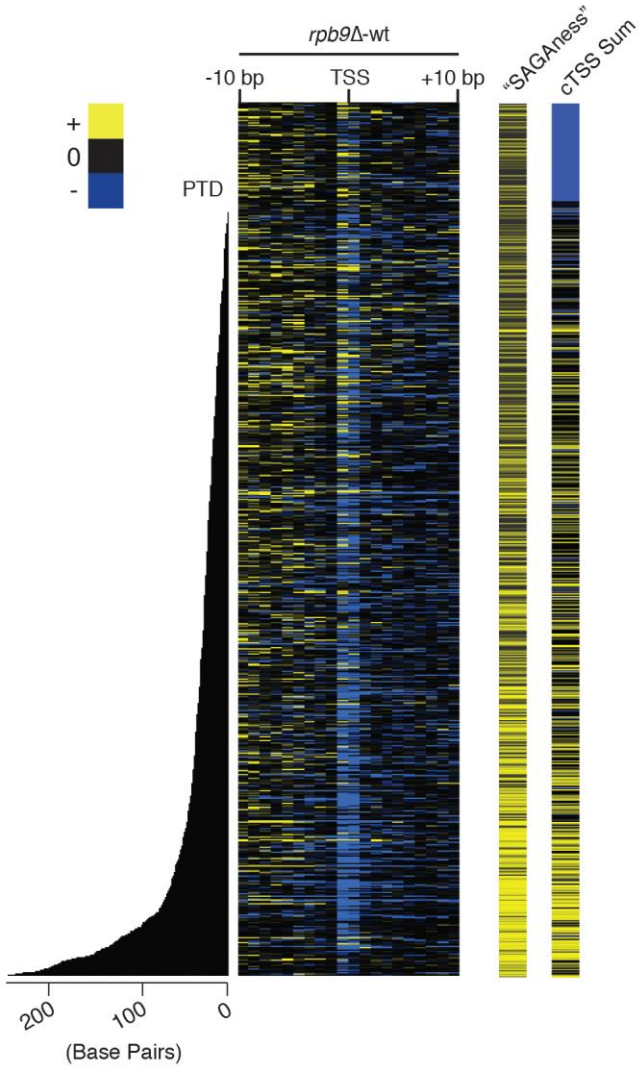

Figure 6-11 – The Effect of rpb9Δ Increases with "SAGAness"

Heat-map demonstrating the difference between 5' ends in rpb9Δ and wildtype samples (left panel). Genes are arranged by increasing PTD. "SAGAness" TAF1-Depletion and Consensus TATA sequence contribute to the "SAGAness" score. "SAGAness" increases with PTD. cTSS sum is defined as the difference between rrp6Δ and wildtype samples within the PTD.

Given the enrichment of cTSS transcription at SAGA promoters, and the previous implication of Gcn5 in start site selection, we speculated that the SAGA complex itself could be involved in regulating cTSS transcript production. Mutations

of various SAGA components have been shown to alter start site selection at the HIS3 promoter (Belotserkovskaya et al. 2000). Further, *gcn5*Δ is known to exhibit synthetic lethality with *rpb9*Δ, which we were able to confirm (Van Mullem et al. 2002). To test for the participation of SAGA in cTSS selection we deleted GCN5, the acetyltransferase component of SAGA, responsible for acetylation of nucleosomal histones (Kuo et al. 1996; Grant et al. 1997). While the effect of *gcn5*Δ is not as severe as that of *rpb9*Δ, primer extension analysis of TPI1 transcripts in a *gcn5*Δ*rrp6*Δ background verifies that the SAGA complex can indeed influence transcription start site selection (Figure 6-12 B).

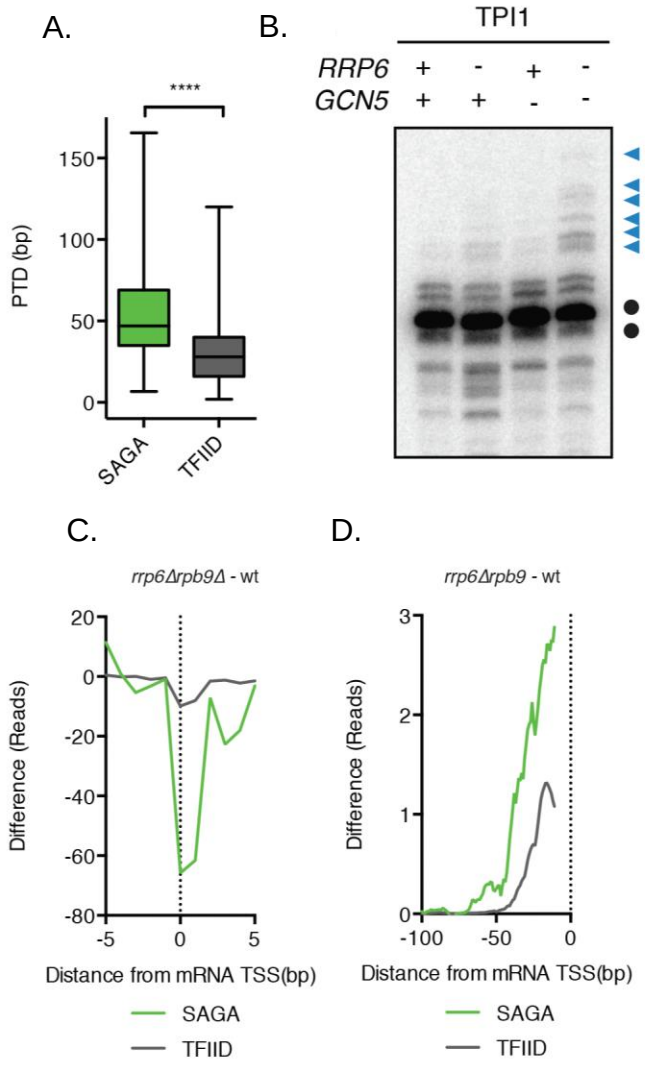

Figure 6-12 – Sensitivity of SAGA Promoters to Cryptic Initiation

A. Box-plot of PTD values associated with SAGA (green) and TFIID (grey) promoters. **B.** Effect of *gcn5*Δ on TSS selection at the *TPI1* locus. mRNA TSS – black dot. cTSS – blue triangles. **C.** Average fold-difference (*rpb9*Δ*rrp6*Δ-wt) in 5' end coverage at SAGA (green) and TFIID (grey) promoters near mRNA transcription start sites. **D.** Average fold-difference (*rpb9*Δ*rrp6*Δ-wt) in 5' end coverage upstream of transcription start sites at SAGA (green) and TFIID (promoters).

6.2.6 - Acute Inhibition of Exosome Activity With 5-Flurouracil

In addition to perturbing exosome activity by deleting RRP6, we were also able to acutely inhibit exosome function by treating cells with the dTTP and UTP precursor, 5-flurouracil (5-FU) (Figure 6-13). The interaction was identified in a screen examining the fitness of hetrozygous mutant strains when treated with various small molecules (Lum et al. 2004). Four strains heterozygous for components of the exosome, *RRP6*, *RRP41*, *RRP44*, and *RRP46* exhibit sensitivity to 5-FU. In addition to 5-FU, RRP6/rrp6Δ diploid yeast also exhibit a significant loss of fitness when grown in the presence of 5-Flurocytidine and 5-Fluorodeoxyuridine (Lum et al. 2004). The effect of 5-FU on an RPB9/rpb9 heterozyote strain was not tested, though considering the synthetic growth defect observed in the *rrp6*Δ*rpb9*Δ background, 5-FU might be expected to compromise the fitness of RPB9/*rpb9*Δ. The incorporation of 5-FU into RNA directly inhibits the activity of the Exosome *in vitro*, suggesting that the loss of fitness observed in the RRP6/*rrp6*Δ heterozygote could be due in part to the stabilization of 1,000s of non-coding transcripts (Fang et al. 2004; Silverstein et al. 2011).

To investigate this possibility, in regards to cryptic alternative start site transcripts, we treated an *rpb9*Δ culture with 5-FU (100uM final concentration) and DMSO as a control and sampled the culture 5, 10, and 20 minutes following the treatment. Total RNA was prepared and primer extension of transcripts initiating at the GCN4 locus was performed. As shown earlier, transcripts initiating from cryptic start sites are observable in an *rrp6*Δ*rpb9*Δ background (Figure 6-13). Upon treatment with

DMSO we observe no stabilization of cryptic RNAs. However, within 5 minutes of treatment of 5-FU we observe a faint accumulation of cryptic start sites, and by 20 minutes after treatment cryptic transcripts are significantly stabilized (Figure 6-13). These results indicate that it is not necessary to chronically stabilize cryptic RNAs with *rrp6*Δ, and for experiments requiring more acute disarming of exosome function treatment with 5-FU can be exercised.

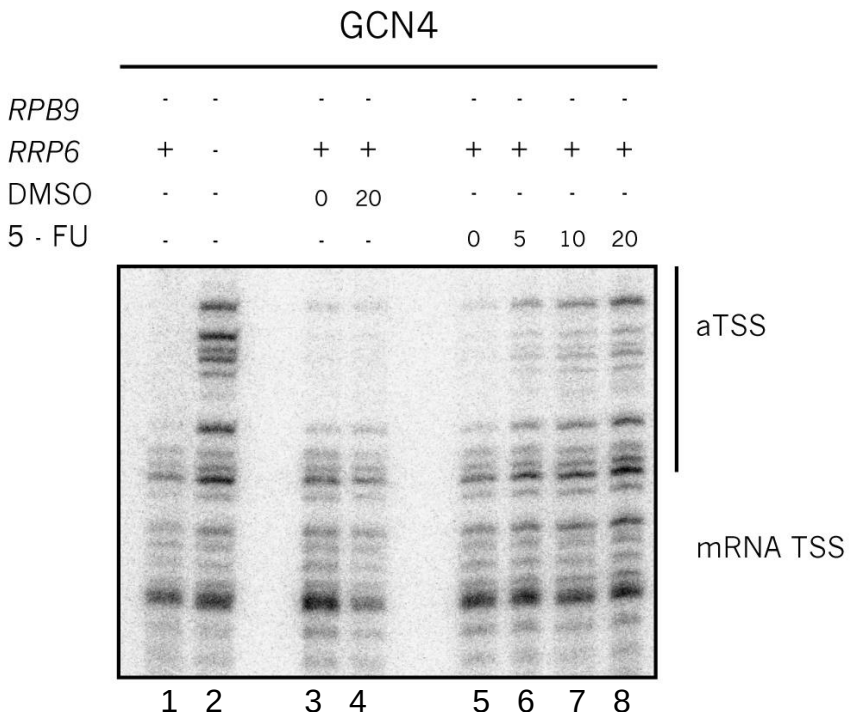

Figure 6-13 – Stabilization of cTSS Transcripts by 5-FU

Primer extension of transcripts initiating from the GCN4 promoter. Lane 1 – *rpb9*Δ. Lane 2 – *rpb9*Δ*rrp6*Δ. Lanes 3 & 4 – rrp6Δ with (20 minutes) and without DMSO treatment (negative control). Lanes 5, 6, 7, & 8 – rpb9Δ without 5-FU treatment and increasing amounts of time in 100uM 5-FU (5, 10, and 20 minutes).

6.2.7 - Extension of cTSS Transcripts by ssu72-2

While destabilization of trigger loop dynamics, and initiation of transcription upstream of canonical TSS induces the transcription of non-coding RNAs, it remains unclear how the termination and degradation pathway of these transcripts is triggered. In an effort to uncouple cryptic transcription initiation from premature termination and degradation by the nuclear exosome, we introduced the *ssu72-2* mutation into the *rpb9*Δ*rrp6*Δ background.

SSU72 encodes a phosphatase of the RNAPII CTD and its activity is focused on serine residues 5 and 7 (Krishnamurthy et al. 2004; Zhang et al. 2012). This gene is essential in *S. cerevisiae*, and the *ssu72-2* allele is defined by the substitution of a highly conserved arginine residue with an alanine (R129A) (Pappas and Hampsey 2000). The *ssu72-2* allele exhibits decreased phosphatase activity and causes defects in transcription termination leading to the generation of elongated transcripts that recognized and degraded by the exosome (Pappas and Hampsey 2000; Dichtl et al. 2002; Reyes-Reyes and Hampsey 2007).

We generated the *ssu72-2* mutant via the mutagenesis method described in Chapter II (Figure 6-15). This strain was then crossed with the *rpb9*Δ*rrp6*Δ double mutant strain, the resulting diploid was then sporulated and dissected with the goal of obtaining an *rpb9*Δ*rrp6*Δ*ssu72-2* triple mutant strain (Figure 6-16). However, we were unable to isolate this mutant and the segregation of the markers amongst the tetrads demonstrates that the triple mutant is synthetic lethal even at the permissive

temperature of 30˚C (Figure 6-16). Further, we find that *ssu72-2* exhibits synthetic sickness with both *rpb9*Δ and *rrp6*Δ, though the synthetic phenotype observed in *ssu72-2*, *rrp6*Δ is much more severe than *ssu72-2*, *rpb9*Δ.

Having previously discovered that *RPO21*-E1103 largely phenocopies *rpb9*Δ, albeit with less severity, we decided to cross *ssu72-2* with *RPO21*-E1103G, *rrp6*Δ in hopes of isolating a triple mutant. The *ssu72-2*, *RPO21*-E1103G, *rrp6*Δ is viable at the permissive temperature, though it grows very slowly, and is presumably likely to obtain suppressor mutations due to tremendous selective pressure (Figure 6-17). Both *ssu72-2*, *RPO21*-E1103G and *ssu72-2*, *RPO21*-E1103G, *rrp6*Δ are not viable at the non-permissive temperature (Figure 6-18). All experiments described below were performed at the permissive temperature.

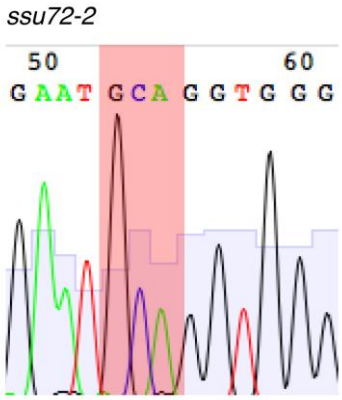

Figure 6-15 - Trace of *ssu72-2* Mutation

AGA (Arg) -> GCA (Ala)

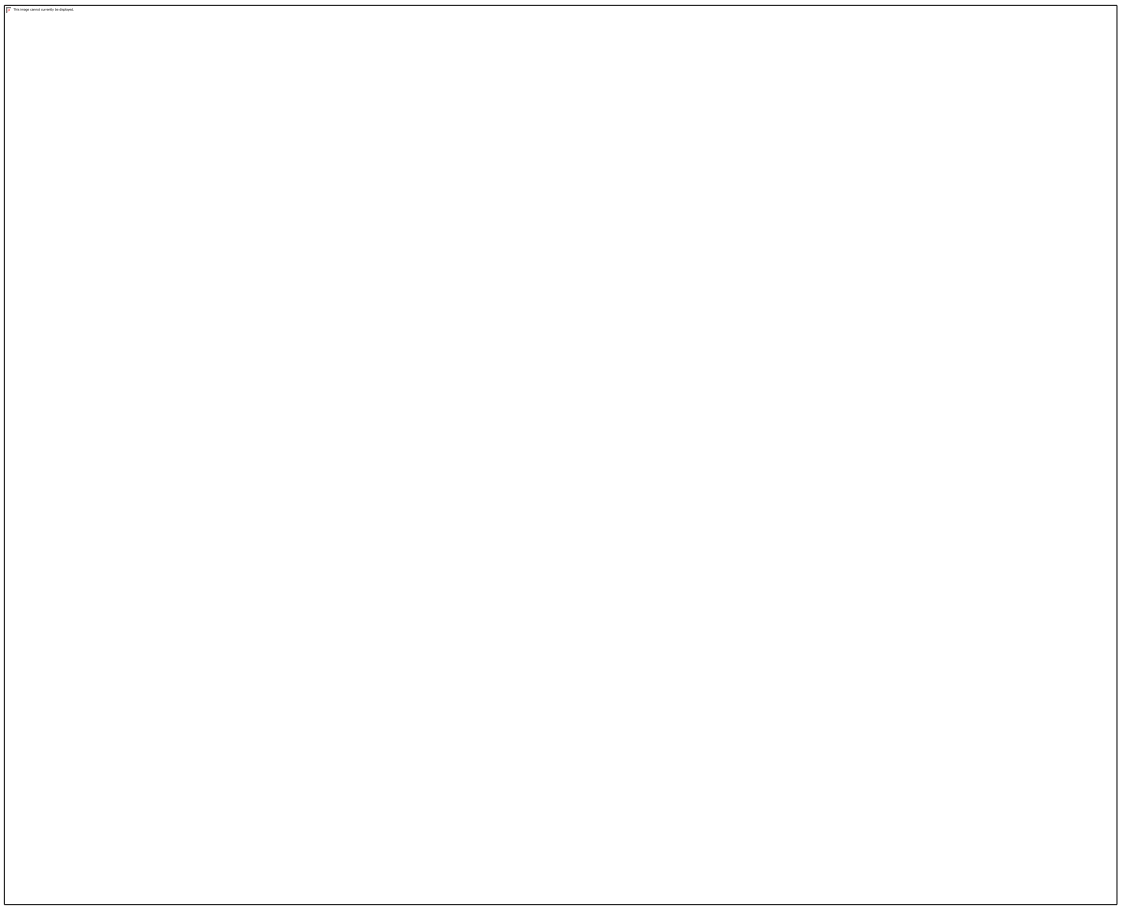

Figure 6-16 – Synthetic Lethality in the Triple Mutant *rpb9*Δ*, ssu72-2, rrp6*Δ

Tetrads dissected onto YPD plates (left panel). Scoring table of tetrad growth on media containing KAN, HYG, and NAT.

		RPO21-E1103G :: HYG	*ssu72-2* :: G418	*rrp6*Δ ::NAT	
1	A	+	+	+	*RPO21-E1103G, ssu72-2, rrp6Δ*
	B	+	+	-	*RPO21-E1103G, ssu72-2*
	C	-	-	+	*rrp6Δ*
	D	-	-	-	wildtype
3	A	+	+	+	*RPO21-E1103G, ssu72-2, rrp6Δ*
	B	-	+	+	ssu72-2 ,*rrp6Δ*
	C	+	-	-	*RPO21-E1103G*
	D	-	-	-	wildtype
5	A	-	-	+	*rrp6Δ*
	B	-	+	-	*ssu72-2*
	C	+	+	-	*RPO21-E1103G, ssu72-2*
	D	+	-	+	*RPO21-E1103G, rrp6Δ*
6	A	-	+	-	*ssu72-2*
	B	-	-	+	*rrp6Δ*
	C	+	+	-	*RPO21-E1103G, ssu72-2*
	D	+	-	+	*RPO21-E1103G, rrp6Δ*
7	A	-	-	-	*wildtype*
	B	-	+	+	*ssu72-2 ,rrp6Δ*
	C	+	-	+	*RPO21-E1103G, rrp6Δ*
	D	+	+	-	*RPO21-E1103G, ssu72-2*
8	A	-	+	+	*ssu72-2 ,rrp6Δ*
	B	+	-	-	*RPO21-E1103G*
	C	+	+	-	*RPO21-E1103G, ssu72-2*
	D	-	-	+	*rrp6Δ*

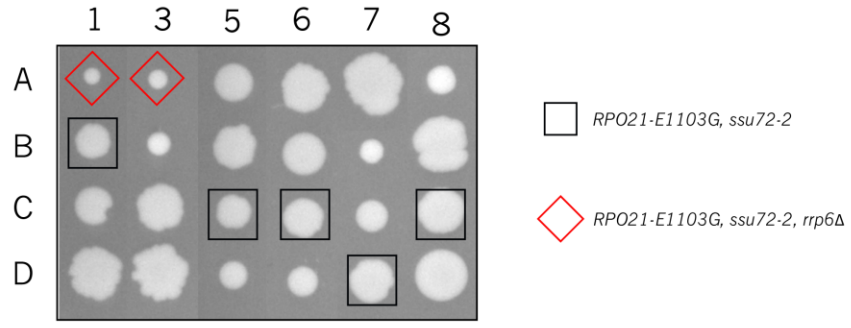

Figure 6-17 - Viability of the Triple Mutant *RPO21*-E1103G, *ssu72-2*, *rrp6*Δ

Scoring table of the tetrad growth on HYG, G418, and NAT. Growth of tetrads on YPD. Black square indicates *RPO21*-E1103G, *ssu72-2* double mutants. Red diamond indicates *RPO21*-E1103G, *ssu72-2*, *rrp6*Δ triple mutants.

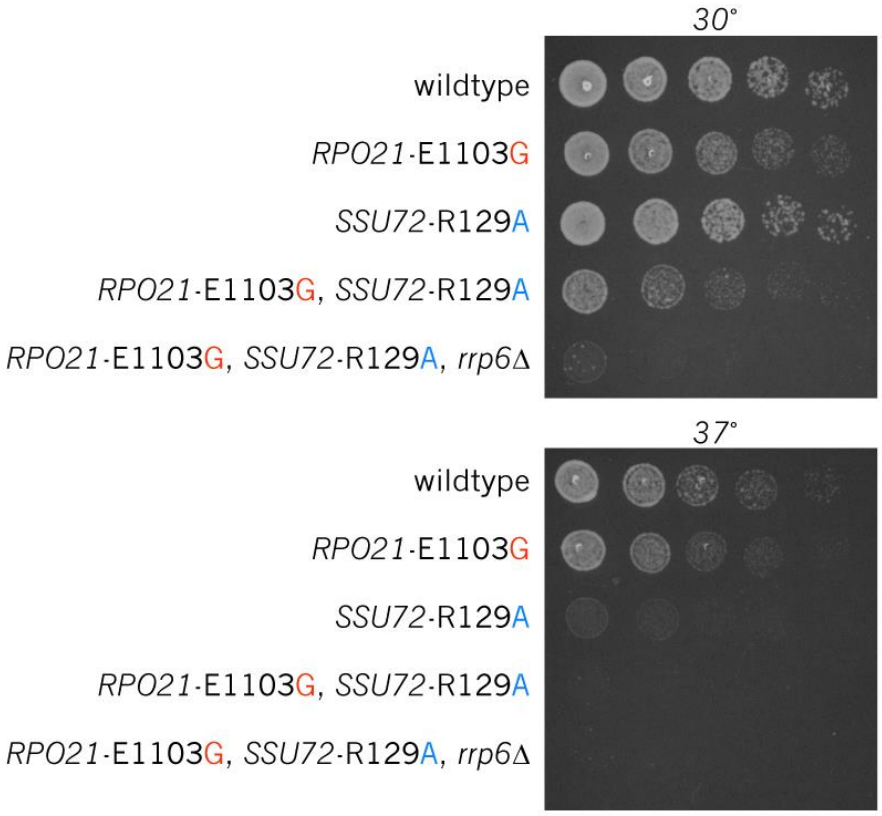

Figure 6-18 - *RPO21*-E1103G, *ssu72-2*, *rrp6*Δ and *RPO21*-E1103G, *ssu72-2* are Extremely Temperature Sensitive

To determine whether *ssu72-2* elongates 3' ends of cTSS transcripts to normal cleavage and polyadenylation sites, or if *ssu72-2* had an impact on transcription start site selection, we first performed primer extension on transcripts from the GCN4 locus. Cryptic transcripts initiating from upstream start sites are not affected by *ssu72-2* in the *RPO21*-E1103G background, comparing lanes 2 and 4 of Figure 6-19. Accordingly, the upstream start site transcripts stabilized in the *RPO21*-E1103G, *rrp6*Δ strain are not observed in the *ssu72-2*, *RPO21*-E1103G background (Figure 6-19 lanes 3 and 4). Thus, this mutation of SSU72 does not have an impact on transcript 5' ends, and any elongation of these transcripts observed on a northern blot can be attributed extension of their 3' ends.

We do observe extension of alternative TSS cryptic transcripts at the GCN4 locus, indicating that Ssu72 is involved in mediating the termination of cryptic alternative start site transcripts (Figure 6-20 A). However, extended cTSS transcripts are still terminated prior to reaching the 3' end of the gene as we might have expected. While 3' ends of cryptic transcripts are typically non-uniformly distributed 200-500 bases downstream of the site of initiation, we find that the hypomorphic allele of *ssu72-2* leads to a uniform site of transcription termination resulting in extended cryptic transcripts that are ~1kb long, still shy of the ~1.5kb of the full-length GCN4 transcript (Figure 6-20). The length of the full-length transcript is unchanged.

We hypothesized that it might be possible to extend these cryptic RNAs even further by shifting cells to the non-permissive temperature. Double and triple mutant cultures were grown at 30˚C and shifted to 37˚, while experiencing logarithmic growth, for two hours. RNA from both cultures was prepared from both cells at the permissive temperatures, and cells harvested subsequent to the temperature shift for analysis via northern blotting (Figure 6-20 B). Surprisingly, we observe no further extension of cryptic transcripts upon shift to the non-permissive temperature. Lethality of *ssu72-2* mutants upon chronic exposure to higher temperatures could perhaps be due to impairment of Ssu72 function in a separate process, not related to the termination of cryptic RNA.

Additionally, it is possible that cells simply die, more or less instantly, upon shift to the non-permissive temperature and thus the response to an increase in temperature is not graded. In this scenario the ~1kb we observe after 2 hours at the non-permissive temperature would simply be residual transcripts produced prior to the shift to 37˚C.

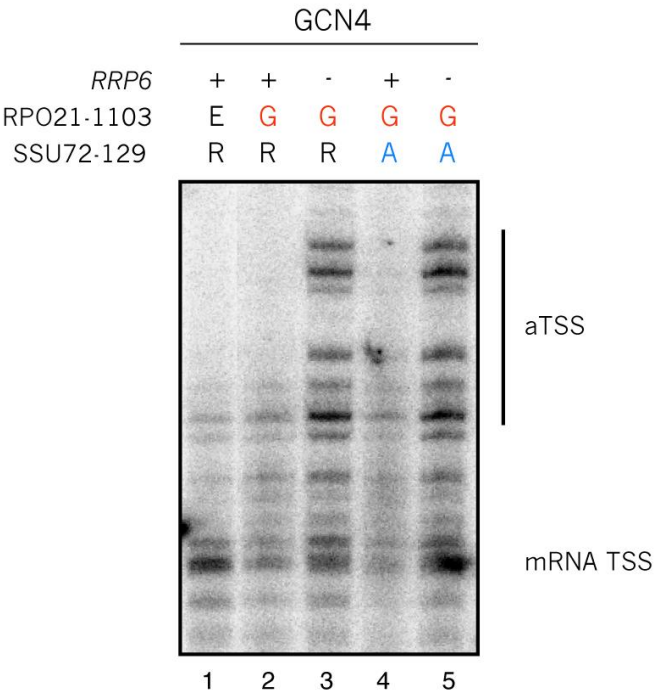

Figure 6-19 – *ssu72-2* Does Not Correct Cryptic Initiation

Lane 1 – Wildtype. Lane 2 – *RPO21*-E1103G. Lane 3 – *RPO21*-E1103G, *rrp6*Δ. Lane 4 – *RPO21*-E1103G, *ssu72-2*. Lane 5 - *RPO21*-E1103G, *ssu72-2*, *rrp6*Δ.

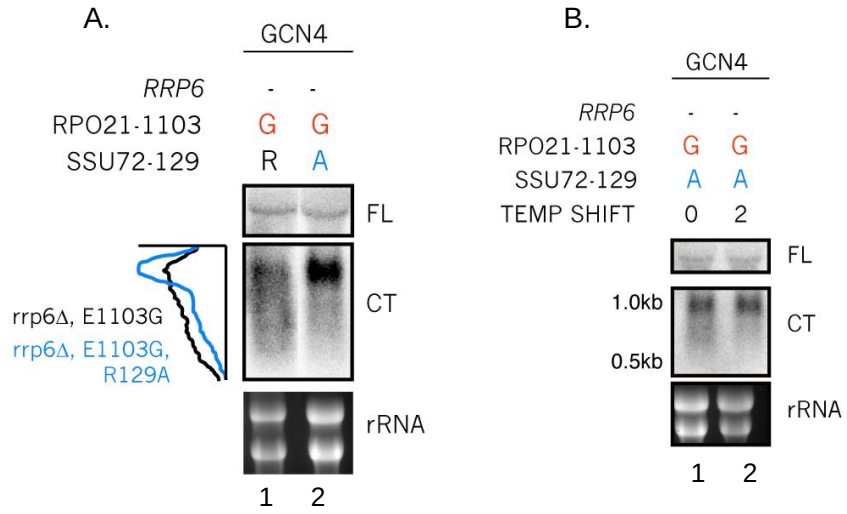

Figure 6-20 – *ssu72-2* Causes the Elongation of cTSS Transcripts

A. Northern blot of GCN4 transcripts. Full length (FL –top panel). Cryptic (CT – middle panel). Loading control (rRNA – bottom panel). Lane 1 – *RPO21*-E1103G, *ssu72-2*. Lane 2 - *RPO21*-E1103G, *ssu72-2*, *rrp6*Δ. **B.** Northern blot of GCN4 transcripts. Lane 1 – No Temperature Shift. Lane 2 – 2 hours at 37˚C

6.3 Discussion

6.3.1 - The relationship between the +1 Nucleosome and the TSS

Our current understanding of how cryptic transcripts differ from mRNA is entirely focused on their distinct 3' end processing and degradation pathways. Here we have shown that a transcript's fate is determined from the moment the first phosphodiester bond of the nascent RNA is formed, and that the nucleosomal context of initiation is crucial in directing towards or away from the cryptic 3' end processing pathway. While +1 nucleosomes and TSSs have long been known to be tightly associated with one another, the causality or significance of this relationship was unknown. Here, we show that transcription can initiate outside of the +1 nucleosome,

likely due to misregulation of the RNAPII trigger loop, and that these transcripts are quickly recognized as aberrant and subsequently degraded. From this observation we can infer that initiation within the +1 nucleosome plays a role in designating transcripts as having coding potential, and masks them from the NNS complex (Figure 6-23). Given the effect that destabilization of the open conformation of the TL has on start site selection and cTSS production, the +1 nucleosome could be prompting the transition of RNAPII from scanning to initiation via an interaction with the TL domain. Further, elongation of these non-coding transcripts can be achieved by altering the phosphorylation state of RNAPII CTD by impairing the activity of the Ssu72 CTD phosphatase. This suggests that posttranslational modifications of RNAPII molecules with altered TL dynamics or elongation kinetics may be distinct from their wildtype counterparts.

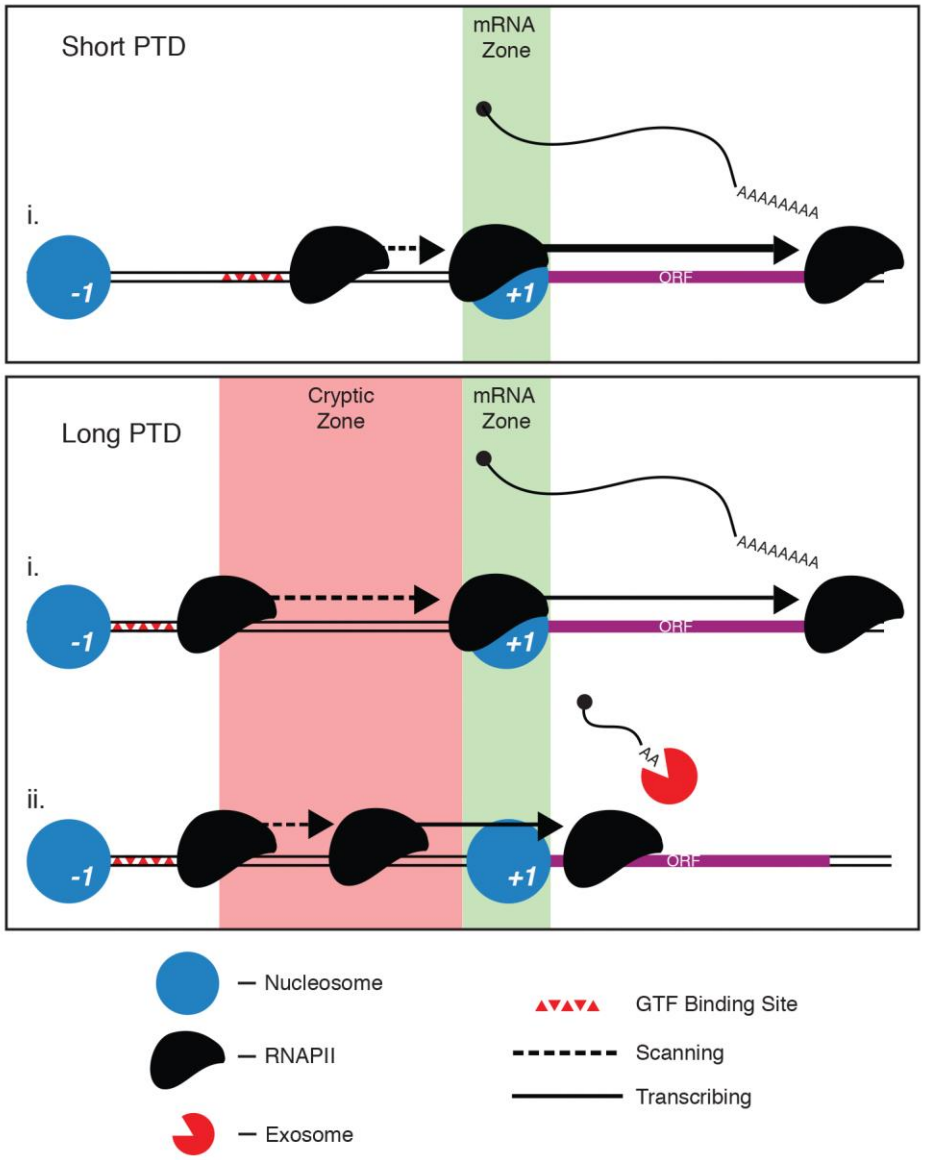

Figure 6-21 - Model Figure

At promoters that maintain a short PIC to TSS distance, the polymerase is highly unlikely to initiate transcription prior to making contact with the +1 nucleosome. For reasons that remain unclear, initiation that takes place within the upstream edge of the +1 nucleosome is highly likely to produce a full-length mRNA product. Alternatively, at promoters exhibiting longer PIC to TSS distances, RNAPII is much more likely to prematurely initiate transcription within the NDR. Transcripts initiating from naked promoter DNA are rapidly terminated and degraded by the nuclear exosome.

6.3.2 - Phosphorylation of Rpb9

We have demonstrated that altering trigger loop dynamics can bias RNAPII towards cTSS *in vivo*. Given the similar phenotypes produced by *rpb9*Δ and *RPO21*-E1103G, and their synthetic lethality, we believe that the effects of *rpb9*Δ can largely be attributed to destabilization of the open conformation of the trigger loop. Rpb9 is a unique component of RNAPII in that is non-essential. We hypothesize that association of Rpb9 with RNAPII can be modulated to ultimately tune transcriptional output via its effects on the TL. Interestingly, several residues on Rpb9 are reported to be phosphorylated (S33, Y34, S40) (Sadowski et al. 2013). These post-translational modifications could potentially be involved in regulating the association of Rpb9 with other components of the RNAPII holoenzyme, and may warrant future investigation.

6.3.3 - Similarities to Transcription Attenuation

Transcription attenuators are found in the 5' UTRs of many prokaryotic transcripts and provide a scaffold for regulatory factors to induce premature transcription termination via recognition of RNA secondary structures (Naville and Gautheret 2010). Once such example involves repression of the pyrimidine synthesis operon in *Bacillus subtilis*. The repressor protein, PyrR, recognizes a loop structure in the 5' leader region of the transcript when UTP levels are high, and its binding to the nascent transcript prevents formation of an antiterminator loop, in turn promoting the emergence of a terminator structure. Recognition of this structure recruits termination

factors and prevents further transcription of the cistron (Bonner et al. 2001; Naville and Gautheret 2010). In yeast, the extended 5'-UTRs generated when transcription initiates from a cTSS could similarly serve as scaffolds to facilitate the binding of the NNS complex.

6.3.4 - Parallels in metazoans

Large-scale analysis of transcription initiation in eukaryotes has demonstrated that their promoters exhibit either a single focused TSS, or a broad distribution of dispersed TSSs (Carninci et al. 2006; Juven-Gershon and Kadonaga 2010; Kadonaga 2012). Similar to how we were able to classify *S. cerevisiae* promoters based in part on the presence of a consensus TATA element, promoters of vertebrates can also be segregated with respect to the presence or absence of promoter elements. Promoters exhibiting a single focused TSS tend to maintain TATA boxes (in addition to other promoter elements) and are more subject to regulation. This is similar to the SAGA class of promoters, many of which we find exhibit cTSSs. Further, promoters from which transcription initiates from a set of dispersed start sites are likely to be expressed at more consistent levels, and lack consensus promoter sequence elements, similar to TFIID genes. It seems possible that focused TSS promoters could potentially behave similarly to SAGA promoters in yeast, with initiation from non-canonical upstream TSSs generating transcripts that are recognized and degraded by the conserved counterpart of the exosome, such that when 5' ends are mapped to these loci, only full-length transcripts escaping the 3'->5' exonuclease complex are detected.

Epilogue

Given the enrichment of SAGA associated characteristics at both cryptic TSS promoters and the +1 Shifter promoters described in Chapter III, we decided to examine if these two classes of genes were one and the same. To do this we calculated the Cryptic Score, defined as the difference in 5' ends initiating within the PTD between *rrp6*Δ and wildtype, and compared it to the standard deviation of +1 nucleosome positioning throughout the YMC (Figure 6-24). Promoters belonging to the Dynamic class exhibit a standard deviation of +1 positions > 10 base pairs. Interestingly, we find that promoters with the least +1 nucleosome movement are much more likely to exhibit cryptic transcription start sites. Suggesting that cTSS and Dynamic promoters individually represent sub-classes of SAGA class promoters.

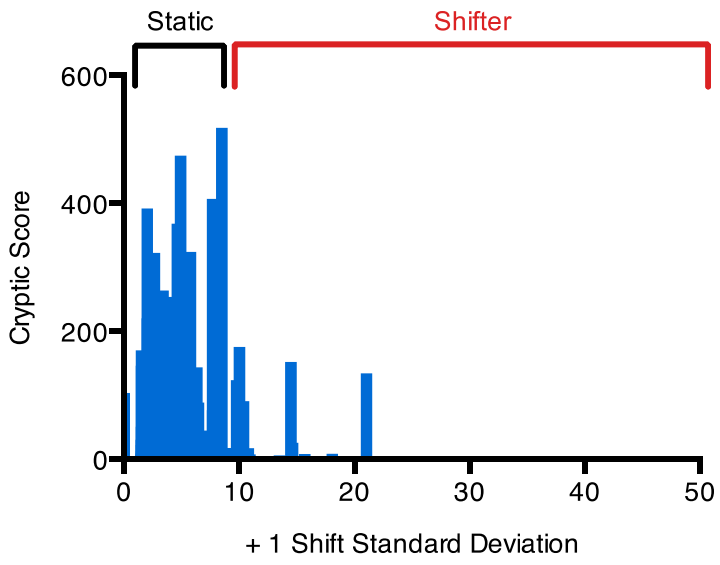

Figure 6-22 – +1 Nucleosomes of cTSS Promoters are Static With Respect to the YMC

Cryptic score, calculated as the sum of 5' ends in an rrp6Δ minus wildtype signal with in the PTD, is plotted against the standard deviation of +1 nucleosome positions through the YMC. +1 nucleosomes with a standard deviation >10 qualify as being Dynamic.

Examining a specific locus, as opposed to performing a meta-analysis, we find many promoters such as the *MAF1* locus. The +1 nucleosome of the MAF1 gene occupies essentially the same position throughout the YMC, however, in an *rpb9Δrrp6Δ* background, this same locus accumulates many cryptic 5' ends within its NDR (Figure 6-25).

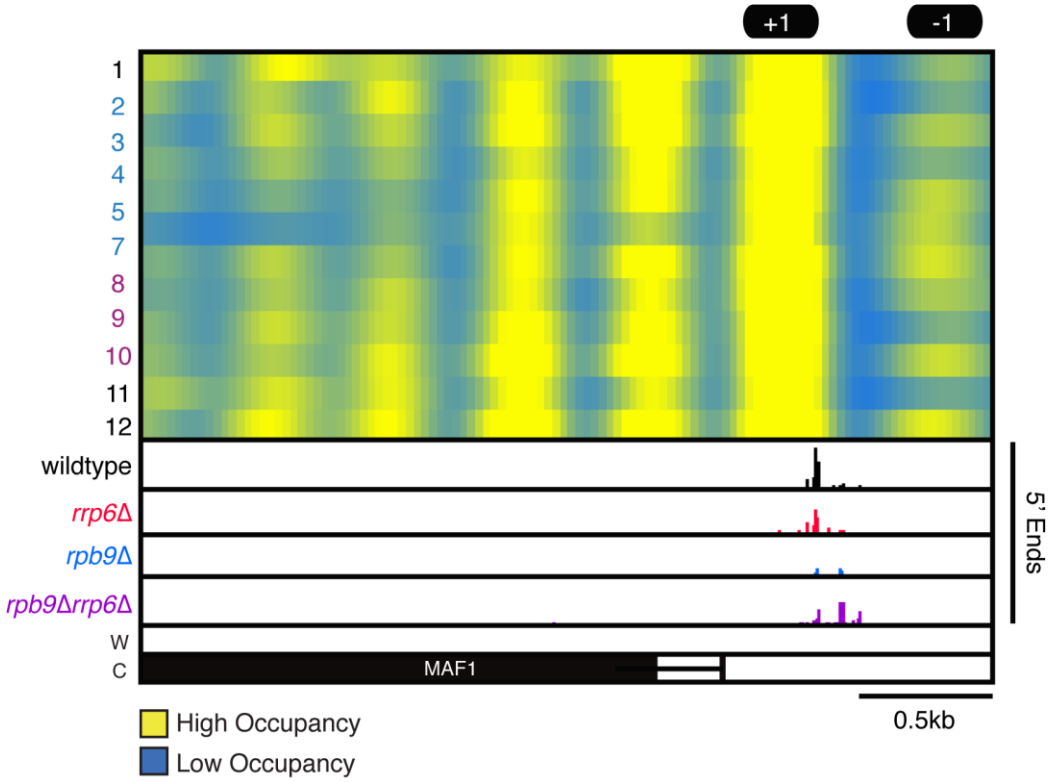

Figure 6-23 – YMC Nucleosome Dynamics and Cryptic Initiation at the MAF1 Locus

Heat-map demonstrating nucleosome positions through the YMC at the MAF1 locus are shown. The +1 nucleosome is relatively stationary through the respiratory oscillation. Also, shown are transcript 5' ends emanating from the locus in the various genetic backgrounds tested. Wildtype (black), *rrp6Δ* (blue), *rpb9Δ* (blue), *rpb9Δrrp6Δ* (purple).

This suggests that Dynamic promoters are primarily regulated at the stage of RNAPII recruitment and assembly of the PIC, while Static promoters are perhaps more likely to be regulated at stages following PIC assembly, such as start site selection. As shown earlier, the Static class of promoters are enriched for histone variant Htz1, and chromatin remodeling factor, Ino80. In fact, *RPB9* and *HTZ1* exhibit synthetic lethality (Malagon et al. 2004), though *HTZ1* is not known to play a role in start site selection.

Further, we tested whether *rrp6*Δ or *rpb9*Δ impacted the ability of the culture to undergo metabolic oscillations (Figure 6-26). We find that disruption of nuclear exosome activity by *rrp6*Δ does not impair the ability of the culture to achieve metabolic oscillations. Thus, the transcription of non-coding RNAs through metabolic oscillations can potentially be examined. Interestingly, *rpb9*Δ inhibits the YMC, suggesting that accurate transcription start site selection is necessary to achieve proper dosage of genes involved in maintaining respiratory oscillations. We hypothesize that bursts of expression from Static promoters during the YMC could be governed in part by regulation of transcription start site selection.

Together the data presented here represent two distinct descriptions of interactions between RNAPII and promoter chromatin. With respect to chromatin remodeling in the context of the YMC the nucleosome reprises its canonical role as a repressor of transcription. Promoter nucleosomes occlude access to general transcription factor binding sites, and generally behave as a barrier to be overcome.

Though these nucleosome represent an impediment to RNAPII recruitment, they are quite literally pushed aside by the activity of ATP-dependent remodeling factors, namely SWI/SNF. However, at a separate class of promoters +1 nucleosomes are fixed in positions that do not inhibit transcription factor binding, and thus transcriptional regulation at these loci is likely achieved at stages downstream of RNAPII recruitment, such as transcription start site selection. To that point, we have demonstrated that cryptic initiation events take place at many promoters, and that these cryptic RNAs utilize start sites in non-nucleosomal linker DNA. This is in stark contrast to the initiation of mRNA transcripts which utilize TSSs buried within +1 nucleosomes. Thus it would appear that transcription initiation outside of context of a nucleosome would set in motion events leading to the premature termination and degradation of a transcript. Given that inappropriate start site selection trigger the cryptic RNA degradation pathway, and that +1 nucleosomes play a crucial role in defining transcription start sites, +1 nucleosomes can be thought of as transcriptional activators, augmenting the likelihood that nascent RNAs mature to full-length transcripts. Together the data demonstrate that the relationship between promoter nucleosomes and transcriptional output is complex and the role of the +1 nucleosome is context dependent.

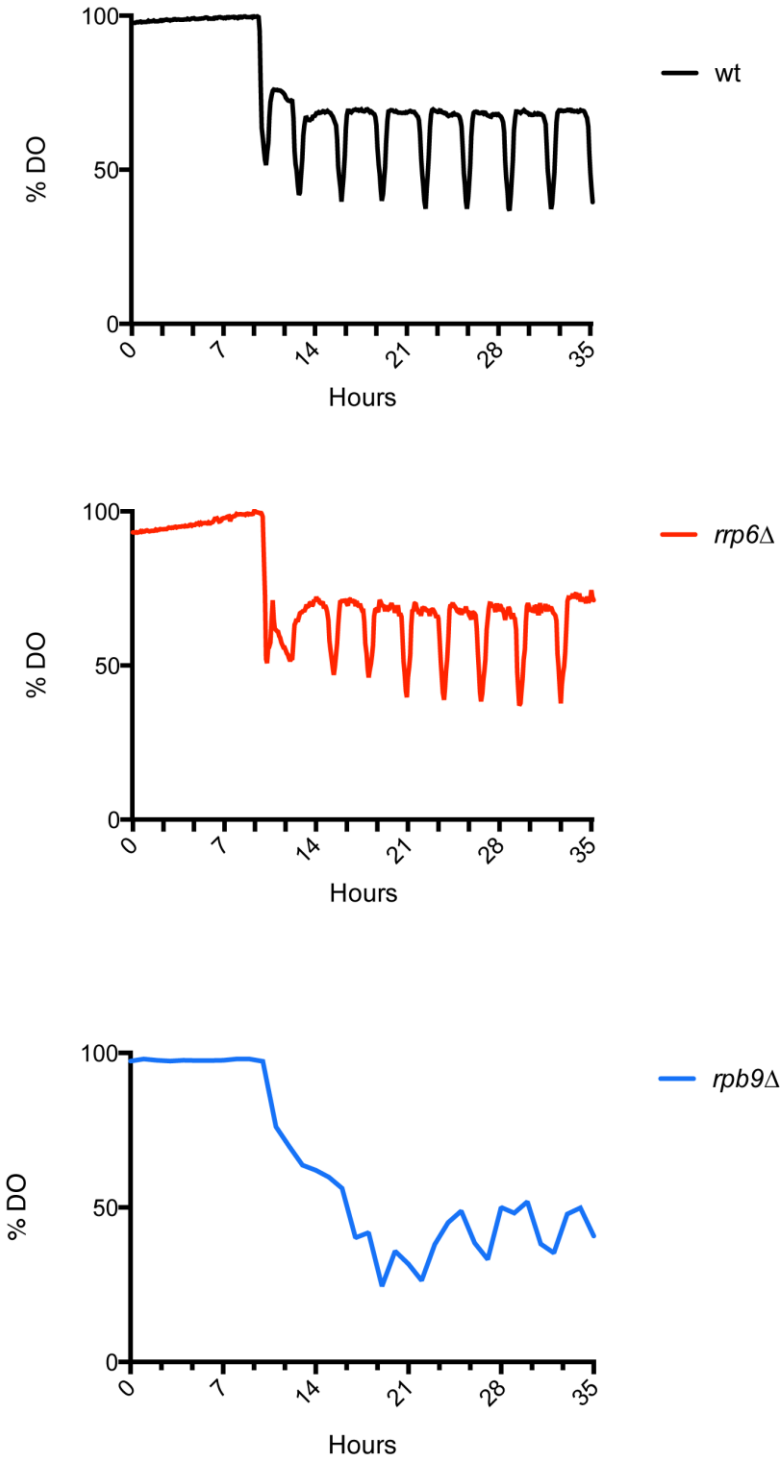

Figure 6-24 – Effects of *rrp6*Δ and *rpb9*Δ on Metabolic Oscillations

DO% traces of wildtype (black), *rrp6*Δ (red), and *rpb9*Δ (blue) cultures through metabolic oscillations. *rpb9*Δ completely disrupts the cycle.

References

Adkins MW, Williams SK, Linger J, Tyler JK. 2007. Chromatin disassembly from the PHO5 promoter is essential for the recruitment of the general transcription machinery and coactivators. *Molecular and cellular biology* **27**(18): 6372-6382.

Akhtar MS, Heidemann M, Tietjen JR, Zhang DW, Chapman RD, Eick D, Ansari AZ. 2009. TFIIH kinase places bivalent marks on the carboxy-terminal domain of RNA polymerase II. *Molecular cell* **34**(3): 387-393.

Altaf M, Auger A, Monnet-Saksouk J, Brodeur J, Piquet S, Cramet M, Bouchard N, Lacoste N, Utley RT, Gaudreau L et al. 2010. NuA4-dependent acetylation of nucleosomal histones H4 and H2A directly stimulates incorporation of H2A.Z by the SWR1 complex. *The Journal of biological chemistry* **285**(21): 15966-15977.

Arndt K, Fink GR. 1986. GCN4 protein, a positive transcription factor in yeast, binds general control promoters at all 5' TGACTC 3' sequences. *Proceedings of the National Academy of Sciences of the United States of America* **83**(22): 8516-8520.

Badis G, Chan ET, van Bakel H, Pena-Castillo L, Tillo D, Tsui K, Carlson CD, Gossett AJ, Hasinoff MJ, Warren CL et al. 2008. A library of yeast transcription factor motifs reveals a widespread function for Rsc3 in targeting nucleosome exclusion at promoters. *Molecular cell* **32**(6): 878-887.

Barbaric S, Luckenbach T, Schmid A, Blaschke D, Horz W, Korber P. 2007. Redundancy of chromatin remodeling pathways for the induction of the yeast PHO5 promoter in vivo. *The Journal of biological chemistry* **282**(38): 27610-27621.

Basehoar AD, Zanton SJ, Pugh BF. 2004. Identification and distinct regulation of yeast TATA box-containing genes. *Cell* **116**(5): 699-709.

Belotserkovskaya R, Sterner DE, Deng M, Sayre MH, Lieberman PM, Berger SL. 2000. Inhibition of TATA-binding protein function by SAGA subunits Spt3 and Spt8 at Gcn4-activated promoters. *Molecular and cellular biology* **20**(2): 634-647.

Bonner ER, D'Elia JN, Billips BK, Switzer RL. 2001. Molecular recognition of pyr mRNA by the Bacillus subtilis attenuation regulatory protein PyrR. *Nucleic acids research* **29**(23): 4851-4865.

Bu Y, Schmidt MC. 1998. Identification of cis-acting elements in the SUC2 promoter of Saccharomyces cerevisiae required for activation of transcription. *Nucleic acids research* **26**(4): 1002-1009.

Burger K, Muhl B, Harasim T, Rohrmoser M, Malamoussi A, Orban M, Kellner M, Gruber-Eber A, Kremmer E, Holzel M et al. 2010. Chemotherapeutic drugs inhibit ribosome biogenesis at various levels. *The Journal of biological chemistry* **285**(16): 12416-12425.

Burns LG, Peterson CL. 1997. The yeast SWI-SNF complex facilitates binding of a transcriptional activator to nucleosomal sites in vivo. *Molecular and cellular biology* **17**(8): 4811-4819.

Cai L, Sutter BM, Li B, Tu BP. 2011. Acetyl-CoA induces cell growth and proliferation by promoting the acetylation of histones at growth genes. *Molecular cell* **42**(4): 426-437.

Cai L, Tu BP. 2012. Driving the cell cycle through metabolism. *Annual review of cell and developmental biology* **28**: 59-87.

Carninci P, Sandelin A, Lenhard B, Katayama S, Shimokawa K, Ponjavic J, Semple CA, Taylor MS, Engstrom PG, Frith MC et al. 2006. Genome-wide analysis of mammalian promoter architecture and evolution. *Nature genetics* **38**(6): 626-635.

Chambers AL, Downs JA. 2012. The RSC and INO80 chromatin-remodeling complexes in DNA double-strand break repair. *Progress in molecular biology and translational science* **110**: 229-261.

Chandy M, Gutierrez JL, Prochasson P, Workman JL. 2006. SWI/SNF displaces SAGA-acetylated nucleosomes. *Eukaryotic cell* **5**(10): 1738-1747.

Chatterjee N, Sinha D, Lemma-Dechassa M, Tan S, Shogren-Knaak MA, Bartholomew B. 2011. Histone H3 tail acetylation modulates ATP-dependent remodeling through multiple mechanisms. *Nucleic acids research* **39**(19): 8378-8391.

Chen HT, Hahn S. 2003. Binding of TFIIB to RNA polymerase II: Mapping the binding site for the TFIIB zinc ribbon domain within the preinitiation complex. *Molecular cell* **12**(2): 437-447.

Chen W, Liu Y, Zhu S, Green CD, Wei G, Han JD. 2014. Improved nucleosome-positioning algorithm iNPS for accurate nucleosome positioning from sequencing data. *Nature communications* **5**: 4909.

Churchman LS, Weissman JS. 2012. Native elongating transcript sequencing (NET-seq). *Current protocols in molecular biology / edited by Frederick M Ausubel [et al]* **Chapter 4**: Unit 4 14 11-17.

Corden JL. 2008. Yeast Pol II start-site selection: the long and the short of it. *EMBO reports* **9**(11): 1084-1086.

Corden JL, Cadena DL, Ahearn JM, Jr., Dahmus ME. 1985. A unique structure at the carboxyl terminus of the largest subunit of eukaryotic RNA polymerase II. *Proceedings of the National Academy of Sciences of the United States of America* **82**(23): 7934-7938.

Cote J, Quinn J, Workman JL, Peterson CL. 1994. Stimulation of GAL4 derivative binding to nucleosomal DNA by the yeast SWI/SNF complex. *Science* **265**(5168): 53-60.

Dahmus ME. 1996. Reversible phosphorylation of the C-terminal domain of RNA polymerase II. *The Journal of biological chemistry* **271**(32): 19009-19012.

Davis CA, Ares M, Jr. 2006. Accumulation of unstable promoter-associated transcripts upon loss of the nuclear exosome subunit Rrp6p in Saccharomyces cerevisiae. *Proceedings of the National Academy of Sciences of the United States of America* **103**(9): 3262-3267.

Dechassa ML, Zhang B, Horowitz-Scherer R, Persinger J, Woodcock CL, Peterson CL, Bartholomew B. 2008. Architecture of the SWI/SNF-nucleosome complex. *Molecular and cellular biology* **28**(19): 6010-6021.

Dichtl B, Blank D, Ohnacker M, Friedlein A, Roeder D, Langen H, Keller W. 2002. A role for SSU72 in balancing RNA polymerase II transcription elongation and termination. *Molecular cell* **10**(5): 1139-1150.

Downey M, Knight B, Vashisht AA, Seller CA, Wohlschlegel JA, Shore D, Toczyski DP. 2013. Gcn5 and sirtuins regulate acetylation of the ribosomal protein transcription factor Ifh1. *Current biology : CB* **23**(17): 1638-1648.

Dror V, Winston F. 2004. The Swi/Snf chromatin remodeling complex is required for ribosomal DNA and telomeric silencing in Saccharomyces cerevisiae. *Molecular and cellular biology* **24**(18): 8227-8235.

Durr H, Flaus A, Owen-Hughes T, Hopfner KP. 2006. Snf2 family ATPases and DExx box helicases: differences and unifying concepts from high-resolution crystal structures. *Nucleic acids research* **34**(15): 4160-4167.

Dutta A, Gogol M, Kim JH, Smolle M, Venkatesh S, Gilmore J, Florens L, Washburn MP, Workman JL. 2014. Swi/Snf dynamics on stress-responsive genes is governed by competitive bromodomain interactions. *Genes & development* **28**(20): 2314-2330.

Eaton ML, Galani K, Kang S, Bell SP, MacAlpine DM. 2010. Conserved nucleosome positioning defines replication origins. *Genes & development* **24**(8): 748-753.

Egloff S, O'Reilly D, Chapman RD, Taylor A, Tanzhaus K, Pitts L, Eick D, Murphy S. 2007. Serine-7 of the RNA polymerase II CTD is specifically required for snRNA gene expression. *Science* **318**(5857): 1777-1779.

Erkina TY, Tschetter PA, Erkine AM. 2008. Different requirements of the SWI/SNF complex for robust nucleosome displacement at promoters of heat shock factor and Msn2- and Msn4-regulated heat shock genes. *Molecular and cellular biology* **28**(4): 1207-1217.

Erkina TY, Zou Y, Freeling S, Vorobyev VI, Erkine AM. 2010. Functional interplay between chromatin remodeling complexes RSC, SWI/SNF and ISWI in regulation of yeast heat shock genes. *Nucleic acids research* **38**(5): 1441-1449.

Ertel F, Dirac-Svejstrup AB, Hertel CB, Blaschke D, Svejstrup JQ, Korber P. 2010. In vitro reconstitution of PHO5 promoter chromatin remodeling points to a role for activator-nucleosome competition in vivo. *Molecular and cellular biology* **30**(16): 4060-4076.

Fang F, Hoskins J, Butler JS. 2004. 5-fluorouracil enhances exosome-dependent accumulation of polyadenylated rRNAs. *Molecular and cellular biology* **24**(24): 10766-10776.

Field Y, Kaplan N, Fondufe-Mittendorf Y, Moore IK, Sharon E, Lubling Y, Widom J, Segal E. 2008. Distinct modes of regulation by chromatin encoded through nucleosome positioning signals. *PLoS computational biology* **4**(11): e1000216.

Forsburg SL, Guarente L. 1989. Identification and characterization of HAP4: a third component of the CCAAT-bound HAP2/HAP3 heteromer. *Genes & development* **3**(8): 1166-1178.

Gasch AP, Spellman PT, Kao CM, Carmel-Harel O, Eisen MB, Storz G, Botstein D, Brown PO. 2000. Genomic expression programs in the response of yeast cells to environmental changes. *Molecular biology of the cell* **11**(12): 4241-4257.

Geng F, Laurent BC. 2004. Roles of SWI/SNF and HATs throughout the dynamic transcription of a yeast glucose-repressible gene. *The EMBO journal* **23**(1): 127-137.

Ghosh S, Pugh BF. 2011. Sequential recruitment of SAGA and TFIID in a genomic response to DNA damage in Saccharomyces cerevisiae. *Molecular and cellular biology* **31**(1): 190-202.

Giardina C, Lis JT. 1993. DNA melting on yeast RNA polymerase II promoters. *Science* **261**(5122): 759-762.

Giniger E, Varnum SM, Ptashne M. 1985. Specific DNA binding of GAL4, a positive regulatory protein of yeast. *Cell* **40**(4): 767-774.

Gkikopoulos T, Havas KM, Dewar H, Owen-Hughes T. 2009. SWI/SNF and Asf1p cooperate to displace histones during induction of the saccharomyces cerevisiae HO promoter. *Molecular and cellular biology* **29**(15): 4057-4066.

Gkikopoulos T, Schofield P, Singh V, Pinskaya M, Mellor J, Smolle M, Workman JL, Barton GJ, Owen-Hughes T. 2011. A role for Snf2-related nucleosome-spacing enzymes in genome-wide nucleosome organization. *Science* **333**(6050): 1758-1760.

Grant PA, Duggan L, Cote J, Roberts SM, Brownell JE, Candau R, Ohba R, Owen-Hughes T, Allis CD, Winston F et al. 1997. Yeast Gcn5 functions in two multisubunit complexes to acetylate nucleosomal histones: characterization of an Ada complex and the SAGA (Spt/Ada) complex. *Genes & development* **11**(13): 1640-1650.

Grant PA, Eberharter A, John S, Cook RG, Turner BM, Workman JL. 1999. Expanded lysine acetylation specificity of Gcn5 in native complexes. *The Journal of biological chemistry* **274**(9): 5895-5900.

Grant PA, Schieltz D, Pray-Grant MG, Steger DJ, Reese JC, Yates JR, 3rd, Workman JL. 1998. A subset of TAF(II)s are integral components of the SAGA complex required for nucleosome acetylation and transcriptional stimulation. *Cell* **94**(1): 45-53.

Gray WM, Fassler JS. 1996. Isolation and analysis of the yeast TEA1 gene, which encodes a zinc cluster Ty enhancer-binding protein. *Molecular and cellular biology* **16**(1): 347-358.

Gregory PD, Schmid A, Zavari M, Munsterkotter M, Horz W. 1999. Chromatin remodelling at the PHO8 promoter requires SWI-SNF and SAGA at a step subsequent to activator binding. *The EMBO journal* **18**(22): 6407-6414.

Grunberg S, Warfield L, Hahn S. 2012. Architecture of the RNA polymerase II preinitiation complex and mechanism of ATP-dependent promoter opening. *Nature structural & molecular biology* **19**(8): 788-796.

Haber JE. 2012. Mating-type genes and MAT switching in Saccharomyces cerevisiae. *Genetics* **191**(1): 33-64.

Hampsey M. 1998. Molecular genetics of the RNA polymerase II general transcriptional machinery. *Microbiology and molecular biology reviews : MMBR* **62**(2): 465-503.

Hartley PD, Madhani HD. 2009. Mechanisms that specify promoter nucleosome location and identity. *Cell* **137**(3): 445-458.

Hassan AH, Awad S, Prochasson P. 2006. The Swi2/Snf2 bromodomain is required for the displacement of SAGA and the octamer transfer of SAGA-acetylated nucleosomes. *The Journal of biological chemistry* **281**(26): 18126-18134.

Hassan AH, Neely KE, Workman JL. 2001. Histone acetyltransferase complexes stabilize swi/snf binding to promoter nucleosomes. *Cell* **104**(6): 817-827.

Hassan AH, Prochasson P, Neely KE, Galasinski SC, Chandy M, Carrozza MJ, Workman JL. 2002. Function and selectivity of bromodomains in anchoring chromatin-modifying complexes to promoter nucleosomes. *Cell* **111**(3): 369-379.

Hemming SA, Edwards AM. 2000. Yeast RNA polymerase II subunit RPB9. Mapping of domains required for transcription elongation. *The Journal of biological chemistry* **275**(4): 2288-2294.

Hemming SA, Jansma DB, Macgregor PF, Goryachev A, Friesen JD, Edwards AM. 2000. RNA polymerase II subunit Rpb9 regulates transcription elongation in vivo. *The Journal of biological chemistry* **275**(45): 35506-35511.

Ho CK, Sriskanda V, McCracken S, Bentley D, Schwer B, Shuman S. 1998. The guanylyltransferase domain of mammalian mRNA capping enzyme binds to the phosphorylated carboxyl-terminal domain of RNA polymerase II. *The Journal of biological chemistry* **273**(16): 9577-9585.

Horikoshi M, Bertuccioli C, Takada R, Wang J, Yamamoto T, Roeder RG. 1992. Transcription factor TFIID induces DNA bending upon binding to the TATA element. *Proceedings of the National Academy of Sciences of the United States of America* **89**(3): 1060-1064.

Hsieh TH, Weiner A, Lajoie B, Dekker J, Friedman N, Rando OJ. 2015. Mapping Nucleosome Resolution Chromosome Folding in Yeast by Micro-C. *Cell* **162**(1): 108-119.

Hsin JP, Sheth A, Manley JL. 2011. RNAP II CTD phosphorylated on threonine-4 is required for histone mRNA 3' end processing. *Science* **334**(6056): 683-686.

Hughes AL, Jin Y, Rando OJ, Struhl K. 2012. A functional evolutionary approach to identify determinants of nucleosome positioning: a unifying model for establishing the genome-wide pattern. *Molecular cell* **48**(1): 5-15.

Huisinga KL, Pugh BF. 2004. A genome-wide housekeeping role for TFIID and a highly regulated stress-related role for SAGA in Saccharomyces cerevisiae. *Molecular cell* **13**(4): 573-585.

Jamonnak N, Creamer TJ, Darby MM, Schaughency P, Wheelan SJ, Corden JL. 2011. Yeast Nrd1, Nab3, and Sen1 transcriptome-wide binding maps suggest multiple roles in post-transcriptional RNA processing. *Rna* **17**(11): 2011-2025.

Jenks MH, O'Rourke TW, Reines D. 2008. Properties of an intergenic terminator and start site switch that regulate IMD2 transcription in yeast. *Molecular and cellular biology* **28**(12): 3883-3893.

Jensen R, Sprague GF, Jr., Herskowitz I. 1983. Regulation of yeast mating-type interconversion: feedback control of HO gene expression by the mating-type locus. *Proceedings of the National Academy of Sciences of the United States of America* **80**(10): 3035-3039.

Jenuwein T, Allis CD. 2001. Translating the histone code. *Science* **293**(5532): 1074-1080.

Jiang C, Pugh BF. 2009a. A compiled and systematic reference map of nucleosome positions across the Saccharomyces cerevisiae genome. *Genome biology* **10**(10): R109.

Jianc C, Pugh BF. 2009b. Nucleosome positioning and gene regulation: advances through genomics. *Nature reviews Genetics* **10**(3): 161-172.

Jorgensen P, Rupes I, Sharom JR, Schneper L, Broach JR, Tyers M. 2004. A dynamic transcriptional network communicates growth potential to ribosome synthesis and critical cell size. *Genes & development* **18**(20): 2491-2505.

Juven-Gershon T, Kadonaga JT. 2010. Regulation of gene expression via the core promoter and the basal transcriptional machinery. *Developmental biology* **339**(2): 225-229.

Kadonaga JT. 2012. Perspectives on the RNA polymerase II core promoter. *Wiley interdisciplinary reviews Developmental biology* **1**(1): 40-51.

Kaplan CD, Jin H, Zhang IL, Belyanin A. 2012. Dissection of Pol II trigger loop function and Pol II activity-dependent control of start site selection in vivo. *PLoS genetics* **8**(4): e1002627.

Kaplan CD, Laprade L, Winston F. 2003. Transcription elongation factors repress transcription initiation from cryptic sites. *Science* **301**(5636): 1096-1099.

Kaplan CD, Larsson KM, Kornberg RD. 2008. The RNA polymerase II trigger loop functions in substrate selection and is directly targeted by alpha-amanitin. *Molecular cell* **30**(5): 547-556.

Kaplan N, Moore IK, Fondufe-Mittendorf Y, Gossett AJ, Tillo D, Field Y, LeProust EM, Hughes TR, Lieb JD, Widom J et al. 2009. The DNA-encoded nucleosome organization of a eukaryotic genome. *Nature* **458**(7236): 362-366.

Kim H, Erickson B, Luo W, Seward D, Graber JH, Pollock DD, Megee PC, Bentley DL. 2010a. Gene-specific RNA polymerase II phosphorylation and the CTD code. *Nature structural & molecular biology* **17**(10): 1279-1286.

Kim JH, Saraf A, Florens L, Washburn M, Workman JL. 2010b. Gcn5 regulates the dissociation of SWI/SNF from chromatin by acetylation of Swi2/Snf2. *Genes & development* **24**(24): 2766-2771.

Kobor MS, Venkatasubrahmanyam S, Meneghini MD, Gin JW, Jennings JL, Link AJ, Madhani HD, Rine J. 2004. A protein complex containing the conserved Swi2/Snf2-related ATPase Swr1p deposits histone variant H2A.Z into euchromatin. *PLoS biology* **2**(5): E131.

Korber P, Barbaric S. 2014. The yeast PHO5 promoter: from single locus to systems biology of a paradigm for gene regulation through chromatin. *Nucleic acids research* **42**(17): 10888-10902.

Korber P, Barbaric S, Luckenbach T, Schmid A, Schermer UJ, Blaschke D, Horz W. 2006. The histone chaperone Asf1 increases the rate of histone eviction at the yeast PHO5 and PHO8 promoters. *The Journal of biological chemistry* **281**(9): 5539-5545.

Kouzine F, Wojtowicz D, Yamane A, Resch W, Kieffer-Kwon KR, Bandle R, Nelson S, Nakahashi H, Awasthi P, Feigenbaum L et al. 2013. Global regulation of promoter melting in naive lymphocytes. *Cell* **153**(5): 988-999.

Krebs JE, Kuo MH, Allis CD, Peterson CL. 1999. Cell cycle-regulated histone acetylation required for expression of the yeast HO gene. *Genes & development* **13**(11): 1412-1421.

Krishnamurthy S, He X, Reyes-Reyes M, Moore C, Hampsey M. 2004. Ssu72 Is an RNA polymerase II CTD phosphatase. *Molecular cell* **14**(3): 387-394.

Krogan NJ, Keogh MC, Datta N, Sawa C, Ryan OW, Ding H, Haw RA, Pootoolal J, Tong A, Canadien V et al. 2003. A Snf2 family ATPase complex required for recruitment of the histone H2A variant Htz1. *Molecular cell* **12**(6): 1565-1576.

Kuang Z, Cai L, Zhang X, Ji H, Tu BP, Boeke JD. 2014. High-temporal-resolution view of transcription and chromatin states across distinct metabolic states in budding yeast. *Nature structural & molecular biology* **21**(10): 854-863.

Kuehner JN, Brow DA. 2008. Regulation of a eukaryotic gene by GTP-dependent start site selection and transcription attenuation. *Molecular cell* **31**(2): 201-211.

Kunkel GR, Martinson HG. 1981. Nucleosomes will not form on double-stranded RNa or over poly(dA).poly(dT) tracts in recombinant DNA. *Nucleic acids research* **9**(24): 6869-6888.

Kuo MH, Brownell JE, Sobel RE, Ranalli TA, Cook RG, Edmondson DG, Roth SY, Allis CD. 1996. Transcription-linked acetylation by Gcn5p of histones H3 and H4 at specific lysines. *Nature* **383**(6597): 269-272.

Langmead B, Salzberg SL. 2012. Fast gapped-read alignment with Bowtie 2. *Nature methods* **9**(4): 357-359.

Larson MH, Zhou J, Kaplan CD, Palangat M, Kornberg RD, Landick R, Block SM. 2012. Trigger loop dynamics mediate the balance between the transcriptional fidelity and speed of RNA polymerase II. *Proceedings of the National Academy of Sciences of the United States of America* **109**(17): 6555-6560.

Lee TI, Causton HC, Holstege FC, Shen WC, Hannett N, Jennings EG, Winston F, Green MR, Young RA. 2000. Redundant roles for the TFIID and SAGA complexes in global transcription. *Nature* **405**(6787): 701-704.

Lee W, Tillo D, Bray N, Morse RH, Davis RW, Hughes TR, Nislow C. 2007. A high-resolution atlas of nucleosome occupancy in yeast. *Nature genetics* **39**(10): 1235-1244.

Li H, Handsaker B, Wysoker A, Fennell T, Ruan J, Homer N, Marth G, Abecasis G, Durbin R, Genome Project Data Processing S. 2009. The Sequence Alignment/Map format and SAMtools. *Bioinformatics* **25**(16): 2078-2079.

Lieleg C, Ketterer P, Nuebler J, Ludwigsen J, Gerland U, Dietz H, Mueller-Planitz F, Korber P. 2015. Nucleosome spacing generated by ISWI and CHD1 remodelers is constant regardless of nucleosome density. *Molecular and cellular biology* **35**(9): 1588-1605.

Lin H, Wong RP, Martinka M, Li G. 2010. BRG1 expression is increased in human cutaneous melanoma. *The British journal of dermatology* **163**(3): 502-510.

Lindquist S. 1986. The heat-shock response. *Annual review of biochemistry* **55**: 1151-1191.

Liu CL, Kaplan T, Kim M, Buratowski S, Schreiber SL, Friedman N, Rando OJ. 2005. Single-nucleosome mapping of histone modifications in S. cerevisiae. *PLoS biology* **3**(10): e328.

Lorch Y, Griesenbeck J, Boeger H, Maier-Davis B, Kornberg RD. 2011. Selective removal of promoter nucleosomes by the RSC chromatin-remodeling complex. *Nature structural & molecular biology* **18**(8): 881-885.

Lorch Y, Maier-Davis B, Kornberg RD. 2006. Chromatin remodeling by nucleosome disassembly in vitro. *Proceedings of the National Academy of Sciences of the United States of America* **103**(9): 3090-3093.

Lubliner S, Keren L, Segal E. 2013. Sequence features of yeast and human core promoters that are predictive of maximal promoter activity. *Nucleic acids research* **41**(11): 5569-5581.

Lubliner S, Regev I, Lotan-Pompan M, Edelheit S, Weinberger A, Segal E. 2015. Core promoter sequence in yeast is a major determinant of expression level. *Genome research* **25**(7): 1008-1017.

Luger K, Mader AW, Richmond RK, Sargent DF, Richmond TJ. 1997. Crystal structure of the nucleosome core particle at 2.8 A resolution. *Nature* **389**(6648): 251-260.

Luk E, Ranjan A, Fitzgerald PC, Mizuguchi G, Huang Y, Wei D, Wu C. 2010. Stepwise histone replacement by SWR1 requires dual activation with histone H2A.Z and canonical nucleosome. *Cell* **143**(5): 725-736.

Lum PY, Armour CD, Stepaniants SB, Cavet G, Wolf MK, Butler JS, Hinshaw JC, Garnier P, Prestwich GD, Leonardson A et al. 2004. Discovering modes of action for therapeutic compounds using a genome-wide screen of yeast heterozygotes. *Cell* **116**(1): 121-137.

Malagon F, Tong AH, Shafer BK, Strathern JN. 2004. Genetic interactions of DST1 in Saccharomyces cerevisiae suggest a role of TFIIS in the initiation-elongation transition. *Genetics* **166**(3): 1215-1227.

Martens JA, Laprade L, Winston F. 2004. Intergenic transcription is required to repress the Saccharomyces cerevisiae SER3 gene. *Nature* **429**(6991): 571-574.

Martens JA, Wu PY, Winston F. 2005. Regulation of an intergenic transcript controls adjacent gene transcription in Saccharomyces cerevisiae. *Genes & development* **19**(22): 2695-2704.

Mavrich TN, Ioshikhes IP, Venters BJ, Jiang C, Tomsho LP, Qi J, Schuster SC, Albert I, Pugh BF. 2008. A barrier nucleosome model for statistical positioning of nucleosomes throughout the yeast genome. *Genome research* **18**(7): 1073-1083.

Mayer A, Lidschreiber M, Siebert M, Leike K, Soding J, Cramer P. 2010. Uniform transitions of the general RNA polymerase II transcription complex. *Nature structural & molecular biology* **17**(10): 1272-1278.

McCracken S, Fong N, Rosonina E, Yankulov K, Brothers G, Siderovski D, Hessel A, Foster S, Shuman S, Bentley DL. 1997. 5'-Capping enzymes are targeted to pre-mRNA by binding to the phosphorylated carboxy-terminal domain of RNA polymerase II. *Genes & development* **11**(24): 3306-3318.

McKnight JN, Boerma JW, Breeden LL, Tsukiyama T. 2015. Global Promoter Targeting of a Conserved Lysine Deacetylase for Transcriptional Shutoff during Quiescence Entry. *Molecular cell* **59**(5): 732-743.

Mitra D, Parnell EJ, Landon JW, Yu Y, Stillman DJ. 2006. SWI/SNF binding to the HO promoter requires histone acetylation and stimulates TATA-binding protein recruitment. *Molecular and cellular biology* **26**(11): 4095-4110.

Mosley AL, Pattenden SG, Carey M, Venkatesh S, Gilmore JM, Florens L, Workman JL, Washburn MP. 2009. Rtr1 is a CTD phosphatase that regulates RNA polymerase II during the transition from serine 5 to serine 2 phosphorylation. *Molecular cell* **34**(2): 168-178.

Nagalakshmi U, Wang Z, Waern K, Shou C, Raha D, Gerstein M, Snyder M. 2008. The transcriptional landscape of the yeast genome defined by RNA sequencing. *Science* **320**(5881): 1344-1349.

Naville M, Gautheret D. 2010. Transcription attenuation in bacteria: theme and variations. *Briefings in functional genomics* **9**(2): 178-189.

Neef DW, Kladde MP. 2003. Polyphosphate loss promotes SNF/SWI- and Gcn5-dependent mitotic induction of PHO5. *Molecular and cellular biology* **23**(11): 3788-3797.

Neely KE, Hassan AH, Brown CE, Howe L, Workman JL. 2002. Transcription activator interactions with multiple SWI/SNF subunits. *Molecular and cellular biology* **22**(6): 1615-1625.

Neely KE, Hassan AH, Wallberg AE, Steger DJ, Cairns BR, Wright AP, Workman JL. 1999. Activation domain-mediated targeting of the SWI/SNF complex to promoters stimulates transcription from nucleosome arrays. *Molecular cell* **4**(4): 649-655.

Neigeborn L, Carlson M. 1984. Genes affecting the regulation of SUC2 gene expression by glucose repression in Saccharomyces cerevisiae. *Genetics* **108**(4): 845-858.

Neil H, Malabat C, d'Aubenton-Carafa Y, Xu Z, Steinmetz LM, Jacquier A. 2009. Widespread bidirectional promoters are the major source of cryptic transcripts in yeast. *Nature* **457**(7232): 1038-1042.

Neumann NP, Lampen JO. 1967. Purification and properties of yeast invertase. *Biochemistry* **6**(2): 468-475.

Ohtsuki K, Kasahara K, Shirahige K, Kokubo T. 2010. Genome-wide localization analysis of a complete set of Tafs reveals a specific effect of the taf1 mutation on Taf2 occupancy and provides indirect evidence for different TFIID conformations at different promoters. *Nucleic acids research* **38**(6): 1805-1820.

Owen-Hughes T, Utley RT, Cote J, Peterson CL, Workman JL. 1996. Persistent site-specific remodeling of a nucleosome array by transient action of the SWI/SNF complex. *Science* **273**(5274): 513-516.

Pan J, Sasaki M, Kniewel R, Murakami H, Blitzblau HG, Tischfield SE, Zhu X, Neale MJ, Jasin M, Socci ND et al. 2011. A hierarchical combination of factors shapes the genome-wide topography of yeast meiotic recombination initiation. *Cell* **144**(5): 719-731.

Papamichos-Chronakis M, Watanabe S, Rando OJ, Peterson CL. 2011. Global regulation of H2A.Z localization by the INO80 chromatin-remodeling enzyme is essential for genome integrity. *Cell* **144**(2): 200-213.

Pappas DL, Jr., Hampsey M. 2000. Functional interaction between Ssu72 and the Rpb2 subunit of RNA polymerase II in Saccharomyces cerevisiae. *Molecular and cellular biology* **20**(22): 8343-8351.

Parnell TJ, Schlichter A, Wilson BG, Cairns BR. 2015. The chromatin remodelers RSC and ISW1 display functional and chromatin-based promoter antagonism. *eLife* **4**: e06073.

Pelechano V, Wei W, Steinmetz LM. 2013. Extensive transcriptional heterogeneity revealed by isoform profiling. *Nature* **497**(7447): 127-131.

Picelli S, Bjorklund AK, Faridani OR, Sagasser S, Winberg G, Sandberg R. 2013. Smart-seq2 for sensitive full-length transcriptome profiling in single cells. *Nature methods* **10**(11): 1096-1098.

Pinon R. 1978. Folded chromosomes in non-cycling yeast cells: evidence for a characteristic g0 form. *Chromosoma* **67**(3): 263-274.

Qiu H, Hu C, Hinnebusch AG. 2009. Phosphorylation of the Pol II CTD by KIN28 enhances BUR1/BUR2 recruitment and Ser2 CTD phosphorylation near promoters. *Molecular cell* **33**(6): 752-762.

Quinlan AR, Hall IM. 2010. BEDTools: a flexible suite of utilities for comparing genomic features. *Bioinformatics* **26**(6): 841-842.

Raisner RM, Hartley PD, Meneghini MD, Bao MZ, Liu CL, Schreiber SL, Rando OJ, Madhani HD. 2005. Histone variant H2A.Z marks the 5' ends of both active and inactive genes in euchromatin. *Cell* **123**(2): 233-248.

Rando OJ, Winston F. 2012. Chromatin and transcription in yeast. *Genetics* **190**(2): 351-387.

Ranjan A, Mizuguchi G, FitzGerald PC, Wei D, Wang F, Huang Y, Luk E, Woodcock CL, Wu C. 2013. Nucleosome-free region dominates histone acetylation in targeting SWR1 to promoters for H2A.Z replacement. *Cell* **154**(6): 1232-1245.

Reyes-Reyes M, Hampsey M. 2007. Role for the Ssu72 C-terminal domain phosphatase in RNA polymerase II transcription elongation. *Molecular and cellular biology* **27**(3): 926-936.

Rhee HS, Pugh BF. 2012. Genome-wide structure and organization of eukaryotic pre-initiation complexes. *Nature* **483**(7389): 295-301.

Rohland N, Reich D. 2012. Cost-effective, high-throughput DNA sequencing libraries for multiplexed target capture. *Genome research* **22**(5): 939-946.

Rougvie AE, Lis JT. 1988. The RNA polymerase II molecule at the 5' end of the uninduced hsp70 gene of D. melanogaster is transcriptionally engaged. *Cell* **54**(6): 795-804.

Rutledge MT, Russo M, Belton JM, Dekker J, Broach JR. 2015. The yeast genome undergoes significant topological reorganization in quiescence. *Nucleic acids research* **43**(17): 8299-8313.

Ryan DP, Owen-Hughes T. 2011. Snf2-family proteins: chromatin remodellers for any occasion. *Current opinion in chemical biology* **15**(5): 649-656.

Sadowski I, Breitkreutz BJ, Stark C, Su TC, Dahabieh M, Raithatha S, Bernhard W, Oughtred R, Dolinski K, Barreto K et al. 2013. The PhosphoGRID Saccharomyces cerevisiae protein phosphorylation site database: version 2.0 update. *Database : the journal of biological databases and curation* **2013**: bat026.

Sainsbury S, Bernecky C, Cramer P. 2015. Structural basis of transcription initiation by RNA polymerase II. *Nature reviews Molecular cell biology* **16**(3): 129-143.

Satchwell SC, Drew HR, Travers AA. 1986. Sequence periodicities in chicken nucleosome core DNA. *Journal of molecular biology* **191**(4): 659-675.

Schawalder SB, Kabani M, Howald I, Choudhury U, Werner M, Shore D. 2004. Growth-regulated recruitment of the essential yeast ribosomal protein gene activator Ifh1. *Nature* **432**(7020): 1058-1061.

Schmitt ME, Brown TA, Trumpower BL. 1990. A rapid and simple method for preparation of RNA from Saccharomyces cerevisiae. *Nucleic acids research* **18**(10): 3091-3092.

Schwer B, Shuman S. 2011. Deciphering the RNA polymerase II CTD code in fission yeast. *Molecular cell* **43**(2): 311-318.

Segal E, Fondufe-Mittendorf Y, Chen L, Thastrom A, Field Y, Moore IK, Wang JP, Widom J. 2006. A genomic code for nucleosome positioning. *Nature* **442**(7104): 772-778.

Shi L, Sutter BM, Ye X, Tu BP. 2010. Trehalose is a key determinant of the quiescent metabolic state that fuels cell cycle progression upon return to growth. *Molecular biology of the cell* **21**(12): 1982-1990.

Shivaswamy S, Bhinge A, Zhao Y, Jones S, Hirst M, Iyer VR. 2008. Dynamic remodeling of individual nucleosomes across a eukaryotic genome in response to transcriptional perturbation. *PLoS biology* **6**(3): e65.

Shivaswamy S, Iyer VR. 2008. Stress-dependent dynamics of global chromatin remodeling in yeast: dual role for SWI/SNF in the heat shock stress response. *Molecular and cellular biology* **28**(7): 2221-2234.

Silverman SJ, Petti AA, Slavov N, Parsons L, Briehof R, Thiberge SY, Zenklusen D, Gandhi SJ, Larson DR, Singer RH et al. 2010. Metabolic cycling in single yeast cells from unsynchronized steady-state populations limited on glucose or phosphate. *Proceedings of the National Academy of Sciences of the United States of America* **107**(15): 6946-6951.

Silverstein RA, Gonzalez de Valdivia E, Visa N. 2011. The incorporation of 5-fluorouracil into RNA affects the ribonucleolytic activity of the exosome subunit Rrp6. *Molecular cancer research : MCR* **9**(3): 332-340.

Singh N, Ma Z, Gemmill T, Wu X, Defiglio H, Rossettini A, Rabeler C, Beane O, Morse RH, Palumbo MJ et al. 2009. The Ess1 prolyl isomerase is required for transcription termination of small noncoding RNAs via the Nrd1 pathway. *Molecular cell* **36**(2): 255-266.

Smale ST, Kadonaga JT. 2003. The RNA polymerase II core promoter. *Annual review of biochemistry* **72**: 449-479.

Smith CL, Peterson CL. 2005. A conserved Swi2/Snf2 ATPase motif couples ATP hydrolysis to chromatin remodeling. *Molecular and cellular biology* **25**(14): 5880-5892.

Spencer SL, Cappell SD, Tsai FC, Overton KW, Wang CL, Meyer T. 2013. The proliferation-quiescence decision is controlled by a bifurcation in CDK2 activity at mitotic exit. *Cell* **155**(2): 369-383.

Steger DJ, Haswell ES, Miller AL, Wente SR, O'Shea EK. 2003. Regulation of chromatin remodeling by inositol polyphosphates. *Science* **299**(5603): 114-116.

Steinmetz EJ, Conrad NK, Brow DA, Corden JL. 2001. RNA-binding protein Nrd1 directs poly(A)-independent 3'-end formation of RNA polymerase II transcripts. *Nature* **413**(6853): 327-331.

Stern M, Jensen R, Herskowitz I. 1984. Five SWI genes are required for expression of the HO gene in yeast. *Journal of molecular biology* **178**(4): 853-868.

Struhl K. 1985. Naturally occurring poly(dA-dT) sequences are upstream promoter elements for constitutive transcription in yeast. *Proceedings of the National Academy of Sciences of the United States of America* **82**(24): 8419-8423.

Sudarsanam P, Iyer VR, Brown PO, Winston F. 2000. Whole-genome expression analysis of snf/swi mutants of Saccharomyces cerevisiae. *Proceedings of the National Academy of Sciences of the United States of America* **97**(7): 3364-3369.

Sun ZW, Tessmer A, Hampsey M. 1996. Functional interaction between TFIIB and the Rpb9 (Ssu73) subunit of RNA polymerase II in Saccharomyces cerevisiae. *Nucleic acids research* **24**(13): 2560-2566.

Tan S, Hunziker Y, Sargent DF, Richmond TJ. 1996. Crystal structure of a yeast TFIIA/TBP/DNA complex. *Nature* **381**(6578): 127-151.

Tantin D, Carey M. 1994. A heteroduplex template circumvents the energetic requirement for ATP during activated transcription by RNA polymerase II. *The Journal of biological chemistry* **269**(26): 17397-17400.

Thiebaut M, Colin J, Neil H, Jacquier A, Seraphin B, Lacroute F, Libri D. 2008. Futile cycle of transcription initiation and termination modulates the response to nucleotide shortage in S. cerevisiae. *Molecular cell* **31**(5): 671-682.

Tirosh I, Sigal N, Barkai N. 2010. Widespread remodeling of mid-coding sequence nucleosomes by Isw1. *Genome biology* **11**(5): R49.

Todeschini AL, Morillon A, Springer M, Lesage P. 2005. Severe adenine starvation activates Ty1 transcription and retrotransposition in Saccharomyces cerevisiae. *Molecular and cellular biology* **25**(17): 7459-7472.

Tolstorukov MY, Sansam CG, Lu P, Koellhoffer EC, Helming KC, Alver BH, Tillman EJ, Evans JA, Wilson BG, Park PJ et al. 2013. Swi/Snf chromatin remodeling/tumor suppressor complex establishes nucleosome occupancy at target promoters. *Proceedings of the National Academy of Sciences of the United States of America* **110**(25): 10165-10170.

Treitel MA, Carlson M. 1995. Repression by SSN6-TUP1 is directed by MIG1, a repressor/activator protein. *Proceedings of the National Academy of Sciences of the United States of America* **92**(8): 3132-3136.

Tu BP, Kudlicki A, Rowicka M, McKnight SL. 2005. Logic of the yeast metabolic cycle: temporal compartmentalization of cellular processes. *Science* **310**(5751): 1152-1158.

Tu BP, Mohler RE, Liu JC, Dombek KM, Young ET, Synovec RE, McKnight SL. 2007. Cyclic changes in metabolic state during the life of a yeast cell. *Proceedings of the National Academy of Sciences of the United States of America* **104**(43): 16886-16891.

Udugama M, Sabri A, Bartholomew B. 2011. The INO80 ATP-dependent chromatin remodeling complex is a nucleosome spacing factor. *Molecular and cellular biology* **31**(4): 662-673.

Vaillant C, Palmeira L, Chevereau G, Audit B, d'Aubenton-Carafa Y, Thermes C, Arneodo A. 2010. A novel strategy of transcription regulation by intragenic nucleosome ordering. *Genome research* **20**(1): 59-67.

Van Mullem V, Wery M, Werner M, Vandenhaute J, Thuriaux P. 2002. The Rpb9 subunit of RNA polymerase II binds transcription factor TFIIE and interferes with the SAGA and elongator histone acetyltransferases. *The Journal of biological chemistry* **277**(12): 10220-10225.

Vasiljeva L, Kim M, Mutschler H, Buratowski S, Meinhart A. 2008. The Nrd1-Nab3-Sen1 termination complex interacts with the Ser5-phosphorylated RNA polymerase II C-terminal domain. *Nature structural & molecular biology* **15**(8): 795-804.

Vignali M, Hassan AH, Neely KE, Workman JL. 2000. ATP-dependent chromatin-remodeling complexes. *Molecular and cellular biology* **20**(6): 1899-1910.

Voss TC, Hager GL. 2014. Dynamic regulation of transcriptional states by chromatin and transcription factors. *Nature reviews Genetics* **15**(2): 69-81.

Walmacq C, Kireeva ML, Irvin J, Nedialkov Y, Lubkowska L, Malagon F, Strathern JN, Kashlev M. 2009. Rpb9 subunit controls transcription fidelity by delaying NTP sequestration in RNA polymerase II. *The Journal of biological chemistry* **284**(29): 19601-19612.

Wang D, Bushnell DA, Westover KD, Kaplan CD, Kornberg RD. 2006. Structural basis of transcription: role of the trigger loop in substrate specificity and catalysis. *Cell* **127**(5): 941-954.

Watson AD, Edmondson DG, Bone JR, Mukai Y, Yu Y, Du W, Stillman DJ, Roth SY. 2000. Ssn6-Tup1 interacts with class I histone deacetylases required for repression. *Genes & development* **14**(21): 2737-2744.

Weiner A, Hsieh TH, Appleboim A, Chen HV, Rahat A, Amit I, Rando OJ, Friedman N. 2015. High-resolution chromatin dynamics during a yeast stress response. *Molecular cell* **58**(2): 371-386.

Whitehouse I, Flaus A, Cairns BR, White MF, Workman JL, Owen-Hughes T. 1999. Nucleosome mobilization catalysed by the yeast SWI/SNF complex. *Nature* **400**(6746): 784-787.

Whitehouse I, Rando OJ, Delrow J, Tsukiyama T. 2007. Chromatin remodelling at promoters suppresses antisense transcription. *Nature* **450**(7172): 1031-1035.

Whitehouse I, Tsukiyama T. 2006. Antagonistic forces that position nucleosomes in vivo. *Nature structural & molecular biology* **13**(7): 633-640.

Wu L, Winston F. 1997. Evidence that Snf-Swi controls chromatin structure over both the TATA and UAS regions of the SUC2 promoter in Saccharomyces cerevisiae. *Nucleic acids research* **25**(21): 4230-4234.

Wu Q, Madany P, Akech J, Dobson JR, Douthwright S, Browne G, Colby JL, Winter GE, Bradner JE, Pratap J et al. 2015. The SWI/SNF ATPases Are Required for Triple Negative Breast Cancer Cell Proliferation. *Journal of cellular physiology* **230**(11): 2683-2694.

Wyers F, Rougemaille M, Badis G, Rousselle JC, Dufour ME, Boulay J, Regnault B, Devaux F, Namane A, Seraphin B et al. 2005. Cryptic pol II transcripts are degraded by a nuclear quality control pathway involving a new poly(A) polymerase. *Cell* **121**(5): 725-737.

Xu Z, Wei W, Gagneur J, Perocchi F, Clauder-Munster S, Camblong J, Guffanti E, Stutz F, Huber W, Steinmetz LM. 2009. Bidirectional promoters generate pervasive transcription in yeast. *Nature* **457**(7232): 1033-1037.

Yatherajam G, Zhang L, Kraemer SM, Stargell LA. 2003. Protein-protein interaction map for yeast TFIID. *Nucleic acids research* **31**(4): 1252-1260.

Yen K, Vinayachandran V, Batta K, Koerber RT, Pugh BF. 2012. Genome-wide nucleosome specificity and directionality of chromatin remodelers. *Cell* **149**(7): 1461-1473.

Yudkovsky N, Logie C, Hahn S, Peterson CL. 1999. Recruitment of the SWI/SNF chromatin remodeling complex by transcriptional activators. *Genes & development* **13**(18): 2369-2374.

Zhang DW, Mosley AL, Ramisetty SR, Rodriguez-Molina JB, Washburn MP, Ansari AZ. 2012. Ssu72 phosphatase-dependent erasure of phospho-Ser7 marks on the RNA polymerase II C-terminal domain is essential for viability and transcription termination. *The Journal of biological chemistry* **287**(11): 8541-8551.

Zhang H, Roberts DN, Cairns BR. 2005. Genome-wide dynamics of Htz1, a histone H2A variant that poises repressed/basal promoters for activation through histone loss. *Cell* **123**(2): 219-231.

Zhang W, Bone JR, Edmondson DG, Turner BM, Roth SY. 1998. Essential and redundant functions of histone acetylation revealed by mutation of target lysines and loss of the Gcn5p acetyltransferase. *The EMBO journal* **17**(11): 3155-3167.

Zhang Y, Moqtaderi Z, Rattner BP, Euskirchen G, Snyder M, Kadonaga JT, Liu XS, Struhl K. 2009. Intrinsic histone-DNA interactions are not the major determinant of nucleosome positions in vivo. *Nature structural & molecular biology* **16**(8): 847-852.

Zhang Z, Wippo CJ, Wal M, Ward E, Korber P, Pugh BF. 2011. A packing mechanism for nucleosome organization reconstituted across a eukaryotic genome. *Science* **332**(6032): 977-980.

Ziegler LM, Khaperskyy DA, Ammerman ML, Ponticelli AS. 2003. Yeast RNA polymerase II lacking the Rpb9 subunit is impaired for interaction with transcription factor IIF. *The Journal of biological chemistry* **278**(49): 48950-48956.

Zofall M, Persinger J, Kassabov SR, Bartholomew B. 2006. Chromatin remodeling by ISW2 and SWI/SNF requires DNA translocation inside the nucleosome. *Nature structural & molecular biology* **13**(4): 339-346.